ASD-TDR-63-102
Part II

RESEARCH ON THE MECHANISM OF THERMAL DECOMPOSITION OF HYDROCARBON FUELS

TECHNICAL DOCUMENTARY REPORT NO. ASD-TDR-63-102, Part II

August 1964

Air Force Aero Propulsion Laboratory
Research and Technology
Air Force Systems Command
Wright-Patterson Air Force Base, Ohio

Project No. 3048, Task No. 304801

(Prepared under Contract No. AF 33(657)-8193 by Monsanto Research Corporation, Everett, Mass;
Bela M. Fabuss, Alexander S. Borsanyi, Dennis A. Duncan, Ralph Kafesjian, and John O. Smith, authors)

NOTICES

When Government drawings, specifications, or other data are used for any purpose other than in connection with a definitely related Government procurement operation, the United States Government thereby incurs no responsibility nor any obligation whatsoever; and the fact that the Government may have formulated, furnished, or in any way supplied the said drawings, specifications, or other data, is not to be regarded by implication or otherwise as in any manner licensing the holder or any other person or corporation, or conveying any rights or permission to manufacture, use, or sell any patented invention that may in any way be related thereto.

Qualified requesters may obtain copies of this report from the Defense Documentation Center (DDC), (formerly ASTIA), Cameron Station, Bldg. 5, 5010 Duke Street, Alexandria 4, Virginia

This report has been released to the Office of Technical Services, U.S. Department of Commerce, Washington 25, D.C., for sale to the general public.

Copies of this report should not be returned to the Aeronautical Systems Division unless return is required by security considerations, contractual obligations, or notice on a specific document.

FOREWORD

This report was prepared by Monsanto Research Corporation under USAF Contract No. AF 33(657)-8193. The contract was initiated under Project No. 3048, "Aviation Fuels", Task No. 304801, "Hydrocarbon Fuels". The program was administered under the direction of the Air Force Aero Propulsion Laboratory, Research and Technology Division. Mr. Jack Fultz was project engineer.

This report covers work done from 15 November 1962 to 15 November 1963.

The work was directed for Monsanto Research Corporation by Dr. Bela M. Fabuss under the general supervision of Dr. John O. Smith.

ABSTRACT

The decomposition and particle formation of 28 naphthenic and 8 paraffinic hydrocarbons were studied. The decomposition was approximately a first-order kinetic process, although self-acceleration was observed with most monocyclic hydrocarbons and self-inhibition was observed for polycyclic hydrocarbons. Pressure increased the decomposition rate.

A detailed study of the effects of organosulfur contaminants was made. These contaminants inhibited the cracking of naphthenes and straight-chain paraffins and accelerated the cracking of branched paraffins. An increase in contaminant concentration and an increase in the number of methyl substituent groups on a hydrocarbon increased this effect.

Several binary hydrocarbon mixtures were cracked. The component hydrocarbons did not crack independently. Nevertheless, the decomposition rate of the mixture could be predicted assuming no mutual interference in decomposition.

The micro-coker, a new small-scale device for studying decomposition and deposit formation in a flow system, was developed.

This technical documentary report has been reviewed and is approved.

Marc P. Dunnam
Chief, Technical Support Division
AF Aero Propulsion Laboratory

TABLE OF CONTENTS

		Page
I.	INTRODUCTION	1
II.	SUMMARY AND CONCLUSIONS	2
III.	EXPERIMENTAL METHOD	3
IV.	THERMAL DECOMPOSITION OF SATURATED CYCLIC HYDROCARBONS	5
	A. CALCULATION OF RATE CONSTANTS	5
	B. ACTIVATION ENERGIES	7
	C. EFFECT OF PRESSURE ON DECOMPOSITION RATE	13
	D. ESTIMATION OF RATE CONSTANT OF DECOMPOSITION	19
	E. RATE OF PARTICLE FORMATION	20
V.	THERMAL DECOMPOSITION OF PARAFFINIC HYDROCARBONS	23
	A. EXPERIMENTAL RESULTS	23
	B. ACTIVATION ENERGIES	27
	C. EFFECT OF BRANCHING ON THE RATE OF DECOMPOSITION	29
	D. EFFECT OF PRESSURE ON THE RATE OF DECOMPOSITION.	33
	E. METHOD FOR ESTIMATION OF THE RATE CONSTANT OF DECOMPOSITION	37
	F. RATE OF PARTICLE FORMATION	39
	G. PRODUCT DISTRIBUTION FROM PARAFFIN CRACKING BY RICE-KOSSIAKOFF METHOD	41
VI.	CONTAMINATION BY SULFUR COMPOUNDS	49
	A. EXPERIMENTAL STUDY OF SULFUR CONTAMINATION VARIABLES	49
	1. Contaminant Concentration	60
	2. Contaminant Structure	60
	3. Hydrocarbon Structure	60
	4. Temperature Effects	61
	B. THEORETICAL CONSIDERATIONS	61
	C. SULFUR CONTAMINATION AND PARTICLE FORMATION	68
	D. DECOMPOSITION IN THE PRESENCE OF AIR AND CONTAMINANT	69
	1. Synergetic Effect	69
	2. Prolonged Air Exposure	71

TABLE OF CONTENTS
(Continued)

		Page
VII.	DECOMPOSITION OF BINARY MIXTURES	74
	A. EXPERIMENTAL	74
	B. RESULTS	76
	1. n-Hexadecane-Decalin	76
	2. Hydrindan-Decalin	79
	3. Tetramethylnonane-t-butylcyclohexane	79
	4. t-Butylcyclohexane-Methylhydrindan	94
	5. n-Hexadecane-Tetramethylnonane	94
VIII.	MICRO-COKER DEVELOPMENT	103
	A. EQUIPMENT	103
	B. TEST RESULTS	105
	1. Effect of Temperature, Pressure, and Plate Material	105
	2. Effect of Feed Material and Comparison of Results with CRC Coker Data	107
IX.	REFERENCES	112
APPENDIX:	SAMPLE CALCULATIONS	115
A.	RATE CONSTANTS OF PURE HYDROCARBONS: STATISTICAL EVALUATION OF DATA	115
B.	RATE CONSTANTS OF BINARY HYDROCARBON MIXTURES	117

LIST OF FIGURES

No.	Title	Page
1	Rate Constant of Decomposition as a Function of Conversion for Cyclohexane at 800°F.....	8
2	Rate Constant of Decomposition as a Function of Conversion of t-Butylcyclohexane at 800°F.....	8
3	Concentration Change in the Decomposition of 1-Ethyldecalin at 800°F.....	9
4	Rate Constants of Decomposition as a Function of Conversion and Temperature for Methylhydrindan.....	11
5	Arrhenius Plot for Cyclohexane.....	12
6	The Effect of Pressure on the Rate of Decomposition of t-Butylcyclohexane at 800°F.....	15
7	Arrhenius Plot for Decalin.....	18
8	Rates of Decomposition of Naphthenic Hydrocarbons at 800°F.....	21
9	Rates of Decomposition of Paraffinic Hydrocarbons at 800°F.....	25
10	Activation Energies of Paraffinic Hydrocarbons.....	26
11	Rate Constants of Thermal Cracking of n-Hexadecane.	28
12	Rate Constants of Decomposition of n-Paraffins.....	30
13	Rate Constants of Isomeric Dodecanes as a Function of Pressure.....	35
14	Relative Rate Constants of Thermal Cracking as a Function of Pressure.....	36
15	Effect of Phase Conditions on the Decomposition Rate Constants of n-Hexadecane.....	38
16	Calculated Product Distribution in the Thermal Cracking of Cetane.....	47
17	Effect of Contaminant Concentration on Rate of Decomposition of Decalin.....	57

LIST OF FIGURES
(Continued)

No.	Title	Page
18	Effect of Contaminant Concentration on Rate of Decomposition of 5-n-Propylnonane.....	58
19	Effect of Contaminant Concentration on Rate of Decomposition of n-Hexadecane.....	59
20	The Variation in the Effect of Sulfur Contamination with Temperature.....	63
21	Typical Chromatograph for Binary Mixture Decomposition.....	75
22	The Effect of Dilution with n-Hexadecane (C) on the Decomposition Rate Constant of Decalin (D) at 700°F	77
23	The Effect of Dilution with Decalin (D) on the Decomposition Rate Constant of n-Hexadecane (C) at 700°F.	78
24	Decomposition Rate Constants of n-Hexadecane-Decalin Mixtures at 700°F.....	81
25	Effect of Dilution with Hydrindan (H) on the Decomposition Rate Constant of Decalin (D) at 750°F.....	83
26	Effect of Dilution with Decalin (D) on the Decomposition Rate Constant of Hydrindan (H) at 750°F.....	84
27	Decomposition Rate Constants of Hydrindan-Decalin Mixtures at 750°F.....	85
28	The Effect of Dilution with 2,2,8,8-Tetramethylnonane (N) on the Decomposition Rate Constant of t-Butylcyclohexane (X) at 800°F.....	87
29	The Effect of Dilution with t-Butylcyclohexane (X) on the Decomposition Rate Constant of 2,2,8,8-Tetramethylnonane (N) at 800°F.....	88
30	Decomposition Rate Constant of 2,2,8,8-Tetramethylnonane-t-Butylcyclohexane Mixtures at 800°F.....	89
31	Effect of Dilution with 2,2,8,8-Tetramethylnonane (N) on the Decomposition Rate Constant of t-Butylcyclohexane (X) at 800°F.....	91

LIST OF FIGURES
(Continued)

No.	Title	Page
32	Effect of Dilution with t-Butylcyclohexane (X) on the Decomposition Rate Constant of 2,2,8,8-Tetramethylnonane (N) at 800°F	92
33	Decomposition Rate Constants of 2,2,8,8-Tetramethylnonane (N)-t-Butylcyclohexane (X) Mixtures at 800°F.	93
34	Effect of Dilution with t-Butylcyclohexane (X) on the Decomposition Rate Constant of Methylhydrindan (M) at 800°F	96
35	Effect of Dilution with Methylhydrindan (M) on the Decomposition Rate Constant of t-Butylcyclohexane (X) at 800°F	97
36	Decomposition Rate Constants of t-Butylcyclohexane-Methylhydrindan Mixtures at 800°F	98
37	Effect of Dilution with 2,2,8,8-Tetramethylnonane (N) on the Decomposition Rate Constant of n-Hexadecane (C) at 800°F	100
38	Effect of Dilution with n-Hexadecane (C) on the Decomposition Rate Constant of 2,2,8,8-Tetramethylnonane (N) at 800°F	101
39	Decomposition Rate Constants of n-Hexadecane-2,2,8,8-Tetramethylnonane Mixtures (800°F)	102
40	Micro-Coker Assembly	104
41	Effect of Temperature on Deposit Length, Type 302 Stainless Steel Test Plates	106
42.	Effect of Temperature on Deposit Length, Aluminum Test Plates	108
43	Effect of Pressure and Temperature on Deposit Length, Aluminum Test Plates	109
44	Comparison of Micro-Coker and CRC Ratings on Various Fuels	111

LIST OF TABLES

No.	Title	Page
1	Boiling Points and Purity of Selected Hydrocarbons	4
2	First-Order Decomposition Rate Constants for Naphthenic Hydrocarbons	6
3	The Effect of Pressure on the Decomposition of t-Butylcyclohexane at 800°F	14
4	Rates of Decomposition (hr^{-1}) of Paraffinic Hydrocarbons	24
5	Rates of Decomposition of Branched Chain Paraffins.	32
6	Effect of Pressure on the Decomposition of Paraffinic Hydrocarbons	34
7	Experimental and Calculated Rate Constants of Decomposition and Rate Constants of Particle Formation at 800°F	40
8	Activation Energies of Particle Formation (E_p) and Decomposition (E_D) (kcal/mole)	41
9	Radicals Formed From 100 Cetane Molecules by Isomerization	43
10	Olefins and R_2 Radicals Formed by Decomposition of 100 Cetane Molecules	45
11	Product Distribution in the Decomposition of n-Hexadecane (in mole per cent)	46
12	Decomposition Rate Data for 5-n-Propylnonane Contaminated with t-Butyldisulfide	50
13	Decomposition Rate Data for 5-n-Propylnonane Contaminated with Thiophenol	51
14	Decomposition Rate for n-Hexadecane Contaminated with t-Butyldisulfide	52
15	Decomposition Rate for n-Hexadecane Contaminated with t-Butyldisulfide	53
16	Decomposition Rate Data for Decalin Contaminated with t-Butyldisulfide	54

LIST OF TABLES
(Continued)

No.	Title	Page
17	Decomposition Rate Data for Decalin Contaminated with Thiophenol.....	55
18	Decomposition Rate Data for Sundry Hydrocarbons Contaminated with t-Butyldisulfide.....	56
19	Change in Decomposition Rate by 0.1% t-Butyldisulfide as a Function of Number of Methyl Groups...	62
20	Particle Formation in Samples Contaminated with t-Butyldisulfide.....	70
21	Particle Formation in n-Hexadecane Decomposition: The Synergetic Effect of Air and Phenyldisulfide...	72
22	Thermal Cracking of Binary Mixtures n-Hexadecane-Decalin.....	80
23	Thermal Cracking of Binary Mixtures Hydrindan-Decalin.....	82
24	Thermal Cracking of Binary Mixtures 2,2,8,8-Tetramethylnonane-t-Butylcyclohexane (N-X).....	86
25	Thermal Cracking of Binary Mixtures 2,2,8,8-Tetramethylnonane-t-Butylcyclohexane (N-X).....	90
26	Thermal Cracking of Binary Mixtures t-Butylcyclohexane-Methylhydrindan.....	95
27	Thermal Cracking of Binary Mixtures n-Hexadecane-2,2,8,8-Tetramethylnonane.....	99

I. INTRODUCTION

The study of the thermal decomposition of hydrocarbons acquires great scientific and technical importance because of the increasingly great demands for thermal stability in hydrocarbons during use.

Data available in this area of research permit a preliminary prediction of the thermal stability of various groups of hydrocarbons, and they also give certain information about the selection of fuels and the purification methods required to obtain fuels of improved thermal stability. The basic objective of this program was to obtain further reliable information about the decomposition of pure hydrocarbons, to investigate the rates of decomposition and solid deposition or particle formation, and to determine the mechanism by which hydrocarbon fuels undergo thermal decomposition. Individual pure hydrocarbons were studied to assemble sufficient data to correlate structure with manifestations of thermal instability.

Effects of fuel contaminants were examined to establish their effectiveness both in promoting and inhibiting decomposition processes. Of the possible contaminants in a hydrocarbon fuel, organosulfur compounds are not only the most prevalent but also appear to have the greatest effect on the decomposition rate. The effects of these compounds as hydrocarbon contaminants were studied in detail.

A further objective of the project was to find means for quantitatively predicting the decomposition behavior of a hydrocarbon mixture using the basic knowledge compiled for the decomposition of the pure hydrocarbon components. Several binary hydrocarbon mixtures were cracked experimentally to test the predictability of their decompositions.

A small-scale dynamic decomposition reactor, the micro-coker, was developed. This equipment permits investigation in situ of the decomposition deposits (coke) that form on the hot metal surfaces of its cracking zone.

Manuscript released by authors 24 October 1963 for publication as an ASD Technical Documentary Report.

II. SUMMARY AND CONCLUSIONS

An analysis of the experimental data on thermal decomposition of various saturated cyclic hydrocarbons indicated that the decomposition is approximately a first-order kinetic process. However, a self-acceleration was observed in the decomposition of most of the monocyclic hydrocarbons. Both fused and non-fused polycyclic naphthenic hydrocarbons generally showed a self-inhibiting behavior. Paraffinic hydrocarbons, on the other hand, showed no deviation from a first-order kinetic decomposition process.

Pressure was found to increase the decomposition rate of the paraffinic and cyclic hydrocarbons investigated.

Methods for estimating decomposition rates under the present experimental conditions were devised for both paraffinic and non-paraffinic saturated hydrocarbons. An approximate correlation of the rate of particle formation with chemical structure and decomposition rate indicates that decalin and cyclohexane derivatives are the more stable of the hydrocarbon types studied.

Organosulfur contaminants were added to various hydrocarbons and the effects on decomposition rate were noted. Cracking of naphthenes and straight-chain paraffins was inhibited. Cracking of t branched paraffins was accelerated. The effect of the sulfur contaminant was increased by increasing the decomposition temperature, the contaminant concentration, and the number of methy groups on the hydrocarbon. Particle formation was commensurate with the degree of decomposition. The type of organosulfur component did not seem to be of primary importance. Thiophenol was roughly equivalent to t-butyldisulfide. Air in the reaction tubes caused increased particle formation when cetane was cracke with a sulfide-type contaminant, but no other instances of such synergetic behavior were observed.

Several binary mixtures of hydrocarbons with widely differing structure were cracked. The components did not crack independently. Instead, their reaction chains interacted resulting in a change of decomposition rate for each individual hydrocarbon. The more stable component became less stable and vice vers It was observed, however, that the extent of cracking (or rate of decomposition) could be predicted very well assuming independe non-interfering, first-order decomposition of each component. Only the decomposition rates of the individual pure hydrocarbons need be known to predict the rates for the various blends.

The development work on the micro-coker was completed. This new device permits the study of hydrocarbon decomposition under flow conditions in the presence of metal surfaces. The micro-coker results are reproducible, and evaluation of decomposition of a series of hydrocarbon fuels gave satisfactory experimental resul

III. EXPERIMENTAL METHOD

"Pure" hydrocarbons, as received, were passed through fresh silica gel and/or activated coconut charcoal and filtered through 0.45-micron Millipore filters. The purity of the hydrocarbons was judged primarily from vapor phase chromatograms. In several cases, when impurities were not removed by the adsorption treatment, the material was fractionated. Final samples were stored in glass containers near 0°F. Table 1 lists the compounds studied and the estimated minimum purity. In some cases, several isomers were present and the minimum purity is taken to be the sum of the areas of the several neighboring peaks, each presumably representing one isomer. Table 1 lists the number of components present as indicated by the number of peaks in the chromatogram and also the area of the main peak as a percentage of the total.

Thermal decomposition rates were measured primarily in a static test apparatus. From 1.26 to 1.5 ml of the hydrocarbon was placed in a Pyrex glass tube, the quantity of hydrocarbon being adjusted so as to constitute in each case 39.5% of the tube volume. All samples were degassed by alternate freezing and thawing under vacuum, and the tubes were then sealed under vacuum. They were preheated to 500°F and then subjected to the reaction temperature (700, 750, 800, or 850°F) for periods from 1 to over 100 hours. All hydrocarbons were studied at 800°F, and some at the other temperatures to determine the effective activation energy. From 4 to 26 runs at different reaction times at 800°F for each hydrocarbon gave the order of the reaction. The per cent conversion was determined by vapor phase chromatographic (VPC) measurements, with corrections being applied corresponding to loss of gaseous products when sample tubes were opened.

Some studies were also made in a stainless steel (type 304) high pressure isoteniscope (ref. 2) to determine the effect of pressure on decomposition. Further studies were also made at 500 psig pressure in a micro flow reactor (ref. 2) that consisted of a hypodermic tube 45 inches long and 0.02 inch inside diameter. The tube was coiled, heated electrically, and held inside a Dewar flask for heat insulation. All runs were made at one fixed inlet liquid flow rate.

Detailed descriptions of the design and operating procedure for this test equipment are given in an earlier report*.

*WADC-TR-59-327 Pt II. Vol. I. "Evaluation of Hydrocarbons for High Temperature Fuels," February 1962.

Table 1

BOILING POINTS AND PURITY OF SELECTED HYDROCARBONS

	Compound	Boiling Point, °F*	Estimated Minimum Purity, %	Vapor Phase Chromatogram Main Area, %	N of pon
	NAPHTHENIC HYDROCARBONS				
1.	Cyclohexane	177.3	99.9+	99.9+	
2.	Methylcyclohexane	213.6	99.9+	100	
3.	Ethylcyclohexane	267	99.9+	100	
4.	n-Propylcyclohexane	310	99.5+	99.5	
5.	n-Butylcyclohexane	353	99.9	99.9	
6.	Isopropylcyclohexane	306	98.4+	98.4	
7.	t-Butylcyclohexane	337	99.9	100	
8.	1-Ethyl-4-methyl	298	99.8	77.6	
9.	Diethylcyclohexane (mixed isomers)	346	99.8	44	
10.	1,3,5-Trimethylcyclohexane	281	99.8	63	
11.	1,2,4,5-Tetramethylcyclohexane	331	99.8	51	
12.	Decalin	386	94.9	81	
13.	2,3-Dimethyldecalin	435	99.9+	58.8	
14.	Ethyldecalin	438	98.7	64.5	
15.	Isopropyldecalin	466	99.9+	52.2	
16.	t-Butyldecalin	484	99.4	78.8	
17.	Hydrindan	332	99.8	87	
18.	Methylhydrindan	358	95.9	45	
19.	Ethylhydrindan	396	99.4	51	
20.	Isopropylhydrindan (distilled)	428	96	56	
21.	n-Propylcyclopentane	266	99.9+	99.9+	
22.	n-Butylcyclopentane	310	99.99+	100	
23.	Bicyclopentyl	372	98.9	98.9	
24.	Bicyclohexyl	-	99.2	99	
25.	Isopropylbicyclohexyl	542	99.6	45	
26.	Dicyclohexylmethane	486	99.98	99.9	
27.	1,3-Dicyclohexylbutane	574**	95.8	95.8	
28.	9-Ethyl-perhydro-anthracene	573**	99	99	
	PARAFFINIC HYDROCARBONS				
29.	n-Dodecane	414	99.5	99.5	
30.	Undecane, 3-methyl-	404	99.9	99.9	
31.	Decane, 2,9-dimethyl-	392	100	100	
32.	Nonane, 2,4,8-trimethyl-	384	98+	98	
33.	Nonane, 5-n-propyl-	388	99.9	99.9	
34.	Nonane, 2,2,8,8-tetramethyl-	396	99.9	99.9	
35.	n-Hexadecane	532	99.0	99.0	
36.	n-Nonadecane	-	97.4	97.4	

*Or 50% point of boiling range

**Estimated value (see ref. 1)

IV. THERMAL DECOMPOSITION OF SATURATED CYCLIC HYDROCARBONS

The objective of this study was to develop a general correlation between rate of decomposition and molecular structure from measurements of the rates of decomposition of various pure cyclic saturated hydrocarbons chosen to represent the major structural groups with varying degrees of substitution.

A. CALCULATION OF RATE CONSTANTS

For each hydrocarbon, a plot of the logarithm of the mole fraction of initial hydrocarbon remaining versus time showed roughly a straight line; i.e., the decomposition is a first-order kinetic process, to a first approximation. However, the first-order rate constant is a function of degree of conversion for a substantial fraction of the compounds studied. Table 2 summarizes the experimental results from the studies in the static test apparatus at 800°F. The first two columns of data give the range of per cent conversions studied and the number of runs made on each compound. The data scattered somewhat for a number of the compounds, so the results were analyzed statistically to determine whether or not the variation of first-order rate constant with conversion was significant. Two values of the rate constant were calculated, as shown in Table 2. The first is the average value for all the runs made. The second expresses the first-order rate constant in the form

$$k = k_o + Ax \qquad (1)$$

where x is the fractional conversion, k_o is the rate constant at zero conversion, and A is a constant. The values of the constants in this equation were determined from each set of data by the method of least squares. The F-test was then applied to judge whether the second expression fitted the data better than the use of an average value of k; i.e., whether k, indeed, varied significantly with conversion. The standard deviation from each of the two methods of representing k was calculated. In general, if the standard deviation from the average rate constant substantially exceeds that from the linear expression for k, the F-test is positive as shown in the table. If the number of experiments is very small, however, the standard deviation of the value of k from the linear expression may be substantially less than the standard deviation from the average value of k, and yet not make the F-test positive. This occurs, for example, with dimethyldecalin. Although the data strongly indicate a self-inhibition effect, the effect is not within the 95% confidence level. Borderline cases are designated by both a plus and minus sign. Where the effect of conversion on the first-order rate constant is significant, a positive value of A indicates self-acceleration of the reaction, and a negative value, self-inhibition.

Table 2

FIRST-ORDER DECOMPOSITION RATE CONSTANTS FOR NAPHTHENIC HYDROCARBONS
(Static Tests, 800°F)

Compound	Conversion Range, wt-%	No. of Experiments	Average Rate Constant k_{avg}, hr^{-1}	Rate Constant k, hr^{-1}	Standard Deviation From Avg. Rate Constant(%)	Standard Deviation From Linear Expression(%)	F Test
Cyclohexane	12-72	13	0.00944	0.00788 + 0.00432x	12.4	8.8	+
Cyclohexane, methyl-	7-50	17	0.0138	0.0112 + 0.094x	21.2	7.6	+
Cyclohexane, ethyl-	19-70	13	0.0558	0.0682 - 0.0028x	11.9	8.7	+
Cyclohexane, n-propyl-	25-55	7	0.0844	0.0658 + 0.0447x	10.1	9.0	-
Cyclohexane, n-butyl-	22-87	14	0.126	0.109 + 0.029x	13.1	13.1	-
Cyclohexane, isopropyl-	16-83	13	0.129	0.0986 + 0.0482x	15.1	13.4	±
Cyclohexane, tert-butyl-	28-80	15	0.127	0.187 - 0.096x	13.8	6.2	-
Cyclohexane, 1-ethyl-4-methyl-	15-71	15	0.0668	0.0645 + 0.0055x	9.8	10.0	-
Cyclohexane, diethyl-	14-89	11	0.135	0.169 - 0.063x	15.3	11.0	+
Cyclohexane, 1,3,5-trimethyl-	15-56	7	0.0312	0.0267 + 0.0097x	8.4	7.9	-
Cyclohexane, 1,2,4,5-tetramethyl-	17-75	4	0.0772	0.0722 + 0.0093x	27.2	32.8	-
Decalin	23-62	15	0.0431	0.0569 - 0.0349x	19.0	15.0	+
Decalin, dimethyl-	34-64	4	0.0582	0.124 - 0.139x	33.8	17.9	-
Decalin, 1-ethyl-	28-62	6	0.146	0.194 - 0.106x	12.9	11.8	-
Decalin, isopropyl-	21-83	26	0.161	0.260 - 0.161x	19.6	11.1	+
Decalin, 1-tert-butyl-	39-89	18	0.139	0.319 - 0.252x	28.8	8.2	+
Hydrindan	31-60	7	0.0559	0.0613 - 0.0120x	13.8	11.9	-
Hydrindan, methyl-	8-61	15	0.110	0.148 - 0.101x	21.5	17.7	+
Hydrindan, ethyl-	19-65	12	0.151	0.282 - 0.247x	7.6	3.8	+
Hydrindan, isopropyl-	42-80	6	0.314	0.429 - 0.172x	21.5	22.2	-
Cyclopentane, n-propyl-	12-48	10	0.104	0.104 - 0.003x	10.1	10.5	-
Cyclopentane, n-butyl-	7-60	16	0.132	0.043 + 0.259x	32.9	21.4	+
Bicyclopentyl	4-50	12	0.0768	0.0501 + 0.0889x	18.7	11.8	+
Bicyclohexyl	18-83	7	0.171	0.184 - 0.023x	19.6	18.0	-
Bicyclohexyl, isopropyl-	60-94	9	0.401	0.662 - 0.307x	26.9	26.9	-
Methane, dicyclohexyl-	51-89	8	0.260	0.314 - 0.069x	10.5	10.5	-
Butane, 1,3-dicyclohexyl-	51-93	6	0.644	0.877 - 0.302x	10.4	7.8	±
9-ethyl-perhydro-anthracene	35-82	6	0.355	0.538 - 0.278x	22.8	19.9	-

Cyclohexane and its derivatives were studied in greatest detail. Cyclohexane and its methyl derivatives showed self-acceleration, but the ethyl, di-ethyl, and t-butyl derivatives showed self-inhibition. With the other derivatives, little effect of conversion was noted. Decalin and all its homologs showed self-inhibition, even though the inhibition with the 1-ethyl and dimethyl derivatives did not lie within 95% confidence limits. All of the hydrindans seemed to show self-inhibition although the 95% confidence level was again found only for the methyl and ethyl derivatives. The n-butylcyclopentane showed a very rapid self-acceleration, but the n-propyl derivative did not. Bicyclopentyl showed rapid self-acceleration, but bicyclohexyl showed no effect of degree of conversion. With a few of the compounds studied, e.g., some of the cyclohexanes and the last four compounds in Table 2, the number of runs or the conversion range, or both, were insufficient to establish very clearly whether a significant effect of conversion on the reaction rate occurred.

Figures 1 and 2 show experimental data for two compounds in which self-acceleration and self-inhibition, respectively, are statistically significant. The straight lines through the experimental points were calculated by the method of least squares and the dotted envelopes give the 95% confidence limits of the experimental data. A complete sample calculation is given in the Appendix.

There are several reasons for the observed self-inhibition. In the decomposition of paraffin hydrocarbons (refs. 4,5,6,7,8,9), in which self-inhibition is generally observed, the cause is believed to be the formation of olefins, which are known to be good inhibitors of free radical reactions. With decalin and its derivatives, the starting "pure" material is a mixture of cis and trans isomers. During the decomposition, the cis-isomer is gradually converted into the more stable trans-isomer, as clearly shown by vapor phase chromatograms. Figure 3 shows this effect for 1-ethyl decalin; the starting material contained 35.2% trans- and 64.8% cis-isomer. The dashed line on Figure 3 shows the composition path that would be followed if the two isomers decomposed at the same rate. The real path shows that the concentration of trans-isomer (based on total material present, reactants and products) goes through a maximum with time, proving that isomerization from cis to trans isomer was occurring simultaneously with decomposition of both isomers. An approximate calculation showed that the cis-isomer decomposed about 2.5 times faster than the trans-isomer. Other mixtures of isomers would be expected to show the same effect.

B. ACTIVATION ENERGIES

When the reaction rate constant varies with degree of conversion, the most reliable value for the constant is usually that extrapolated back to zero per cent conversion. If the ratio of rate constants

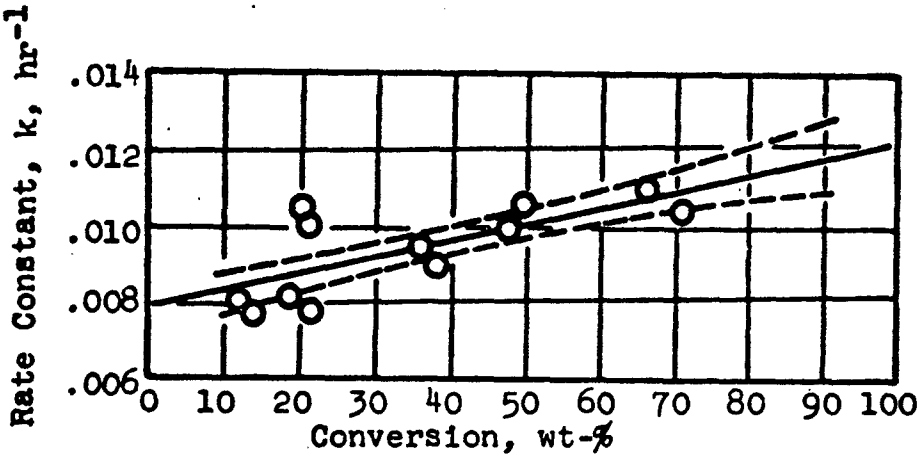

Figure 1. Rate Constant of Decomposition as a Function of Conversion for Cyclohexane at 800°F

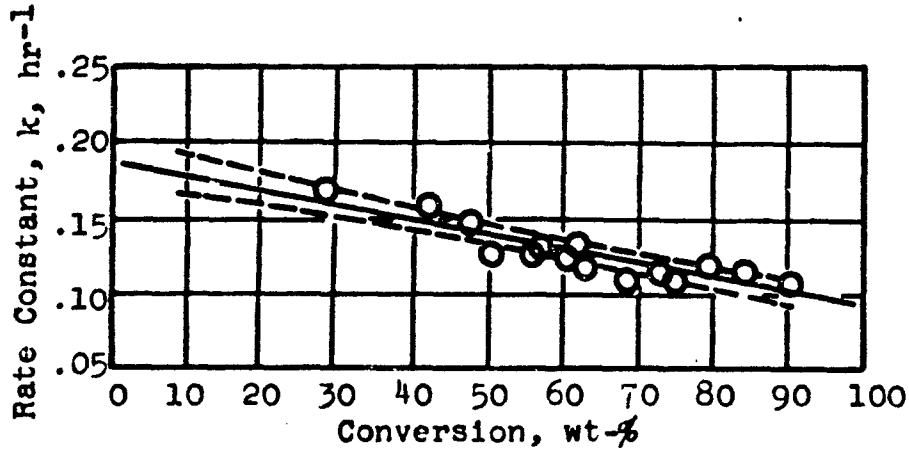

Figure 2. Rate Constant of Decomposition as a Function of Conversion of t-Butylcyclohexane at 800°F

1/2 FRAMES

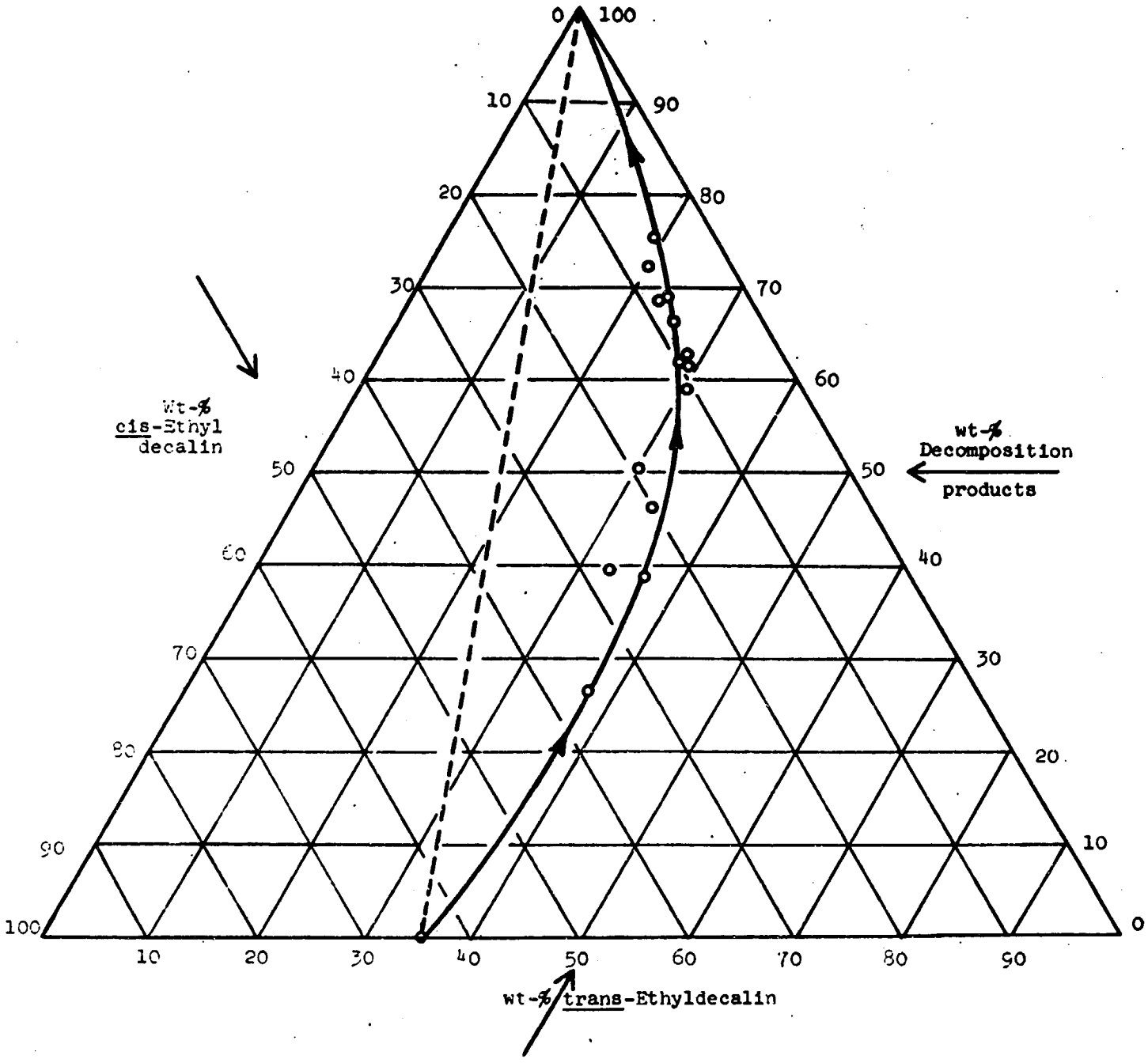

Figure 3. Concentration Change in the Decomposition of 1-Ethyldecalin at 800°F

at two temperatures is independent of degree of conversion, then the calculated activation energy will be independent also. This was found to be so in the present studies. If equation 1 is obeyed, and rate constant is plotted versus per cent conversion, the data points for each temperature will fall on a straight line, and the straight lines for each temperature will have a common intersection on the abscissa. Figure 4 shows such a plot for methylhydrindan, based on 15 experimental points at 800°F and 3 points each at 750 and 825°F, respectively. The corresponding activation energy is 59,600 cal/mole. Similarly, by studies at either 850 or 750°F, with the ethyl, isopropyl, butyl, diethyl, and 1,3,5-trimethyl derivatives of cyclohexane, activation energies between 59,500 and 63,500 cal/mole were found. Considering the accuracy with which the rate constants are known and the fact that only a 50 to 100°F temperature range was covered, the variation of activation energy with the nature of the derivative cannot be regarded as significant. An average value of 61,000 cal/mole adequately represents them all. The activation energies for cyclohexane and decalin are 63,300 and 64,300 cal/mole, respectively, on the basis of an extensive amount of data available as discussed below. The only activation energy found that differs significantly from the values of 60,000 to 65,000 cal/mole generally ascribed to hydrocarbon decomposition reactions was that for n-butylcyclopentane. On the basis of three runs at 750°F, sixteen runs at 800°F, three at 850°F, and two at 900°F, the activation energy was 48,000 cal/mole. However, the n-butylcyclopentane showed an unusually great increase in first-order rate constant with degree of conversion, so this unusually low apparent activation energy may reflect a different overall decomposition process.

Cyclohexane has been the most widely studied naphthenic hydrocarbon. Figure 5 shows the first-order decomposition rate constants of cyclohexane as compiled from the literature (ref. 10-16). It is not clear how the constants of Jost and Müffling (ref. 10) were calculated, so they are omitted from the plot. The data of Schultze and Wassermann (ref. 11) are based only on total pressure measurements. If we disregard Küchler's data (ref. 13), since his rate constants at the higher temperature were based on conversions of only 0.6 and 4 wt-%, the remaining data fall on two straight lines and agree quite well with each other; the lower line represents studies at sub-atmospheric pressure, and the upper line, elevated pressures, primarily in the 400-500 psig pressure range. The equations of these lines are:

$$\text{at low pressures:} \quad \log k = 17.332 - 24.916 \times 10^3 (1/T) \qquad (2)$$

$$\text{at high pressures:} \quad \log k = 17.818 - 24.916 \times 10^3 (1/T) \qquad (3)$$

where T is expressed in °R, and the corresponding activation energy is 63,300 cal/mole in both pressure regions.

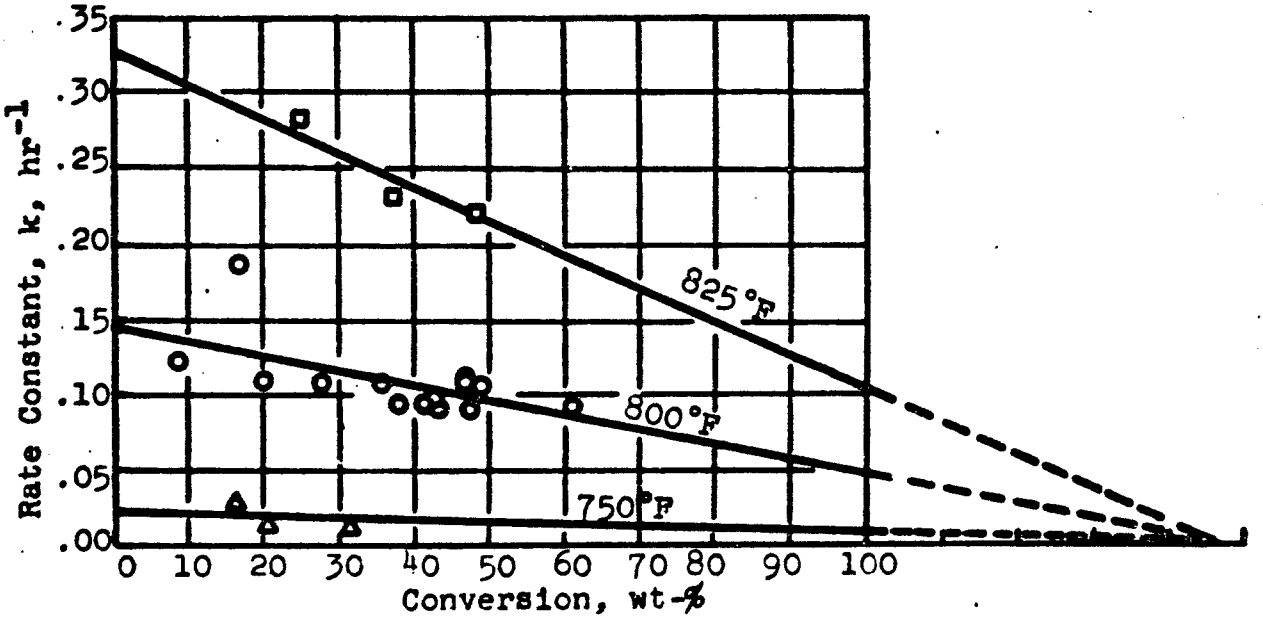

Figure 4. Rate Constants of Decomposition as a Function of Conversion and Temperature for Methylhydrindan

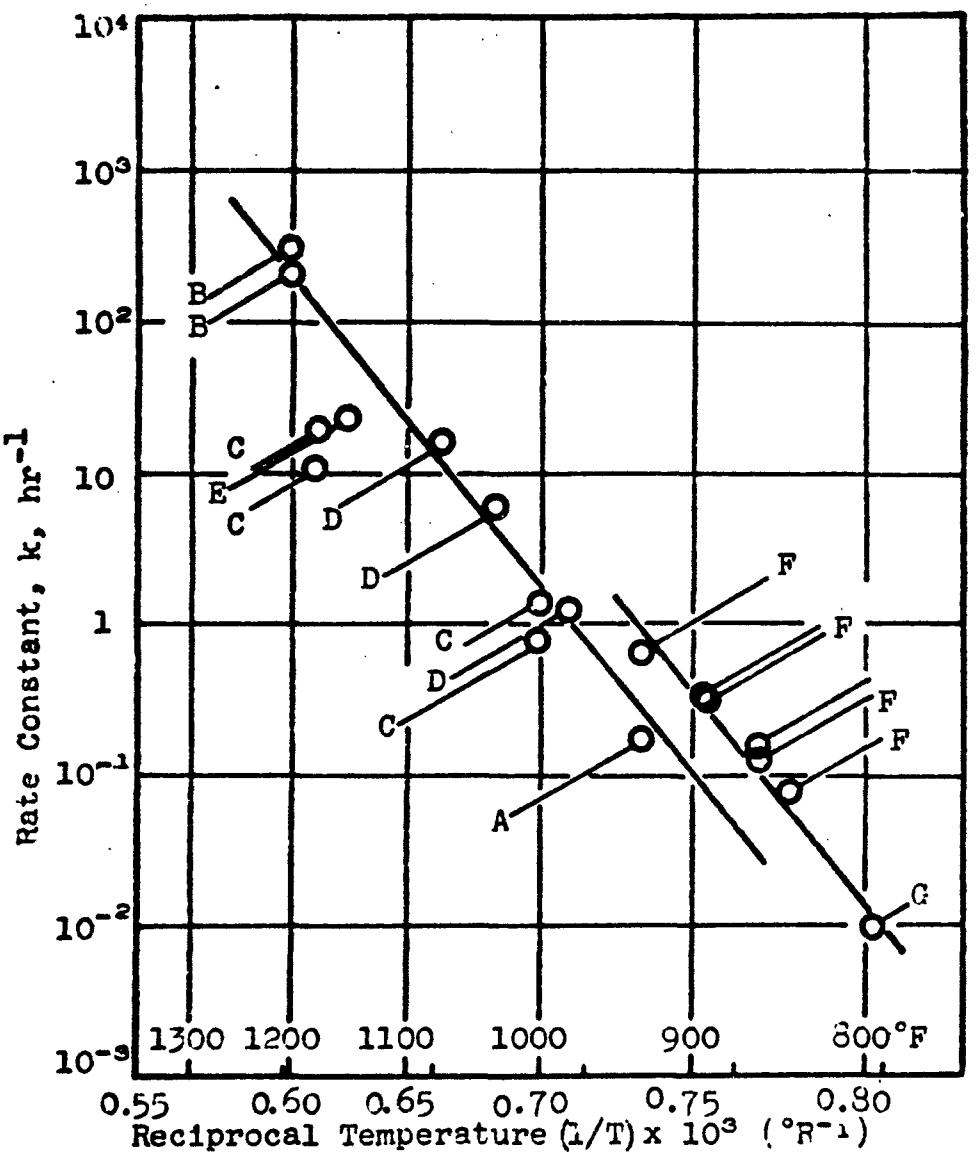

		Conversion, wt-%	Pressure, atm
A	Schultze and Wasserman	-	~1
B	Kasansky and Plate	27-67	1
C	Küchler	0.6-25	1
D	Pease and Morton	-	1
E	Frey	24	1
F	Bachman et al.	10-55	28-33
G	Present data (13 expts)	12-71	130

Figure 5. Arrhenius Plot for Cyclohexane

Some of the earlier compilations of data on rate constants of hydrocarbon decomposition may contain values greatly in error.

C. EFFECT OF PRESSURE ON DECOMPOSITION RATE

In the sealed glass tubes, pressure increased as the hydrocarbon decomposed since the products are of lower average molecular weight than the starting material. The pressure to which the hydrocarbon was initially subjected at the reaction temperature and the change in pressure with degree of reaction depended upon the ratio of liquid-to-void volume in the filled but unheated tube. This ratio had to be kept fixed in order to obtain reproducible results if the first-order rate constant was affected by pressure.

The effect of pressure on decomposition rate was studied in some detail with t-butylcyclohexane with results shown in Table 3. Studies were made in the conventional glass tubes at a series of ratios of liquid-to-void volumes in order to vary the pressure. Three experiments were made in the high pressure isoteniscope that permitted pressure measurements to be made during the decomposition process. For each experiment, the initial pressure was calculated from an estimated value for the compressibility. Table 3 shows that these were in very good agreement with the measured pressures in isoteniscope experiments, except for that with the smallest void volume, which showed a significant deviation.

For each experiment, both the first-order rate constant of decomposition and the initial rate constant of decomposition for zero conversion were calculated from the equation given in Table 2.

$$k = k_o - 0.0959x \qquad (4)$$

Figure 6 shows the initial rate constants as determined from these studies as a function of calculated pressure. The diagram confirms our earlier studies, which showed that essentially no differences are observed between decomposition rates of hydrocarbons on contact with Pyrex glass and in contact with 304 stainless steel. The horizontal arrows in the figure indicate the initial and final pressure in the isoteniscope experiments. It is seen that over the pressure range studied (roughly 400 to 1000 psig), the first-order initial rate constant increased exponentially with pressure. The equation of the line is

$$\log (k_o \cdot 10^2) = 0.583 + 0.886 \times 10^{-3} P \qquad (5)$$

where P is expressed in psia. According to this plot, the initial rate of decomposition doubled for a pressure increase in this range of about 340 psi. An increase in first-order rate constant with pressure is found for the decomposition of hydrocarbons in general.

Table 3

THE EFFECT OF PRESSURE ON THE DECOMPOSITION OF t-BUTYLCYCLOHEXANE AT 800°F

Liquid Volume at 70°F, vol-%	Pressure Calculated, psi	Isoteniscope Studies Pressure Measured		Conversion, wt-%	k_{avg}, hr^{-1}	k_o, hr^{-1}
		Initial, psi	Final, psi			
12.5	395			29.6	0.0585	0.0869
13.1	397	400	600	25.0	0.0575	0.0815
18.8	501			38.0	0.0797	0.116
25.0	552			38.0	0.0797	0.116
26.3	561	555	980	30.5	0.0809	0.110
31.3	622			47.0	0.106	0.151
37.5	701			48.9	0.112	0.159
39.5	767	655	1510	26.0	0.151	0.176
43.8	935			49.5[a]	0.114	0.163
40.5	777			-	-	0.187

[a] Uncorrected for gas loss

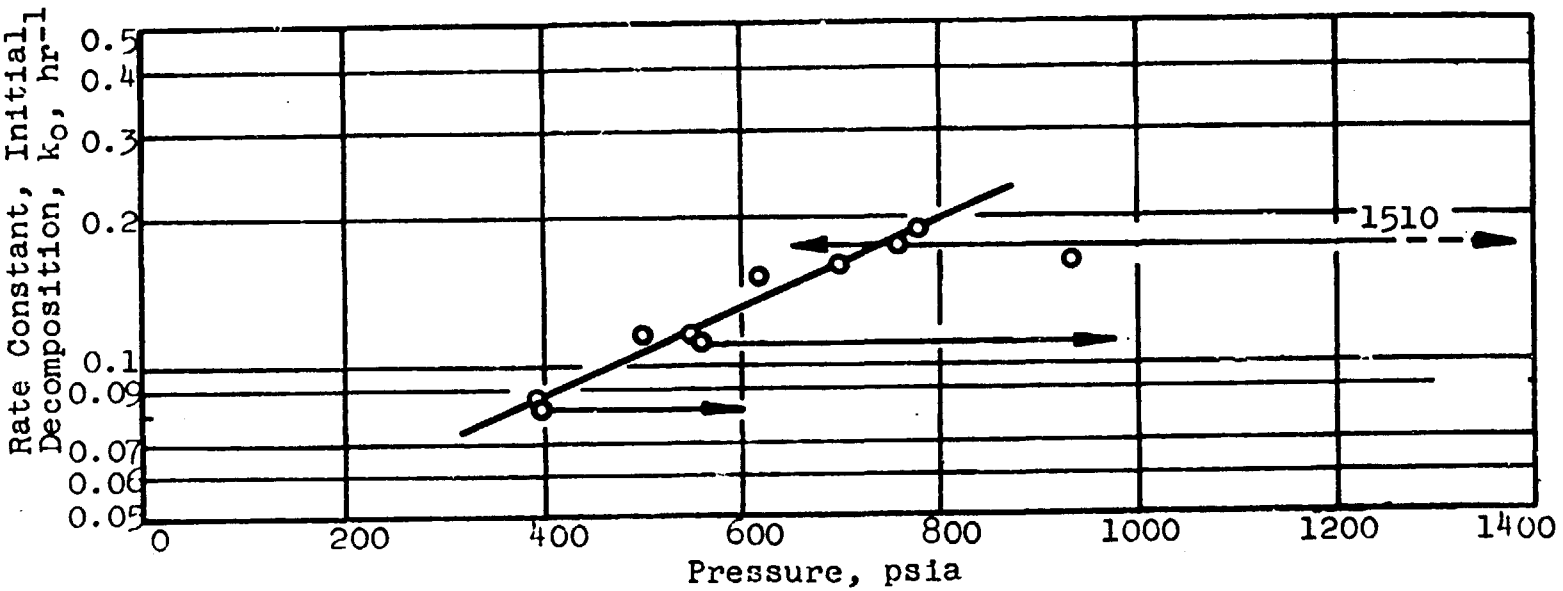

Figure 6. The Effect of Pressure on the Rate of Decomposition of t-butylcyclohexane at 800°F

The above result implies that in the standard glass tube experiment in which the pressure increases with per cent conversion, the amount of reactant found to remain at high per cent conversion should be less than that predicted from the first-order rate consta obtained from data at lower conversions. The opposite actually occurred with butylcyclohexane. It is clear that in the standardiz tube experiment, two opposing effects were at work. The decrease i rate constant with conversion, for reasons previously discussed, wa counteracted by the increase in rate constant caused by the pressur increase. Whichever effect predominated determined whether a so-called self-acceleration or self-inhibition was observed. A net accelerating effect was found here with only a few of the monocycli hydrocarbons. With polycyclic naphthenic hydrocarbons, in general, the opposite effect was observed.

Another factor that may affect the comparison of rate of decomposition of related compounds was the phase condition during the reaction. For most compounds, including all of the cyclohexane derivatives, the reaction temperature of 800°F was above the critical temperature. The decalin derivatives, however, all have estimated critical temperatures above 800°F, which, if true, means that a mixed phase was present during reaction with possibly different rates occurring in the two phases.

A batch reactor such as a sealed tube is useful and reliable in measuring reaction rates when the rate of reaction is sufficiently slow that temperature and other transients at the beginning and end of the run are relatively unimportant. In contrast to the situatior in flow reactors, all the material present is known to be subjected to the reaction temperature for the same time, and generally isothermal conditions are achieved. Pressure changes during reaction may introduce some uncertainty in interpretation, as discussed above and there always remains the possibility of interaction between products and reactants. To make studies at higher temperatures and correspondingly faster rates requires the use of a flow method. This also provides a means of checking on the validity of the batch studies.

However, three principal uncertainties may be encountered in obtaining and interpreting kinetic data in a flow system. First, if the reaction is substantially endothermic or exothermic, temperature gradients may exist both axially and radially. This factor was essentially eliminated in our work by the use of an extremely small diameter reactor (0.02 inch) (see Section VIII).

The second uncertainty concerns the flow and mixing pattern in the reactor. In a tubular reactor, plug flow is generally assumed although, in fact, major departures from this assumption frequently occur. The effect was analyzed for our reactor using the recently published correlations of Levenspiel (ref. 17). Under typical

reaction conditions, the Reynolds number here was about 100, and the Schmidt number about 2. The intensity of dispersion, D/ud, (reciprocal of the axial Peclet number) was about 1 (where D is the diffusivity, u the linear velocity, and d the tube diameter), and the reactor dispersion number, (D/ud)(d/L), where L is reactor length, was about 0.00052. From the correlations of Levenspiel, such a reactor would be expected to behave in identical fashion to a plug flow reactor. In qualitative terms, the plug flow behavior of our micro reactor was due to the low Reynolds number and the extremely high length-to-diameter ratio.

The third possible uncertainty occurs if there is a change in number of moles during reaction. To determine true residence time it is then necessary to have a complete analysis of reaction products as a function of degree of conversion.

Decalin was studied in the micro flow reactor at a series of temperatures between 1000 and 1100°F and at a pressure of 500 psig, to obtain kinetic data on a hydrocarbon over a wider temperature range. The results are shown in the form of an Arrhenius plot in Figure 7, which also includes data from the static tests and other sources. Tilicheev (ref. 18) measured the rate of decomposition in the 425-500°C (797-932°F) temperature range, and one experimental point is given by Malinovsky and Stoyanovskaya (ref. 19), but their residence time is not clearly defined. A number of rate constants can be calculated from Sundgren's work (ref. 20), but he was not primarily interested in obtaining kinetic data, and there is some uncertainty in our interpretation of his work. Recently reported data on cracking of cis-decalin (ref. 15) in a static apparatus are also included. The rate constant of decomposition can be expressed as

$$\log k = 18.649 - 25.298 \times 10^3 (1/T) \qquad (6)$$

where T is expressed in °R. The activation energy is 64,300 cal/mole. As with cyclohexane, the first-order rate constant appears to increase with pressure although the effect cannot be evaluated quantitatively from the available data.

The agreement between the two different methods of measuring kinetic constants gives confidence in the validity of both method and data. The constant pressure of 500 psig used in the flow reactor was close to the average occurring in a typical batch study. The studies with decalin correspond to conversions up to 30%, so no correction was made in analyzing these data for the change in number of moles on reaction.

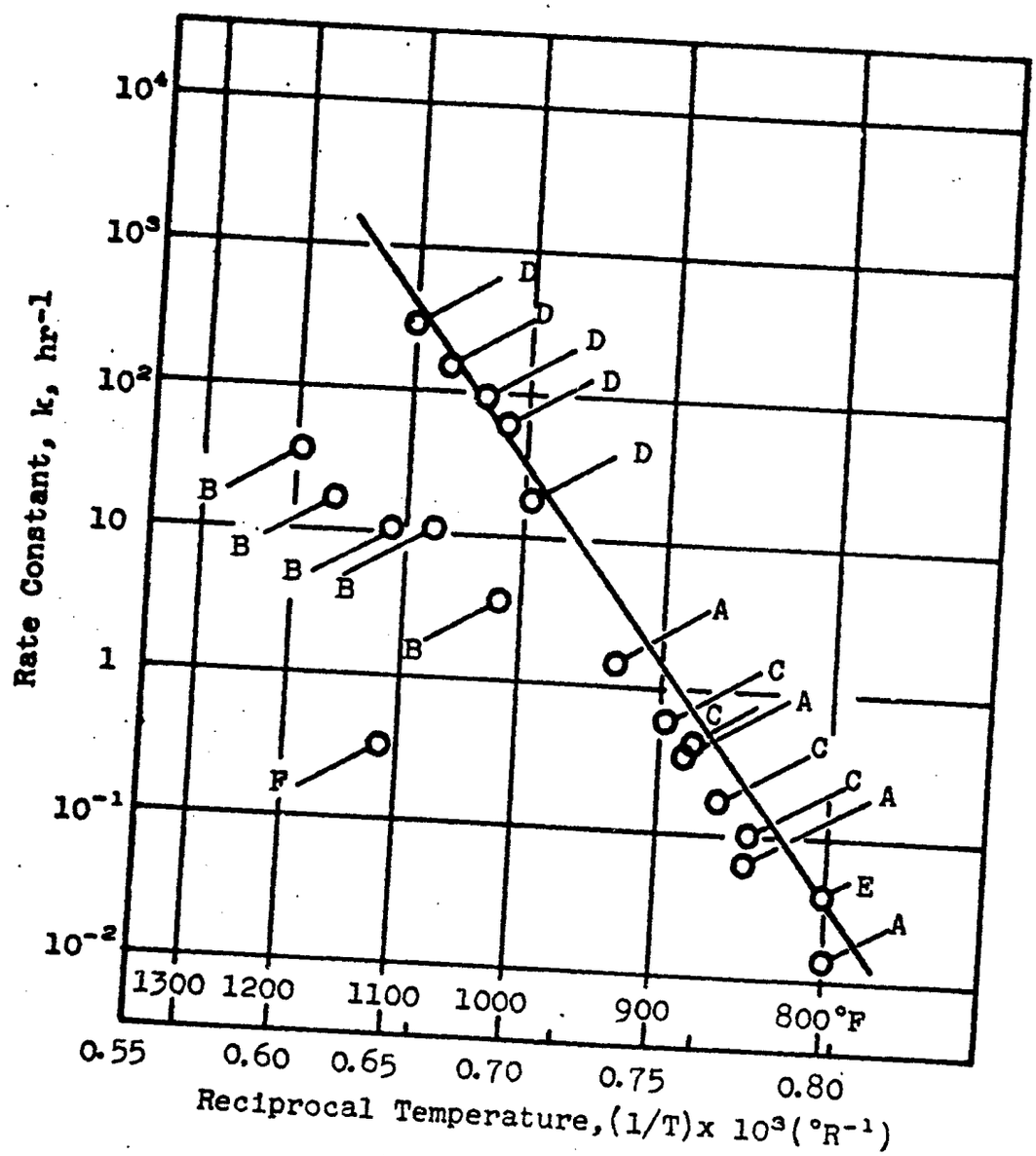

		Conversion, wt-%	Pressure atm
A	Tilicheev (ref. 18)	8-96	40
B	Sundgrén (ref. 20)	18-99	1
C	Bachman et al. (ref. 15)	10-32	33-47
D	Dynamic expts.	15-90	35
E	Static expts.	24-62	40
F	Malinovsky et al. (ref. 19)	12	1

Figure 7. Arrhenius Plot for Decalin

D. ESTIMATION OF RATE CONSTANT OF DECOMPOSITION

Table 2 shows that the rates of decomposition varied widely. The most stable compounds were the non-substituted rings; within each set of derivatives the rates increased with number and size of substituent groups. A simple empirical group contribution method was developed to correlate the decomposition rate data and permit estimation of rates for unknown cyclic saturated hydrocarbons. The basic assumption was that the rate was determined by the kind of bonds present and that it was proportional to the number of bonds of a given type. Each molecular structure is represented by a characterization number, n, which consists of (1) the characterization number of the basic ring compound minus one for each substituent that replaces a C-H bond in the unsubstituted ring, plus (2) the sum of the characterization numbers for any side chains present. From the above sums, a slight correction is subtracted for bicyclics and tricyclics.

The characterization number of the basic ring compounds is taken equal to the number of C-H bonds, except for decalin, for which the n value was empirically adjusted to 14. These values are therefore as follows:

	n
Cyclopentane	10
Cyclohexane	12
Hydrindan	16
Decalin	14
Perhydroanthracene	24

The characterization numbers for side chains and corrections for separated polycyclics are as follows:

	n
CH_3	+2
CH_2	+4
CH	+6
C	+4
C (in ring)	+4
Bicyclics (separated)	-1
Tricyclics (separated)	-2

Examples of the calculation of the characterization number are given below:

n-Propylcyclohexane	n
Characterization number of the ring = 12-1	11
2 CH_2 groups = 2 x 4	+8
CH_3 group	+2
n =	21

Isopropyldecalin	
Characterization number of the ring = 14-1	13
CH group	+6
2 CH_3 groups = 2 x 2	+4
n =	23

Dicyclohexylmethane	
n for two rings = (2 x 12) - 2 =	22
CH_2 group	4
Correction	-1
n =	25

A plot of the rate constant as a function of the characterization number is shown in Figure 8. Very few compounds deviated from the line, the equation of which is

$$k = 0.044 - 0.114n + 0.0008n^2 \qquad (7)$$

Since the characterization number increases by 4 units for the next member in a series of homolog compounds, the precision of this graph is always within this range. This means that the error of an estimated rate constant is smaller than the differenc between the rate constants for two consecutive members of the given series. Figure 8 should be useful for estimating rate data for a variety of naphthenes and other saturated cyclic hydrocarbons. It does not apply to paraffins and probably becomes less reliable for alkyl side chains exceeding C_4 in length.

E. RATE OF PARTICLE FORMATION

The rate of particle formation in the static experiments was expressed as reciprocal of the induction period, in hours, until initial particle formation. In our previous results, a simple expression was obtained for the rate constant of particle formation k_P

$$k_P = ak_D \qquad (8)$$

where a is a constant for a homologous series of cyclic compounds and k_D is the rate of decomposition at 50% conversion.

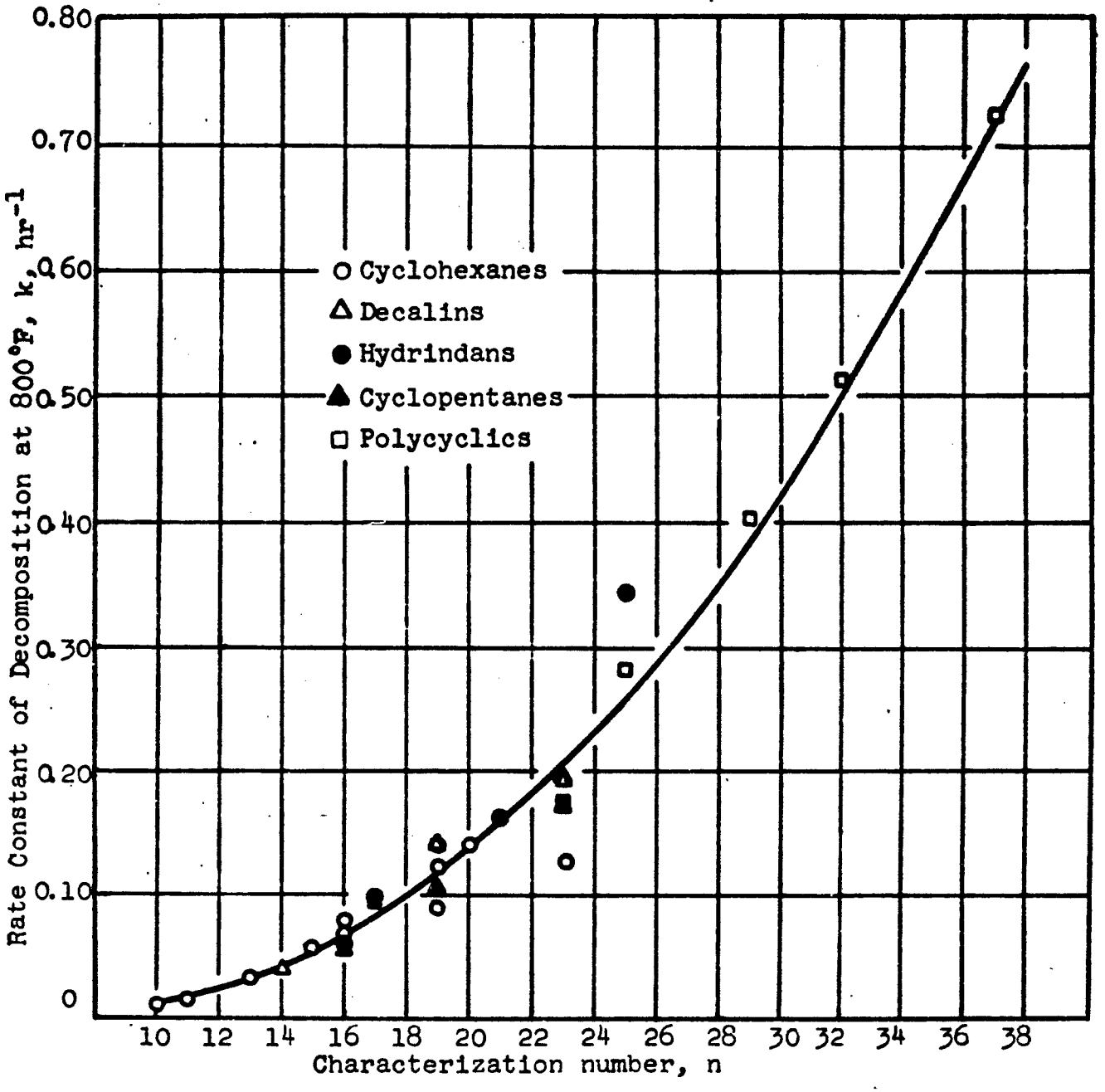

Figure 8. Rates of Decomposition of Naphthenic Hydrocarbons at 800°F

The average "a" values are:

Cyclohexane derivatives	1.37
Decalin derivatives	0.78
Cyclopentane derivatives	1.98
Hydrindan derivatives	1.70
Separated polycyclics	0.36

Usually, methyl derivatives show an exceptionally high a value; isopropyl and t-butyl derivatives show a lower a value than the average of the group.

These data show that condensed bicyclics are more stable if we compare

decalin and cyclohexane
hydrindan and cyclopentane

but, at the same time, six-membered rings are much more resistant to particle formation than five-membered rings. Although the separated polycyclics show a very attractive a value, their rate of decomposition is so high as to limit their application as fuels or fuel components.

This investigation clearly points to the decalin and cyclohexane derivatives as stable fuels, eliminating, more or less, other cyclic structures as potential fuel candidates.

V. THERMAL DECOMPOSITION OF PARAFFINIC HYDROCARBONS

A. EXPERIMENTAL RESULTS

The decomposition of paraffinic hydrocarbons was a pseudo-first order process under our experimental conditions. In the static test apparatus, all materials were at 800°F in vapor phase, with the exception of n-hexadecane and n-nonadecane, which were present as a liquid and a vapor at 800°F and at the vapor pressure corresponding to that temperature. Most of our decomposition experiments were carried out at an initial void volume in the tube of 60%, but several runs were also carried out with different void volumes to determine the effect of pressure on the rate of decomposition.

No change of the rate constants of decomposition with increasing conversion was observed in the decomposition of paraffinic hydrocarbons, which indicates that the decomposition of paraffinic hydrocarbons is a first-order kinetic process without any self-accelerating or inhibiting effects.

The experimentally determined rate constants are summarized in Table 4, giving the number of experiments, the conversion range investigated in wt-%, the average rate constant in hr^{-1}, and the deviation from the average. In those experiments where the amount of liquid hydrocarbon introduced into the glass tube was varied, the initial pressure was calculated from the equation of state of real gases. Since the experimental conditions were quite close to the critical temperature and pressure, these pressures can be considered only as an approximation of the pressure in the system.

The second column of the table gives the void volume, or per cent of vapor phase at room temperature (70°F). The third column gives the volume per cent of the vapor phase at reaction temperature (800°F) at the beginning of the decomposition.

Figure 9 compares the experimentally determined rate constants with the data calculated by two equations for the rate constants of n-paraffins.

Tilicheev's equation (ref. 21) gives the rate constants as a function of carbon atom number at 425°C (797°F) as

$$k = (2.3n-15.6) \times 10^{-5} \text{ sec}^{-1} \qquad (9)$$

Voge and Good (ref. 22) give the same equation at 500°C (932°F) as

$$k = (n-1)(1.57n-3.9) \cdot 10^{-5} \text{ sec}^{-1} \qquad (10)$$

Both equations were used to calculate the rate constants as a function of carbon atom number. The results were adjusted to 800°F, with an activation energy of 60,000 cal/mole and are given in Figure 9.

As can be seen from Figure 9, the measured rate constant for

Table 4

RATES OF DECOMPOSITION (hr^{-1}) OF PARAFFINIC HYDROCARBONS

Phase Conditions	Compound	Void Volume At 70°F, %	Void %**	800°F n	800°F Pressure, psig	800°F Conversion Range, wt %	800°F k, hr^{-1}	750°F n	750°F Pressure, psig	750°F Conversion Range, wt %	750°F k, hr^{-1}	700°F n	700°F Pressure, psig	700°F Conversion Range, wt %	700°F k, hr^{-1}
Homogeneous Vapor Phase	n-dodecane	60		5		41-88	0.469 ± 0.025	5		9-70	0.0614 ± 0.0031				
	undecane, 3-methyl-	60		6		39-84	0.463 ± 0.025								
	decane, 2,9-dimethyl-	80		2	309	58-75	0.444 ± 0.008	2	270	31-34	0.0725 ± 0.0088	1	242	17	0.0127
		60		2	434	42-80	0.503 ± 0.022	6	355	23-82	0.0315 ± 0.0060	3	289	36-64	0.0145 ± 0.0006
		40		2	595	47-68	0.579 ± 0.015	2	459	18-36	0.0779 ± 0.0138	1	351	19	0.0134
	nonane, 2,4,8-trimethyl-	80		2	315	42-50	0.493 ± 0.058	3		24-54	0.129 ± 0.004	3	239	30-53	0.0226 ± 0.0008
		60		7	440	45-83	0.637 ± 0.022					1	324	30	0.0150
		40		4	612	44-88	0.792 ± 0.046								
	nonane, 5-n-propyl-	47		2	569	52-88	0.618 ± 0.153								
		60		6	1074	54-83	0.887 ± 0.071								
	nonane, 2,2,8,8-tetramethyl-	60		6		31-66	0.323 ± 0.012	5		12-67	0.0412 ± 0.0042	2*		43-55	0.549 ± 0.020
Two Phase Conditions	n-hexadecane	86.7	81.5	5		43-76	0.510 ± 0.042								
		80	69.8	2		46-81	0.621 ± 0.004								
		73.3	58.1	2		45-86	0.632 ± 0.022								
		66.7	46.5	2		46-91	0.606 ± 0.010								
		60	34.8	24		48-95	0.709 ± 0.058	3		9-35	0.116 ± 0.013				
		53.3	23.2	2		49-91	0.671 ± 0.002								
	n-nonadecane	60		3		55-90	0.765 ± 0.002	3		21-55	0.101 ± 0.021				

*325°F

**Void per cent or per cent of vapor phase at 500°F

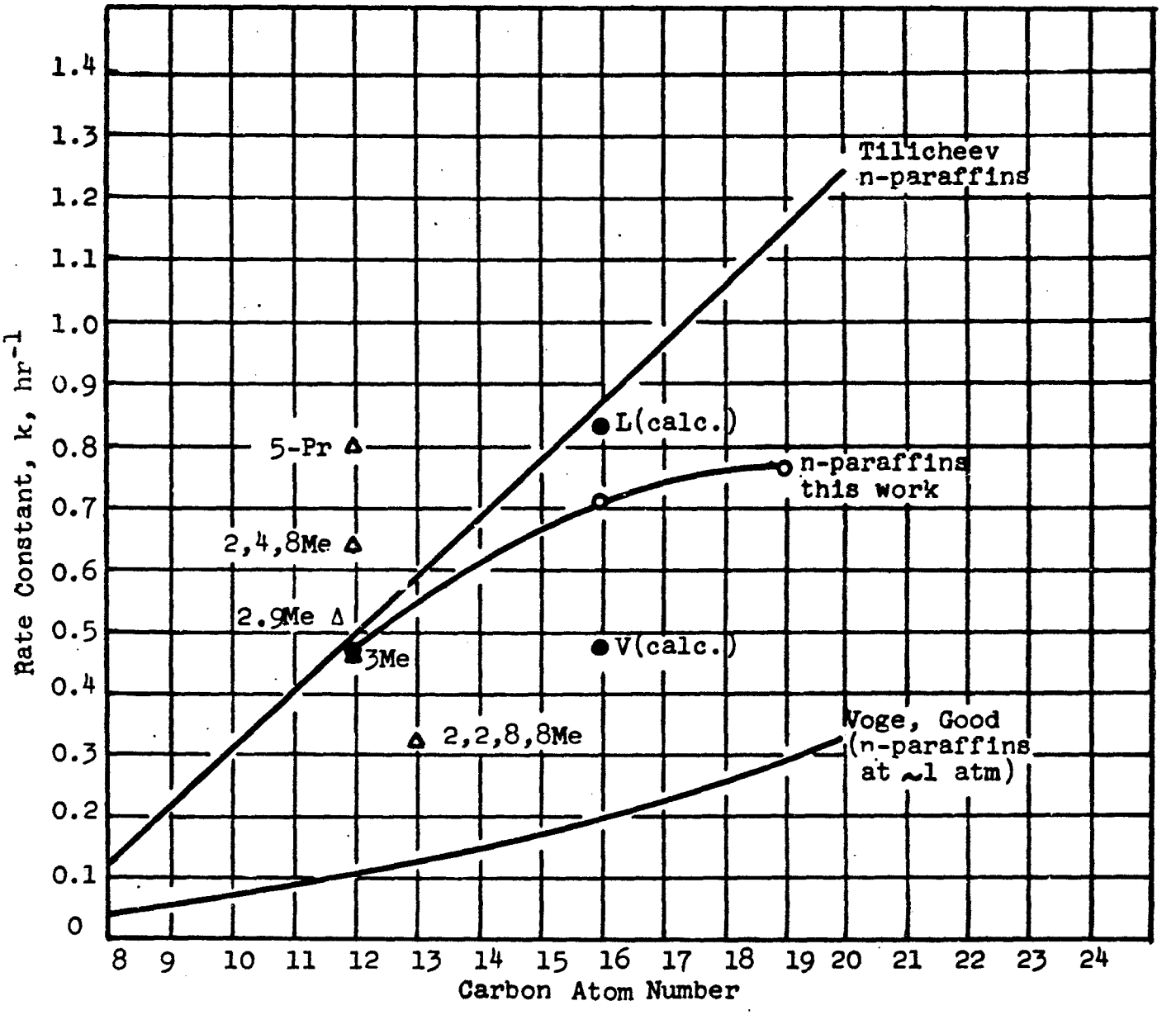

Figure 9. Rates of Decomposition of Paraffinic Hydrocarbons at 800°F

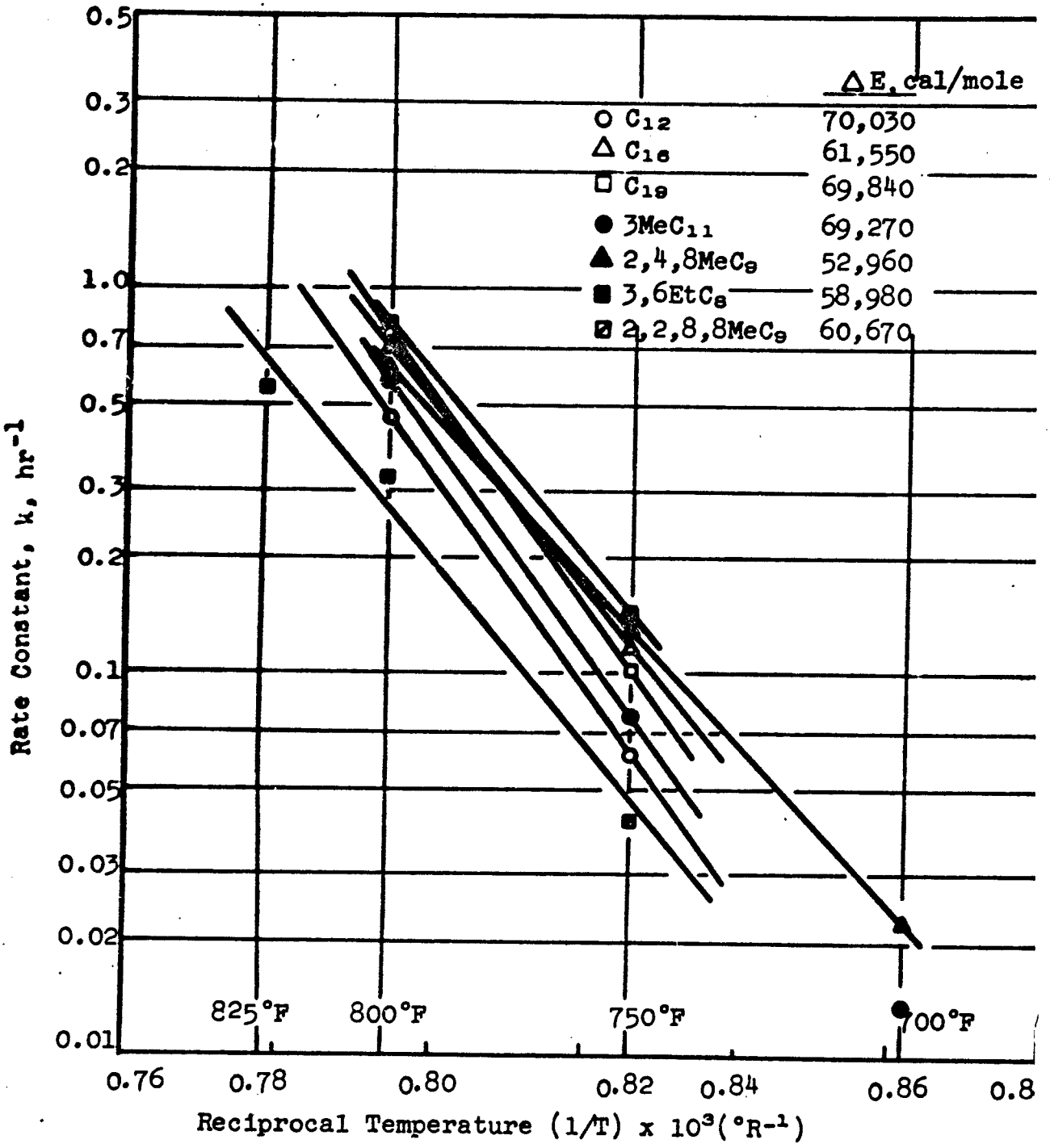

Figure 10. Activation Energies of Paraffinic Hydrocarbons

dodecane agrees very well with Tilicheev's curve; the experimental rate constants for hexadecane and nonadecane deviate more and more from Tilicheev's values. This deviation was partly explained earlier in the discussion of the effect of pressure on the rate constants of decomposition of saturated cyclic hydrocarbons.

B. ACTIVATION ENERGIES

From the experimental data, the Arrhenius plot given in Figure 10 was prepared. The activation energies are in the range of 53-70 kcal/mole. These activation energies can also be calculated from the tabulated data given in Table 4, according to the Arrhenius equation,

$$E = \frac{2.3R}{\frac{1}{T_1} - \frac{1}{T_2}} (\log k_2 - \log k_1) \qquad (11)$$

If we disregard completely the error in temperature measurement, and consider that the entire error of the determination is represented by the tabulated average deviations, the error of the activation energy can be calculated. The partial derivatives of the equation on the assumption that k_1 or k_2 are the only variables are:

$$\frac{\partial E}{\partial k_2} = \frac{2.3R}{\frac{1}{T_1} - \frac{1}{T_2}} \frac{1}{k_2} \qquad (12)$$

and

$$\frac{\partial E}{\partial k_1} = \frac{2.3R}{\frac{1}{T_1} - \frac{1}{T_2}} \left(-\frac{1}{k_1}\right)$$

and the error is

$$\Delta E = \frac{2.3R}{\frac{1}{T_1} - \frac{1}{T_2}} \left(\frac{\Delta k_2}{k_2} - \frac{\Delta k_1}{k_1}\right) \qquad (13)$$

and the maximum error is

$$\Delta E = \frac{2.3R}{\frac{1}{T_1} - \frac{1}{T_2}} \left(\frac{\Delta k_2}{k_2} + \frac{\Delta k_1}{k_1}\right) \qquad (14)$$

Using the data for n-dodecane

$T_2 = 800°F$ $\quad k_2 = 0.469 \pm 0.025$

$T_1 = 750°F$ $\quad k_1 = 0.0614 \pm 0.0031$

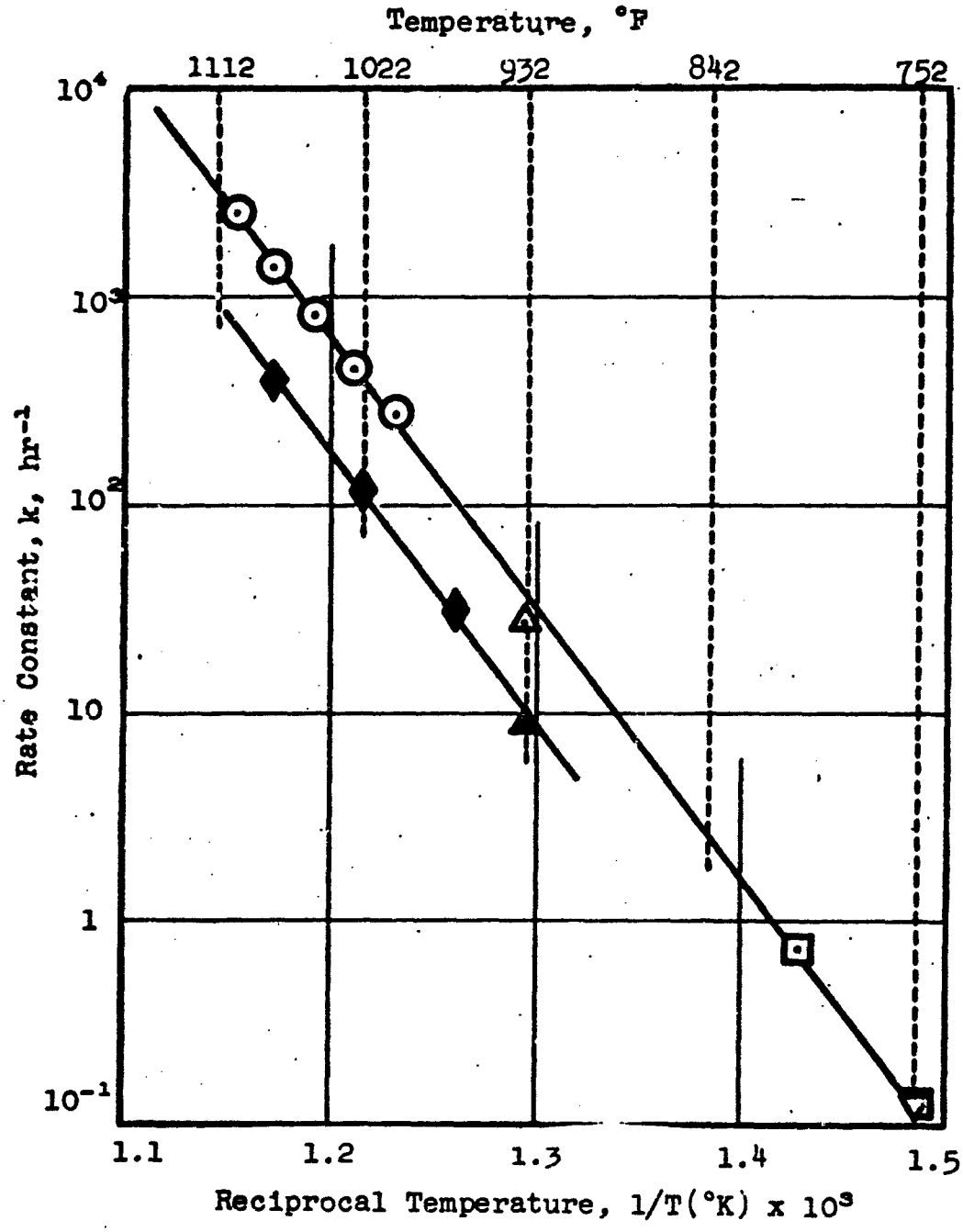

	Pressure, atm
○ Fabuss, et al. (ref. 3)	35
△ Voge and Good (ref. 22)	21
□ Fabuss, et al. (ref. 23)	6-10
▽ Tilicheev and Zimina (ref. 24)	6
◆ Panchenkov and Baranov (ref. 25)	1
▲ Voge and Good (ref. 22)	1

Figure 11. Rate Constants of Thermal Cracking of n-Hexadecane

$$\Delta E = \frac{4.5678}{\frac{1}{1210} - \frac{1}{1260}} \left(\frac{0.025}{0.469} + \frac{0.0031}{0.0614}\right) =$$

$$139.555(0.0533 + 0.0505) = 5 \text{ Btu/lb-mole} = 8.032 \text{ cal/mole}$$

This result indicates that while the precision of the rate constants is about 5%, which is excellent for kinetic measurements of this kind, the deviations may add up to give an error in the activation energy of as much as 13% or more. The situation improves only when measurements are made over a much wider temperature range, but this implies the use of different decomposition methods. The error can also be decreased by determining the rate constants at a series of temperatures.* For this reason, not too much significance should be assigned to the activation energy values given in Figure 10. The average value of the measured activation energies is 63,000 cal/mole.

The Arrhenius plot in Figure 11 shows good agreement among studies by four different investigators in both batch and flow reactors covering a temperature range of 350°F. The activation energy is 59,700 cal/g-mole ± 150 cal/g-mole standard deviation. The rate constant for 427°C and 1 atmosphere pressure agrees very closely with the Voge and Good correlation. Similar plots were prepared for each hydrocarbon but the available data are less complete and scatter much more. The data of C_{12} indicate values roughly double those of the Voge and Good correlation, but the results are much more fragmentary than those for cetane. Data on C_8, C_{14} and C_{20} were obtained at elevated pressures and exceed those predicted by the correlation.

The Voge and Good correlation remains as the best representation of first order kinetic constants at atmospheric pressure. Figure 12 shows rate constants as a function of temperature for n-paraffins from C_4 to C_{20} and may be used for each calcuation. A constant activation energy of 60,000 cal/g-mole is used.

C. EFFECT OF BRANCHING ON THE RATE OF DECOMPOSITION

Unfortunately, only scattered data are available in the literature about the decomposition of branched chain paraffinic hydrocarbons. A summary is given in Table 5, which gives the structure of the isoparaffinic hydrocarbon in an abbreviated form, the temperature range investigated, the reference, and the ratio of the rate constant of the isoparaffin to that of the corresponding n-paraffin. The most complete investigation in this field, on isomeric dodecanes and hexadecanes, was carried out at 500°C by Terres and Gropenbacher (ref. 26) on a chromia-cracking catalyst (Chromperbespaltkatalysator of Kali-Chemie A.G., Hannover, Germany).

* The activation energies previously given for naphthenic hydrocarbons are estimated to be in error by ± 5%.

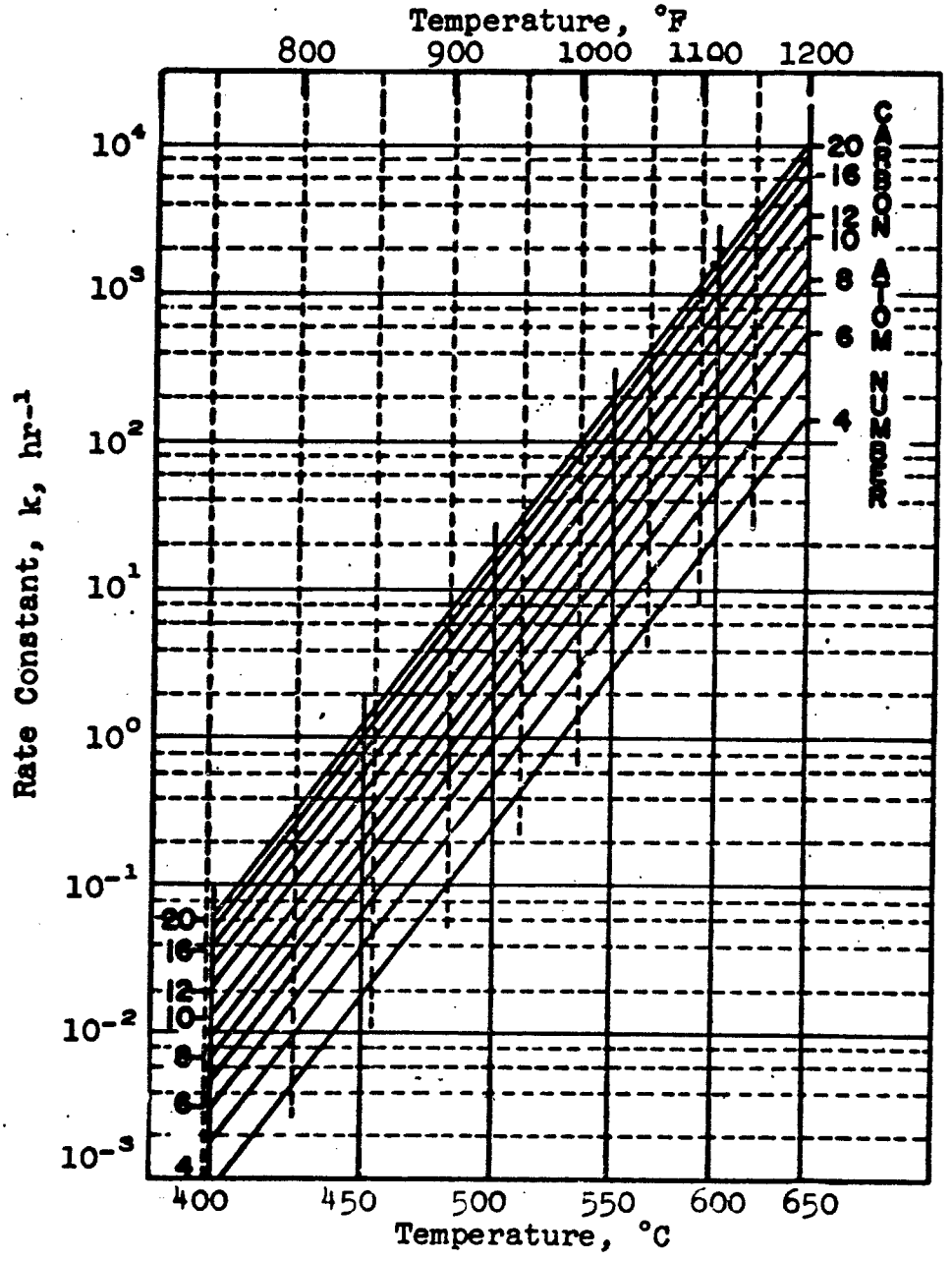

Figure 12. Rate Constants of Decomposition of n-Paraffins

Their results are included in Table 5, although they are not strictly comparable to the thermal cracking studies.

In Table 5, five branched chain hydrocarbons show a lower rate of decomposition than the corresponding n-paraffin hydrocarbon. All these compounds contain in their structure one or more quaternary carbon atoms. This suggests a comparison of the relative rate of decomposition with the relative rate of free radical formation. According to Rice and Kossiakoff, the relative rates of free radical formation by abstraction of a hydrogen atom from a primary, secondary, or tertiary carbon atom at 600°C is about 1:3.2:10.3. Using these values, the relative rate of free radical formation from the branched chain hydrocarbons and straight chain hydrocarbons was calculated and shown as (r_i/r_n) in Table 5. For each compound the calculated rate is taken to be proportional to the number of C-H bonds present of each type, multiplied by the relative rate of abstraction as given by the above ratio.

Table 5 shows general correspondence between the observed relative rates of decomposition and the predicted relative rates of hydrogen abstraction. The essential effects of isomeric structures on decomposition rates are as follows:

(1) The presence of a quaternary carbon atom decreases the rate of decomposition compared to that of the n-paraffin by 50 per cent or more.

(2) The presence of a tertiary carbon atom increases the rate of decomposition by as much as 40 per cent over that of the corresponding n-paraffin.

(3) If both a quaternary and a tertiary carbon atom are present, the effect of the quaternary carbon atom is predominant and the rate of decomposition is decreased over that of the corresponding n-paraffin.

(4) The deviations from this behavior in the case of some of the dodecanes most probably can be attributed to catalytic effects. The catalyst seems to have little effect with the hexadecanes, which would thermally decompose more rapidly than the dodecanes. Since the studies of Terres and Gropenbacher were made at 932°F. it is possible that a substantial amount of thermal cracking occurred in addition to the catalytic cracking. The relative importance of the two processes would vary with the nature of the reactant.

Table 5

RATE OF DECOMPOSITION OF BRANCHED CHAIN PARAFFINS

C-atom Number	Structure	k_1/k_n	T, °F	Reference	r_1/r_n
C_4	$2MeC_3$	1.11-1.49	1067-1202	27,28,29,30	1.03
C_5	$2MeC_4$	1.23-1.78	748-1067	27	1.02
	$2,2MeC_3$	0.46	1067	27	0.48
C_6	$2,3MeC_4$	1.67	1068	27	1.03
C_8	$2,2,4MeC_5$	0.15	935-1060	31	0.71
	$2,5MeC_6$	1.34	935-1047	31	1.02
C_{12}	$2MeC_{11}$	2.03	932	26	1.01
	$3MeC_{11}$	1.00	800	23	1.01
	$2,4MeC_{10}$	2.00	932	26*	1.01
	$2,9MeC_{10}$	1.09	800	23	1.01
	$2,4,6MeC_9$	1.07	932	26*	1.02
	$2,4,8MeC_9$	1.07	932	26*	1.02
	$2,2,4,6MeC_8$	0.80	932	26*	0.63
	$5PrC_9$	1.08	800	23	1.01
	$3,6EtC_8$	1.09	800	23	1.01
C_{13}	$2,2,8,8MeC_9$	0.57	800	23	0.65
C_{16}	$2MeC_{15}$	1.30	932	26*	1.01
	$2,4MeC_{14}$	1.19	932	26*	1.01
	$2,4,6MeC_{13}$	1.19	932	26*	1.02
	$2,4,5MeC_{13}$	1.23	932	26*	1.02
	$2,2,4,4,6,8,8MeC_9$	0.3-1.75	685-815	15	0.59
	$2,2,4,4,6,8,8MeC_9$	0.59	932	26*	0.59

*Catalytic cracking

D. EFFECT OF PRESSURE ON THE RATE OF DECOMPOSITION

Experimental data on the effect of pressure on the thermal cracking rate of paraffinic hydrocarbons were limited until the last decade to pressures not exceeding 50 atm. It has been generally reported that in the range of several atmospheres pressure, the first order rate constant of cracking increases with increased pressure.

Table 6 summarizes the experimental data on the effect of pressure in cracking of paraffinic hydrocarbons. If possible, the rate constants of decomposition measured at an elevated pressure were compared with the rate constant of decomposition measured by the same author at atmospheric pressure; if such data were not given, the rate constant at atmospheric pressure was obtained by interpolation or extrapolation of data from other authors. For isomeric dodecanes, the rate of decomposition of n-dodecane was adjusted by using the k_i/k_n factors given in Table 5. Such values are designated by an asterisk in Table 6. Figure 13 shows the medium pressure range (up to 75 atm.) for isomeric dodecanes, and Figure 14 shows all experimental data up to pressures of about 1000 atm. The straight lines in both figures, which represent approximately the average of all data, indicate that in the low pressure range an increase of pressure by 10 atmospheres increases the rate of decomposition by a factor of about 1.2, and the rate constant doubles for a pressure increase of about 35 to 40 atmospheres.

For propane the studies of Hepp and Frey (ref. 32) at 1500 and 2500 psi (102-170 atm) gave first order rate constants about double those of Steacie and Puddington (ref. 33) at atmospheric pressure, but for butane the constants were about four times greater than those of Steacie and Puddington. Judging from these facts, pressure effects on methane and ethane rate constants may be less pronounced than for the higher members of the series. The first order rate constant increases up to a maximum at about 100 to 300 atm. pressure and then gradually decreases. At the maximum, the first order rate constant decomposition is as much as 20 to 40 times greater than the value at atmospheric pressure (ref. 35).

The important effect of pressure on the phase conditions will be shown for n-hexadecane. While the estimated critical temperature of the hydrocarbons in the C_{12}-C_{13} range is below 800°F, the estimated critical data for n-hexadecane are: critical temperature 885°F, and critical pressure 198.4 psi. This means that the n-hexadecane is present in both phases, and the pressure in the system is initially determined by the vapor pressure of n-hexadecane, which is 115 psi at 800°F. Using the estimated critical data, and the equation of state of real gases (compressibility factor) and liquids (expansion factor), respectively, the densities of the two phases are:

$$d_L = 0.449 \text{ g/ml and } d_G = 0.0203 \text{ g/m.}$$

Table 6

EFFECT OF PRESSURE ON THE DECOMPOSITION OF PARAFFINIC HYDROCARBONS

Hydrocarbon	Temp, °F	Press, atm	Rate Constant k_1, hr^{-1}	Reference	k_p/k_1
C_3H_6	600	1	22.9	30	
	600	7	28.7	30	1.25
	650	1	80.3	30	
	650	7	136	30	1.69
	700	1	618	30	
	700	7	402	30	0.65
$n\text{-}C_4H_{10}$	555	1	5.66	28	
	555	48.4	35.9	28	6.34
	600	1	47.3	30	
	600	7	61.8	30	1.31
	650	1	230	30	
	650	7	251	30	1.09
$i\text{-}C_4H_{10}$	555	1		*	
	555	48.4	33.1	28	3.31
$n\text{-}C_6H_{14}$	420	1	0.0	*	
	420	280-500	1.03	34	39.9
	420	420-700	0.740	34	28.7
	420	400-750	0.782	34	30.3
	420	750-980	0.486	34	18.8
	430	1		*	
	430	140-180	0.293	34	6.44
	430	800-920	0.162	34	3.56

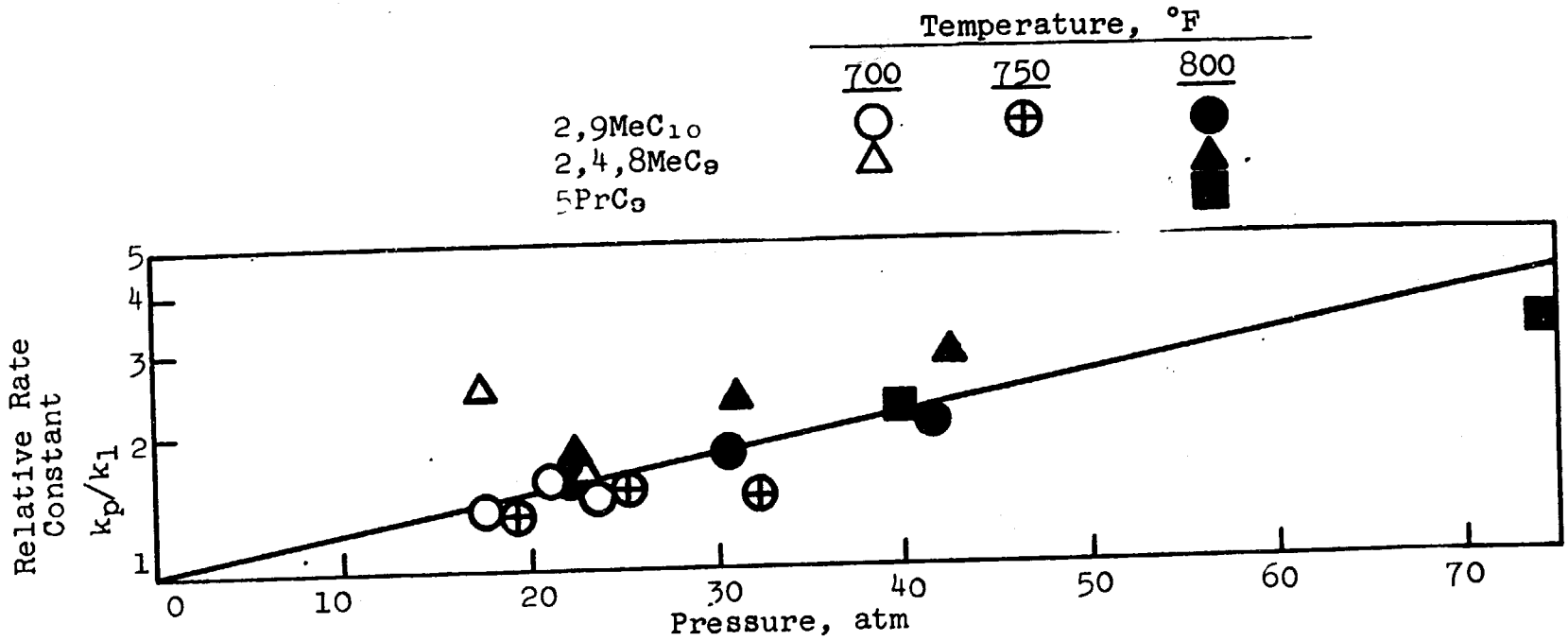

Figure 13. Rate Constants of Isomeric Dodecanes as a Function of Pressure

1/2 FRAMES

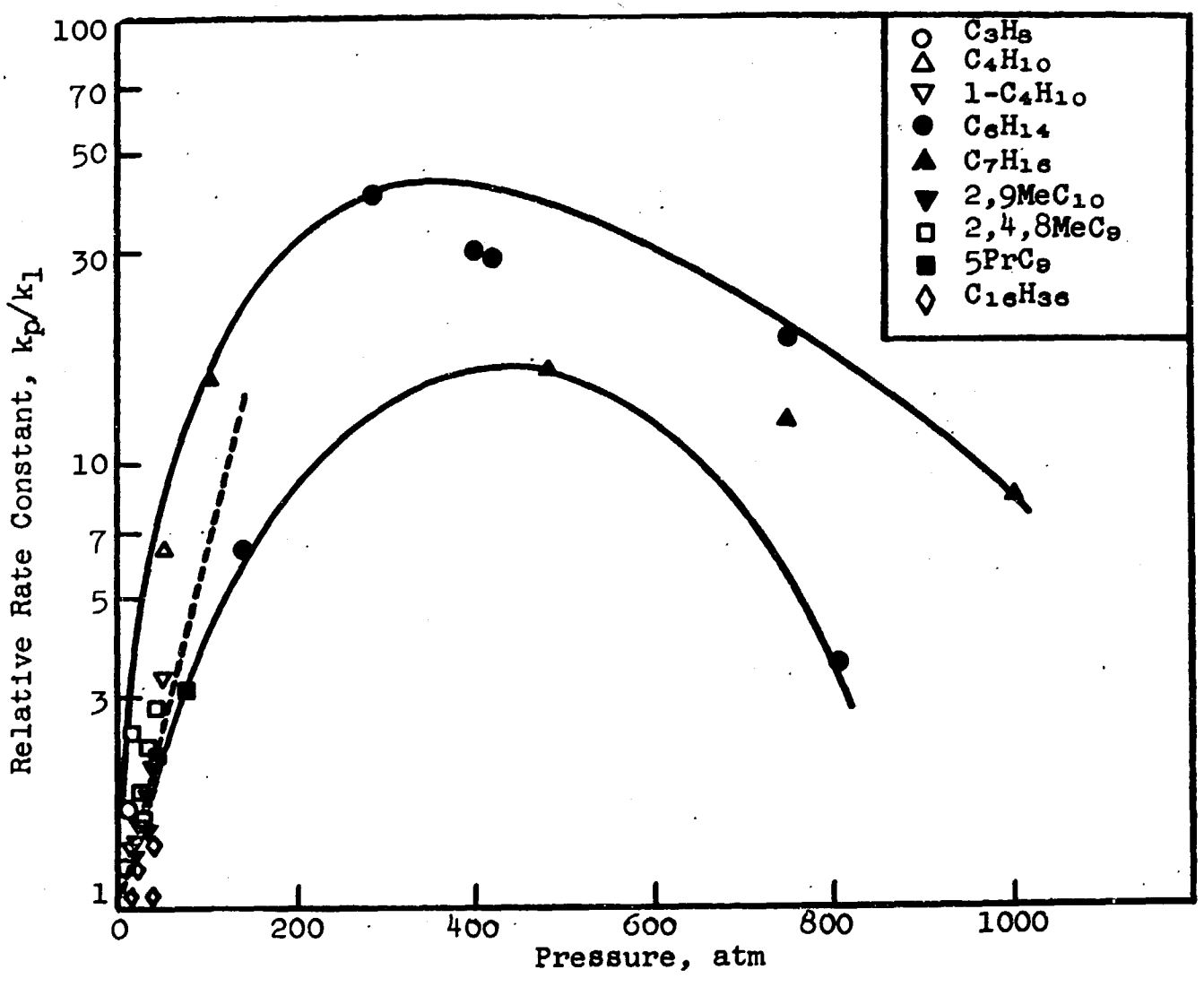

Figure 14. Relative Rate Constants of Thermal Cracking as a Function of Pressure

From these data the volume of the vapor and liquid phase in the reactor was calculated. The volume per cent of vapor phase is given in Table 4. Figure 15 shows the rate constant of decomposition as a function of the per cent of reactor filled with liquid phase at the initial point of decomposition at 800°F. The experimental points show a gradual increase of the rate of decomposition with the amount of liquid phase present in the reactor, indicating that the liquid phase decomposition is faster than the decomposition in the vapor phase. The equation of the line is

$$k = 0.465 + 0.361 V_L/VR \qquad (16)$$

where

V_L is the volume of liquid phase at 800°F
V_R is the volume of the reactor

From this plot, the rate of decomposition in the liquid phase is $k_L = 0.826\ hr^{-1}$ and in the vapor phase $k_V = 0.465$, that is, the decomposition in the liquid phase is nearly twice that in the vapor phase.

The rate of decomposition in a closed system can be calculated as

$$k = k_L \frac{V_L}{V_R} + k_v \frac{V_V}{V_R} \qquad (17)$$

if a simple additivity is assumed for the decomposition taking place in a two-phase system. Figure 9 shows the k_L and k_v values for cetane as blackened circles. The point representing the liquid phase decomposition is very close to Tilichcev's curve. No similar evaluation was made for nonadecane and therefore the rate constant cannot be separated into two points for comparison with hexadecane.

E. METHOD FOR ESTIMATION OF THE RATE CONSTANT OF DECOMPOSITION

Although at this stage no comprehensive method for estimating rate constants can be given, our data, together with those published by Terres and Gropenbacher (ref. 26), give certain leads to the effect of structure on the rate of decomposition. In the C_{12} to C_{18} range, the rate constant of decomposition can be expressed for normal paraffins as

$$k = 0.06n - 0.25 \quad \text{at } 800°F \qquad (18)$$

If we replace a number of CH_2 groups in the chain by side chains, the following corrections must be applied

Methyl group	0
Ethyl or propyl group	+0.16
i-Propyl group	+0.48
Two symmetrical i-propyl groups	+0.11
Two symmetrical t-butyl groups	-0.18

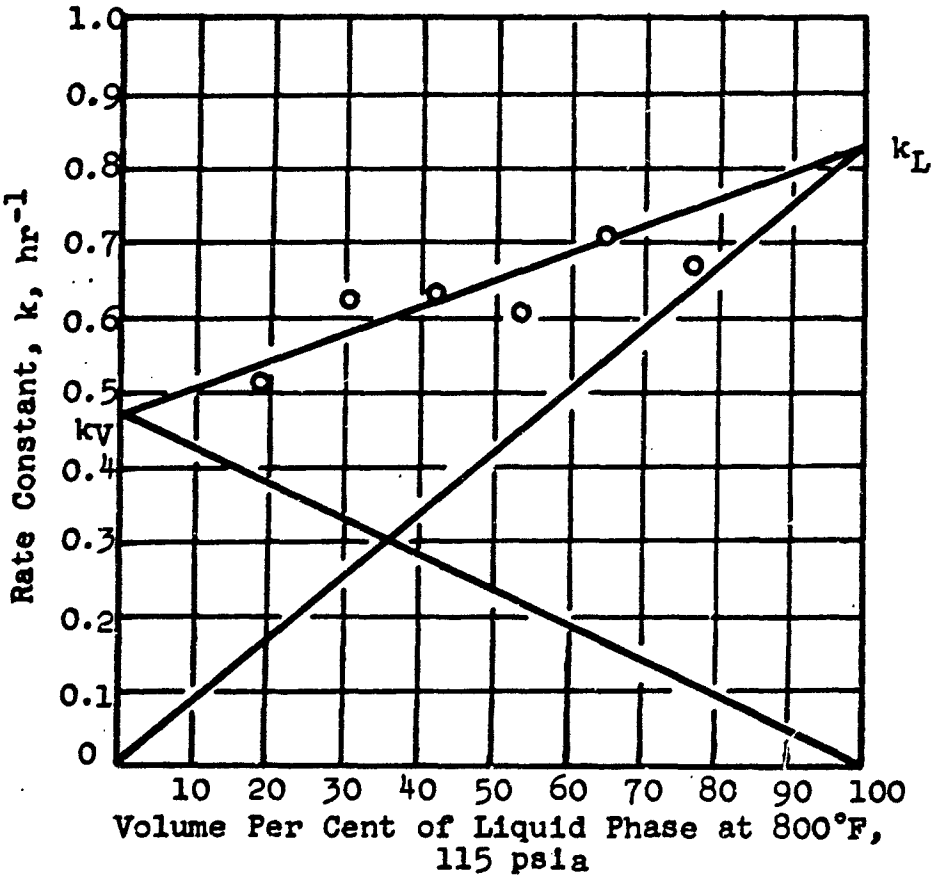

Figure 15. Effect of Phase Conditions on the Decomposition Rate Constants of n-Hexadecane

To show this simple method on a few examples

2-methyl undecane	C_{12} $k = 0.06 \times 12 - 0.25$	0.47
	Me group	0
		0.47
2,9-dimethyl undecane	C_{12}	0.47
	two i-propyl groups	0.11
		0.58
3,6-diethyl octane	C_{12}	0.47
	2 ethyl groups	0.32
		0.79 hr^{-1}

The experimental and calculated data are compared in Table 7. The agreement is satisfactory with the exception of 2,4,8-trimethylnonane, where the crowding effect of side chains may be responsible for the deviation. Included in Table 5 are the data of Terres and Gropenbacher (ref. 26) on isomeric dodecanes.

These results indicate that methyl substitutions have little effect on the rate of decomposition, except when they are in a terminal position on a tertiary carbon atom in an asymmetric molecule (corresponding to an i-propyl ending). Then they increase the rate of decomposition. Symmetrical methyl substitutions on quaternary carbon atoms at both ends significantly increase the stability of the compound toward thermal decomposition.

If we compare the rate constants for isomers, a maximum threefold increase in rate of decomposition was experienced for the isomers investigated, which means that only minor effects in the thermal stability field can be achieved by variation of isomers, corresponding to an increase or decrease of thermal stability of about $\pm(30\text{-}35)°F$.

F. RATE OF PARTICLE FORMATION

The rate of particle formation expressed as the reciprocal induction time to initial particle formation is given in Table 7. All the compounds investigated formed particles after 2-3 hours of exposure at 800°F.

It can be stated that n-paraffinic hydrocarbons seem to be slightly more stable toward particle formation than the branched chain compounds.

The activation energy of the particle forming process (E_P) was determined for two hydrocarbons and is compared with the activation energy of decomposition (E_D) in Table 8.

Table 7

EXPERIMENTAL AND CALCULATED RATE CONSTANTS OF DECOMPOSITION AND RATE CONSTANTS OF PARTICLE FORMATION AT 800°F

	Rate Constants, hr^{-1}		
	$k_{D,exp}$	$k_{D,calc}$	k_p
C_{12}	0.47	0.47	0.33
* $2MeC_{11}$	0.95	0.95	
$3MeC_{11}$	0.46	0.47	0.40
$2,9MeC_{10}$	0.58	0.58	0.40
* $2,4MeC_{10}$	0.94	0.95	
$2,4,8MeC_9$	0.79	0.58	0.50
* $2,4,6MeC_9$	0.88	0.95	
* $2,2,4,6,6MeC_7$	0.31	0.29	
$2,2,8,8MeC_9$	0.32	0.35	0.40
$3,6EtC_8$	0.80	0.79	0.50
$5PrC_9$	0.62	0.63	0.33
C_{18}	0.71	0.71	0.33

* Data from Terres and Gropenbacher (ref. 26).

Table 8

ACTIVATION ENERGIES OF PARTICLE FORMATION (E_P) AND DECOMPOSITION (E_D) (kcal/mole)

	E_P	E_D
n-Dodecane	58-63	70
3,6-Diethyloctane	45-58	59

The values given in Table 8 indicate that the activation energy for particle formation is lower by several kcal/mole than that of decomposition. This means that at lower temperatures, particle formation takes place at lower conversions than at higher temperatures.

G. PRODUCT DISTRIBUTION FROM PARAFFIN CRACKING BY RICE-KOSSIAKOFF METHOD

The Rice-Kossiaskoff modified free radical theory (ref. 36) may be used to predict the product composition from the cracking of paraffinic hydrocarbons. The following is an example of the application of their theory to the calculation of the distribution of products from cetane (n-hexadecane) thermally cracked at 1200°F (922°K). One of the variables is the extent to which the large free radical initially formed is assumed to undergo C-C bond fission versus being converted into a paraffin by H-abstraction. Increased pressure increases the likelihood of H-abstraction (a bimolecular process) over fission (a unimolecular process). The following calculation shows how the product distribution would be predicted to change with an increasing number of decomposition steps of the large free radical before it becomes stabilized by H-abstraction.

Consider first the case in which only one C-C bond in the free radical is broken before the resulting radical is converted into a paraffin. This would be typical of relatively high pressure operation.

One-Step Decomposition Process

(1)	$M \longrightarrow R_1$	radical formation	(19)
(2)	$R_1 \longrightarrow R'_1 \longrightarrow Ol_1 + R_2$	isomerization and fission	(20)
(3)	$R_2 + M \longrightarrow R_2H + R_1$	hydrogen transfer	(21)

The decomposing hydrocarbon, M, is converted in step (1) to a first generation free radical R_1, which will generally be a large free radical. In step (2), R_1 isomerizes to R_1'. Fission at a C-C bond converts the R_1' radical into an olefin (Ol_1) and a smaller second generation free radical, R_2. In this case, R_2 is assumed to become converted into a paraffin by hydrogen abstraction.

Rice and Kossiakoff assumed that the difference in activation energy for removing a secondary and primary hydrogen is 2000 cal/g-mole and the difference between a tertiary and primary hydrogen is 4000 g-mole; at 922.2°K (1200°F), the relative rates of removal of hydrogen atoms in step (1) would be in the ratio

$$\log \frac{k_2}{k_1} = \frac{2000}{4.576 \times 922.2} = 0.474 \qquad (22)$$

or

$$k_2 = 2.98\ k_1 \qquad (23)$$

$$k_3 = 8.87\ k_1 \qquad (24)$$

In n-hexadecane there are six primary hydrogen atoms and 28 secondary hydrogen atoms available. Multiplying the relative rate by the statistical factor, we obtain

primary $6 \times 1 = 6.00$ 6.71% primary free radicals

secondary $28 \times 2.98 = \frac{83.44}{89.44}$ 93.29% secondary free radicals

These radicals have a long skeleton and therefore they may coil around and react with themselves to produce isomers. Thus, the 1-cetyl radical can isomerize into a free radical in which the hydrogen vacancy may be found in any of the positions from 5 to 16. The isomerization of a 1-cetyl to a 2,3 or 4-cetyl radical by a coiling mechanism is not likely for geometrical reasons. For this isomerization in step (2), Rice and Kossiakoff assume that the activation energy difference for internal transfer of a hydrogen atom between a primary and a secondary position is 4000 cal, resulting in a Boltzmann factor of 8.87 at 922°K. Assuming that the different secondary radicals are formed in equal amounts, we obtain by isomerization of a C^1_{16} radical (the lower index gives the length of the radical, the upper index the place of hydrogen abstraction).

$3 \times 1 = 3.00$ 1.51% primary free radicals (C^1_{16} or C^{16}_{16})

$22 \times 8.87 = \frac{195.14}{198.14}$ 98.49% secondary free radicals (C^5_{16} to C^{15}_{16})

In this calculation, 3 and 22 are the numbers of hydrogen atoms available for isomerization forming primary or secondary free radicals, respectively. The same calculation in the case of C^2_{16} radical is

$3 \times 1 = 3.00$ 1.66% primary free radicals (C^1_{16} or C^{16}_{16})

$20 \times 8.87 = \frac{177.40}{180.40}$ 98.34% secondary free radicals (C^8_{16} to C^{15}_{16})

All radicals formed in this initial step are C_{16} radicals. On the basis of a total of 100 C_{16} radicals, the isomer distribution is given by the top line below.

Table 9

RADICALS FORMED FROM 100 CETANE MOLECULES BY ISOMERIZATION

R_i		C_{16}^1	C_{16}^2	C_{16}^3	C_{16}^4	C_{16}^5	C_{16}^6	C_{16}^7	C_{16}^8	Total
		6.71	13.33	13.33	13.33	13.33	13.33	13.33	13.33	
R_1'	C_{16}^1	0.10	0.22	0.2[illegible]	0.28	0.61	0.61	0.61	0.61	3.29
	C_{16}^2	0.60	1.31	1.45	1.63	1.82	3.63	3.63	3.63	17.70
	C_{16}^3	0.60	1.31	1.45	1.63	1.82	1.82	3.63	3.63	15.89
	C_{16}^4	0 60	1.31	1.45	1.63	1.82	1.82	1.82	3.63	14.08
	C_{16}^5	1.20	1.31	1.45	1.63	.82	1.82	1.82	1.82	12.87
	C_{16}^6	1.20	2.62	1.45	1.63	1.82	1.82	1.82	-	12.36
	C_{16}^7	1.20	2.62	2.91	1.63	1.82	1.82	-	-	12.00
	C_{16}^8	1.20	2.62	2.91	3.26	1.82	-	-	-	11.81
		6.70	13.32	13.32	13.32	13.35	13.34	13.33	13.32	100.00

In the first column, the entries below the first line show the distribution of the C_{16} radical isomers formed by isomerization of the 6.71 C_{16}^1 radicals formed in step (1). Likewise, in the second column, the entries below the first line show the distribution obtained by isomerization of the 13.33 C_{16}^2 radicals formed in step (1). The last column gives the final distribution of isomers obtained by applying the set of rules given below.

(1) The decompostion reaction of the large alkyl radical is faster than bimolecular reaction with another hydrocarbon.

(2) The kind of radical initially formed depends upon the relative ease of abstraction of a hydrogen atom from the hydrocarbon. Taking the same pre-exponential factor for all reactions, removal of a secondary hydrogen is assumed to require about 2.0 kcal. of activation energy less than that of a primary hydrogen (an activation energy difference of 2.0 corresponds to a ratio of the two rate constants of 3.66 at 500°C); a tertiary hydrogen is assumed to require about 4 kcal. less of activation energy than a primary hydrogen (corresponds to a ratio of rate constants of 13.4 at 500°C). The range of initial formation of each type of radical is therefore taken to be proportional to this ratio multiplied by the number of C-H bonds of that type present.

(3) In order to bring the theory into closer harmony with the facts, the above simple theory is amplified to assume that a free radical of C_6 or higher may, prior to rupture, isomerize by a coiling mechanism to a carbon atom four or more carbon atoms from the original carbon atom having the vacant position. This involves movement of a H-atom but not a change in the carbon skeleton. The shifting between a primary, secondary and tertiary position is assumed to require an activation energy twice that taken for initial abstraction of a hydrogen atom, e.g., shifting from a primary to a secondary position is assumed to require an activation energy of 2 x 2 = 4 kcal. The probability of collision of the free radical site with a H-atom is taken to be the same for all H-atoms on C atoms four or more C atoms from the position of the H- vacancy.

(4) The free radical formed above undergoes carbon-carbon bond rupture at the β bond relative to the carbon atom from which the hydrogen is missing. If more than one such bond exists, the mechanism leading to a radical of greater stability will occur preferentially, e.g., a tertiary radical will be formed more readily than a secondary; a secondary more readily than a primary.

The theory in its various extensions has been developed primarily from studies on paraffins and paraffin radicals up to about C_6 in size. It cannot be expected to yield detailed predictions of product distribution in unknown systems since a number of simplifying assumptions have had to be made to make the theory manageable. The values for the effect of structure on the activation energies assigned for initial H-abstraction, for H-isomerization, and for carbon-carbon bond rupture are somewhat arbitrary. The coiling mechanism may not be the only way in which isomerization can occur, and the set of rules for calculating isomer distribution is clearly a simplification. Nevertheless, the theory provides good agreement with the broad nature of the experimental facts.

In the latter part of step (2) these free radicals decompose into an olefin and a shorter second generation free radical by splitting of the chain at a β-carbon-carbon bond from the location of the free radical. The C_6^1 and C_6^2 radicals can decompose in only one way, but the rest of the free radicals have two β-positions available. The probability for these two processes is assumed to be equal, except when one of the routes yields a methyl radical. This process is less likely, and it was assumed by Rice and Kossiakoff that the splitting to yield a higher primary radical is three times faster than the splitting to yield a methyl radical. Applying these assumptions, the amounts of olefins and free radicals obtained by decomposition of the R_i radicals are as follows:

Table 10

OLEFINS AND R_2 RADICALS FORMED BY DECOMPOSITION OF 100 CETANE MOLECULES

	Olefins	R_2 Radicals		Olefins	R_2 Radicals
C_1		3.97	C_9	5.90	6.18
C_2	3.29	7.04	C_{10}	5.90	6.43
C_3	17.70	6.43	C_{11}	6.00	7.04
C_4	11.92	6.18	C_{12}	6.18	11.92
C_5	7.04	6.00	C_{13}	6.43	17.70
C_6	6.43	5.90	C_{14}	7.04	3.29
C_7	6.18	5.90	C_{15}	3.97	-
C_8	6.00	6.00			

In this case we assume that the second generation free radicals react with cetane molecules to form paraffins and cetyl radicals, which then undergo again the isomerization and decomposition steps. Under these conditions, disregarding the chain termination step, the product distribution per 100 molecules of cetane decomposed is shown in the first column of Table 9 and is given in Figure 16 as the "one-step decomposition".

Different product distributions are obtained if it is assumed that two or more fission steps occur in step 2. It is assumed that isomerization of the remaining free radicals occurs after each C-C fission. The two-step decomposition can be represented as:

(1) $M \longrightarrow R_1$ radical formation (25)

(2) $R_1 \longrightarrow R_1' \longrightarrow Ol_1 + R_2$ isomerization and fission (26)

(3) $R_2 \longrightarrow R_2' \longrightarrow Ol_2 + R_3$ (27)

(4) $R_3 + M \longrightarrow R_3H + R_1$ hydrogen transfer (28)

The product distribution according to carbon atom number is given in Table 9 for this case, and also for the case in which three or four fissions occur before the radical becomes converted to a paraffin.

After four decomposition steps, only radicals of C_6 or shorter are left, and the assumption of further decomposition steps before H-abstraction would affect the distribution only slightly. The concentration of C_3 hydrocarbons in the product will be only slightly reduced. The ν number given in Table 9 shows the numbers of moles produced from each cetane mole decomposed. Figure 16 shows all these calculations in graphical form. Experimental studies on paraffin cracking show results in agreement with the general conclusions from this type of calculation. In cetane cracking at

Table 11

PRODUCT DISTRIBUTION IN THE DECOMPOSITION OF n-HEXADECANE
(in mole per cent)

Decompositions Steps	1		2		3		4	
Y, mole/mole Decomposed	2.00		2.88		3.56		3.87	
	Paraffin	Olefin	Paraffin	Olefin	Paraffin	Olefin	Paraffin	Olefin
C_1	2.0	-	4.7	-	10.4	-	14.7	-
C_2	3.5	1.7	6.3	8.6	9.1	19.8	9.7	25.7
C_3	3.2	8.9	7.6	12.3	5.6	13.3	1.1	12.7
C_4	3.1	6.0	4.3	7.5	1.6	7.2	0.2	6.7
C_5	3.0	3.5	3.3	4.2	0.8	3.8	0.04	3.5
C_6	2.9	3.2	2.6	5.5	0.4	5.3	0.01	4.9
C_7	2.9	3.1	2.0	4.7	0.2	4.3	-	4.0
C_8	3.0	3.0	1.4	4.3	0.06	3.3	-	3.1
C_9	3.1	2.9	1.3	3.8	0.01	3.1	-	2.9
C_{10}	3.2	2.9	0.9	3.3	-	2.7	-	2.5
C_{11}	3.5	3.0	0.3	2.7	-	2.2	-	2.0
C_{12}	6.0	3.1	0.02	2.4	-	1.9	-	1.8
C_{13}	8.9	3.2	-	2.2	-	1.8	-	1.7
C_{14}	1.7	3.5	-	2.4	-	2.0	-	1.8
C_{15}		2.0	-	1.4	-	1.1	-	1.0

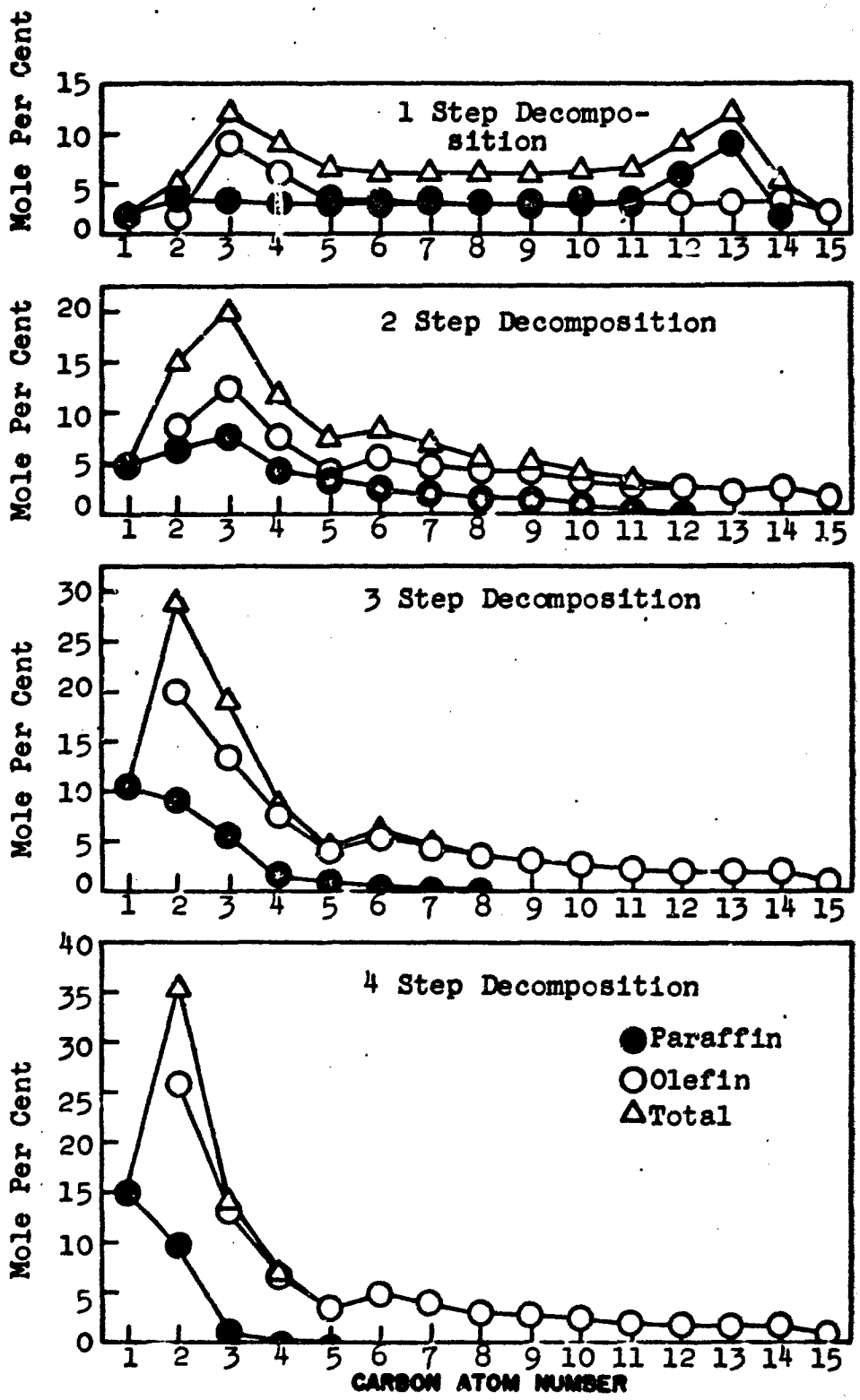

Figure 16. Calculated Product Distribution in the Thermal Cracking of Cetane

atmospheric pressure no paraffins above propane were found and the quantities of larger saturated paraffins increased with pressure.

VI. CONTAMINATION BY SULFUR COMPOUNDS

A. EXPERIMENTAL STUDY OF SULFUR CONTAMINATION VARIABLES

The variables studied were contaminant type, hydrocarbon substrate structure, reaction temperature, contaminant concentration, and the effect of adding air to the reaction tube. The conversion level was about 50%.

Tables 10 through 16 list the decomposition rates (k, hr^{-1}) and fraction of hydrocarbon unconverted for the various pure hydrocarbons tested, together with the reaction time and temperature and the contamination level of the particular run. The decomposition rates were calculated assuming first-order reaction rates in all cases.

In each experiment a control sample of pure hydrocarbon was run to evaluate the effect of the contaminant. Previously reported rate constants were statistical averages of many experimental runs. The results reported here are therefore not intended to revise any previously reported data but only to give relative values for the contamination studies.

The initial study was made on decalin, 5-n-propylnonane, and n-hexadecane, which represented cyclic, branched chain, and straight-chain types of hydrocarbons, respectively. Thiophenol and t-butyldisulfide were chosen as organosulfur contaminants with considerably different structure. Temperatures ranged from 700 to 850°F while the contaminant concentration varied from 0 to 10 wt-%.

The results of this study are graphically portrayed in Figures 17, 18, and 19. From these graphs the following observations can be made:

(1) The decomposition rate of n-hexadecane was strongly inhibited by the sulfur contaminants, and that of decalin was moderately inhibited. On the other hand, the rate of decomposition of 5-n-propylnonane was accelerated.

(2) In every case except 5-n-propylnonane at 700°F, the effect of increasing the contaminant concentration was to increase the effect it produced, either inhibition or acceleration.

(3) The effects from contaminating with t-butyldisulfide or thiophenol were the same qualitatively and quantitatively within the limits of normal experimental error.

With regard to the first observation above, the dramatically different result (rate acceleration) obtained in the case of the branched chain paraffin prompted further exploration into the effect of substrate structure and this subject will be discussed fully later.

Table 12

DECOMPOSITION RATE DATA FOR 5-n-PROPYLNONANE CONTAMINATED WITH t-BUTYLDISULFIDE

Temp, °F	Time, hr	Contaminant, wt-%	Fraction Hydrocarbon Unconverted	k (hr^{-1})
700	64	0	0.466	0.0119
700	64	0.001	0.421	0.0135
700	64	0.01	0.413	0.0142
700	64	0.1	0.368	0.0156
700	64	1.0	0.362	0.0159
700	64	10	0.372*	0.0155
750	5.5	0	0.439	0.150
750	5.5	0.001	0.426	0.155
750	5.5	0.01	0.419	0.158
750	5.5	0.1	0.340	0.196
750	5.5	1.0	0.330	0.202
750	5.5	10	0.276*	0.234
800	1.5	0	0.331	0.737
800	1.5	0.001	0.324	0.751
800	1.5	0.01	0.321	0.757
800	1.5	0.1	0.241	0.949
800	1.5	1.0	0.154	1.247
800	1.5	10	0.071*	1.763

*At the 10% contaminant levels, the VPC data were adjusted to show only the fraction of hydrocarbon unconverted.

Table 13

DECOMPOSITION RATE DATA FOR 5-n-PROPYLNONANE CONTAMINATED WITH THIOPHENOL

Temp., °F	Time, hr	Contaminant, wt-%	Fraction Hydrocarbon Unconverted	k, (hr^{-1})
700	64.25	0	0.358	0.0160
700	64.25	0.01	0.368	0.0156
700	64.25	0.1	0.294	0.0191
750	5.5	0	0.461	0.141
750	5.5	0.01	0.474	0.136
750	5.5	0.1	0.372	0.180
800	1.5	0	0.320	0.760
800	1.5	0.01	0.320	0.522
800	1.5	0.1	0.256	0.908

Table 14

DECOMPOSITION RATE FOR n-HEXADECANE CONTAMINATED WITH THIOPHENOL

Temp, °F	Time, hr	Contaminant, wt-%	Fraction Hydrocarbon Unconverted	k, (hr⁻
700	76	0	0.416	0.011
700	76	0.001	0.453	0.010
700	76	0.01	0.556	0.007
700	76	0.1	0.600	0.006
700	76	1.0	0.711	0.004
700	76	10	0.757	0.003
750	5.5	0	0.487	0.127
750	5.5	0.001	0.524	0.117
750	5.5	0.01	0.645	0.079
750	5.5	0.1	0.660	0.075
750	5.5	1.0	0.748	0.052
750	5.5	10	0.791	0.042
800	1	0	0.587	0.533
800	1	0.001	0.549	0.599
800	1	0.01	0.608	0.498
800	1	0.1	0.654	0.418
800	1	1.0	0.754	0.282
800	1	10	0.849	0.164

Table 15

DECOMPOSITION RATE FOR n-HEXADECANE CONTAMINATED WITH t-BUTYLDISULFIDE

Temp, °F	Time, hr	Contaminant, wt-%	Fraction Hydrocarbon Unconverted	k, (hr^{-1})
700	76	0	0.373	0.0130
700	76	0.01	0.361	0.0134
700	76	0.1	0.413	0.0116
750	5.5	0	0.447	0.146
750	5.5	0.01	0.496	0.127
750	5.5	0.1	0.535	0.114
800	1	0	0.451	0.796
800	1	0.01	0.502	0.689
800	1	0.1	0.543	0.611

Table 14

DECOMPOSITION RATE DATA FOR DECALIN CONTAMINATED WITH t-BUTYLDISULFIDE

Temp., °F	Time, hr	Contaminant, wt-%	Fraction Hydrocarbon Unconverted	k_1 (hr^{-1})
800	30	0	0.460	0.0259
800	30	0.001	0.450	0.0266
800	30	0.01	0.494	0.0235
800	30	0.1	0.540	0.0205
800	30	1.0	0.550	0.0199
800	30	10	0.552	0.0198
750	136	0	0.639	0.00329
750	136	0.001	0.607	0.00367
750	136	0.01	0.656	0.00310
750	136	0.1	0.681	0.00282
750	136	1.0	0.732	0.00229
750	136	10	0.760	0.00202
850	3	0	0.440	0.274
850	3	0.001	0.475	0.248
850	3	0.01	0.463	0.257
850	3	0.1	0.493	0.236
850	3	1.0	0.602	0.169
850	3	10	0.615	0.162

Table 17

DECOMPOSITION RATE DATA FOR DECALIN CONTAMINATED WITH THIOPHENOL

Temp., °F	Time, hr	Contaminant, wt-%	Fraction Hydrocarbon Unconverted	$k(hr^{-1})$
800	29.7	0	0.437	0.0279
800	29.7	0.01	0.512	0.0225
800	29.7	0.1	0.565	0.0192
850	3	0	0.473	0.250
850	3	0.01	0.493	0.236
850	3	0.1	0.610	0.165

Table 18

DECOMPOSITION RATE DATA FOR SUNDRY HYDROCARBONS CONTAMINATED WITH t-BUTYLDISULFIDE

Hydrocarbon	Temp, °F	Time, hr	Contaminant, wt-%	Fraction Unconverted	k, (hr^{-1})
3-Methylundecane	700	55	0.1	0.539	0.0112
	700	55	0	0.530	0.0115
	800	1.5	0.1	0.314	0.794
	800	1.5	0	0.393	0.623
2,9-Dimethyldecane	700	48	0.1	0.517	0.0137
	700	48	0	0.550	0.0125
	800	1.5	0.1	0.359	0.683
	800	1.5	0	0.489	0.477
1-Propyldecalin	700	88	0.1	0.925	0.000885
	700	88	0	0.820	0.00226
	800	3	0.1	0.684	0.127
	800	3	0	0.510	0.225
Decalin	800	22.5	0.1	0.541	0.0273
	800	22.5	0	0.503	0.0305
	800	46	0.1	0.402	0.0198
	800	46	0	0.363	0.0220
	750	136	0.1	0.698	0.00265
	750	136	0	0.667	0.00298
2,3-Dimethyldecalin	800	7	0.1	0.600	0.0730
	800	7	0	0.436	0.1186
Methylhydrindan	800	6	0.1	0.606	0.0835
	800	6	0	0.507	0.1132
Ethyldecalin	800	5	0.1	0.608	0.0996
	800	5	0	0.572	0.1117
2,2,8,8-Tetramethylnonane	800	3	0.1	0.279	0.426
	800	3	0	0.463	0.257
	800	1.5	0.1	0.446	0.538
	800	1.5	0	0.689	0.248
Hydrindan	800	3	0.1	0.800	0.0744
	800	3	0	0.841	0.0577
n-Dodecane	800	1.5	0.1	0.541	0.409
	800	1.5	0	0.521	0.435

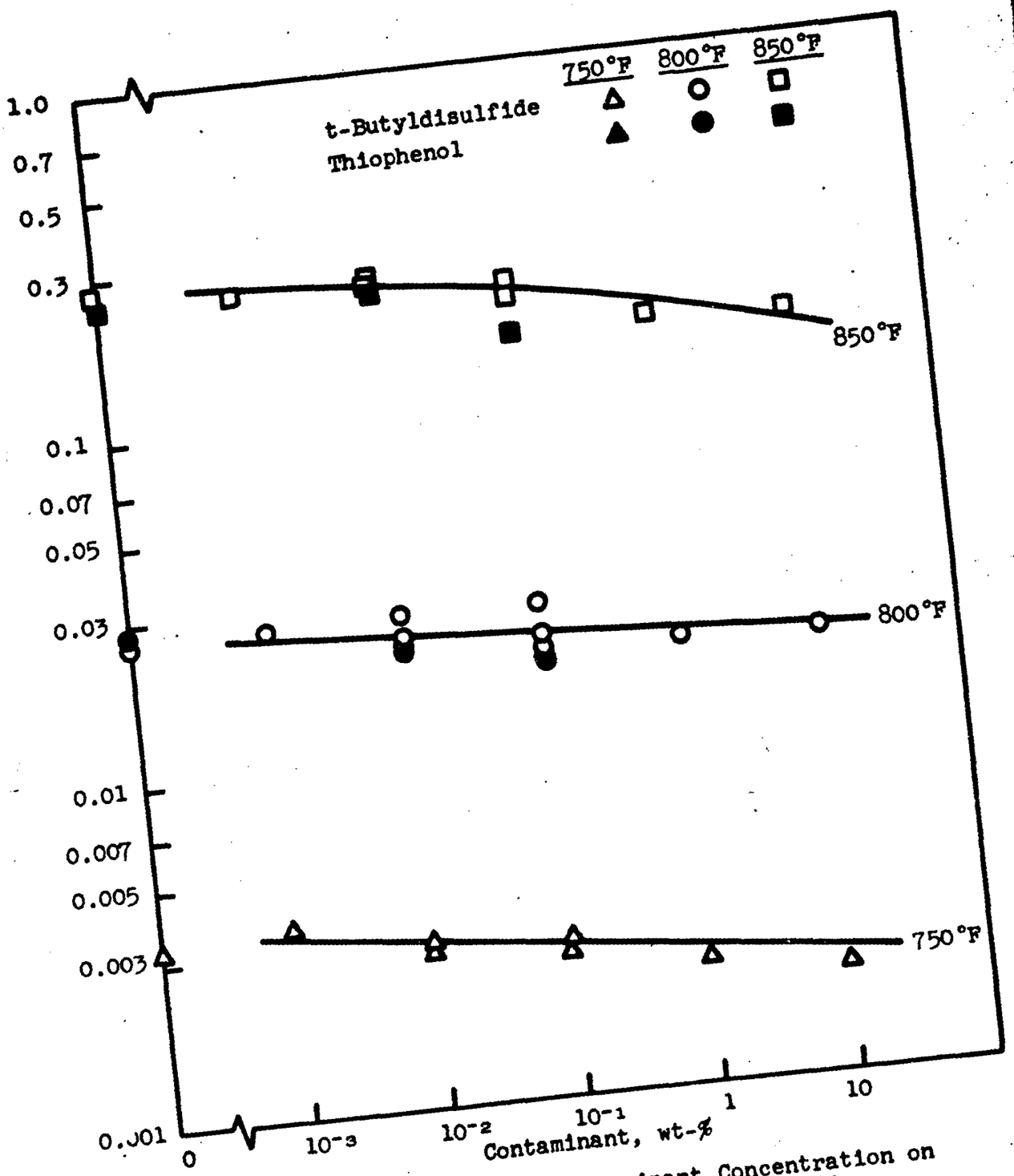

Figure 17. Effect of Contaminant Concentration on Rate of Decomposition of Decalin

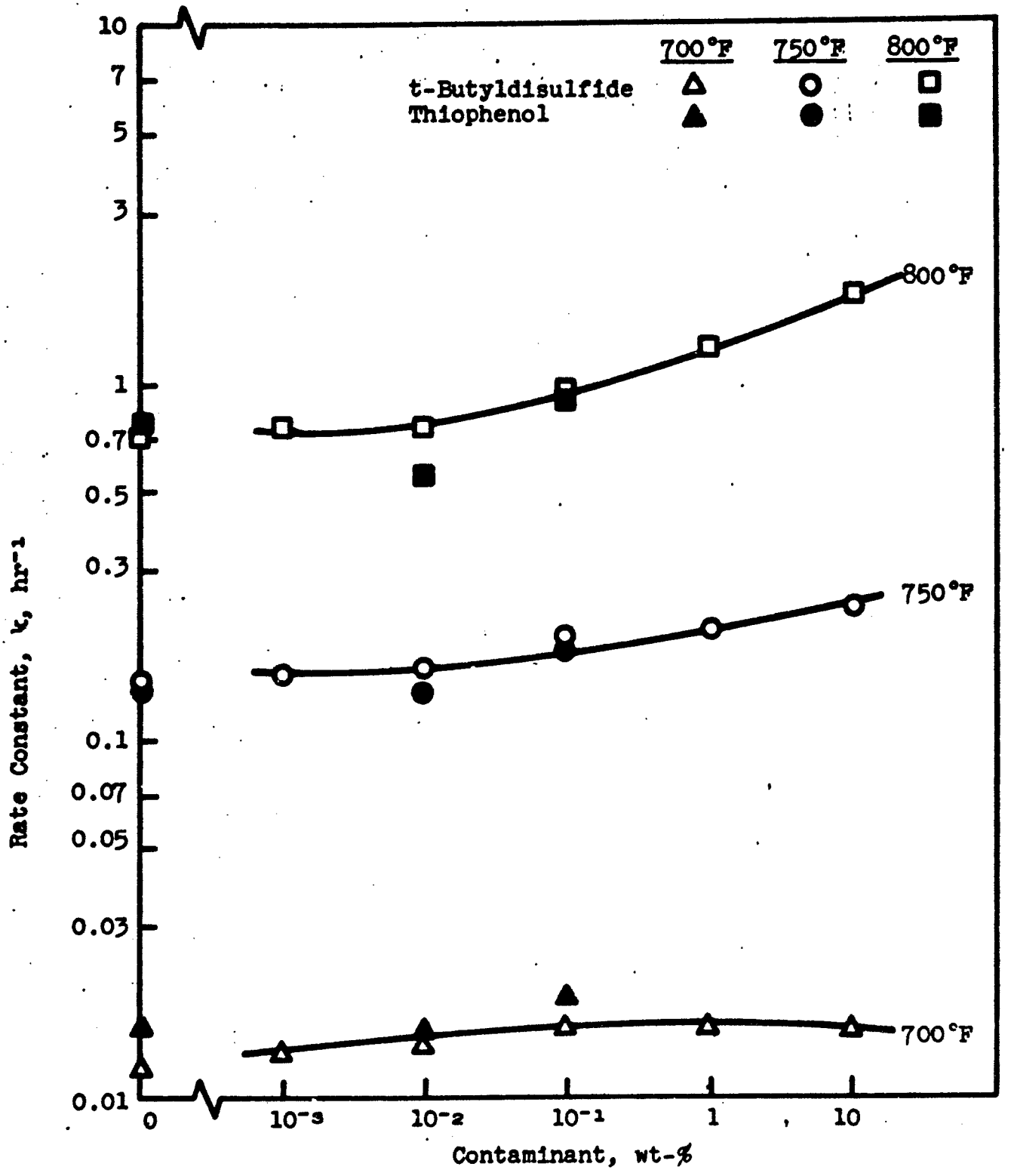

Figure 18. Effect of Contaminant Concentration on Rate of Decomposition of 5-n-propylnonane

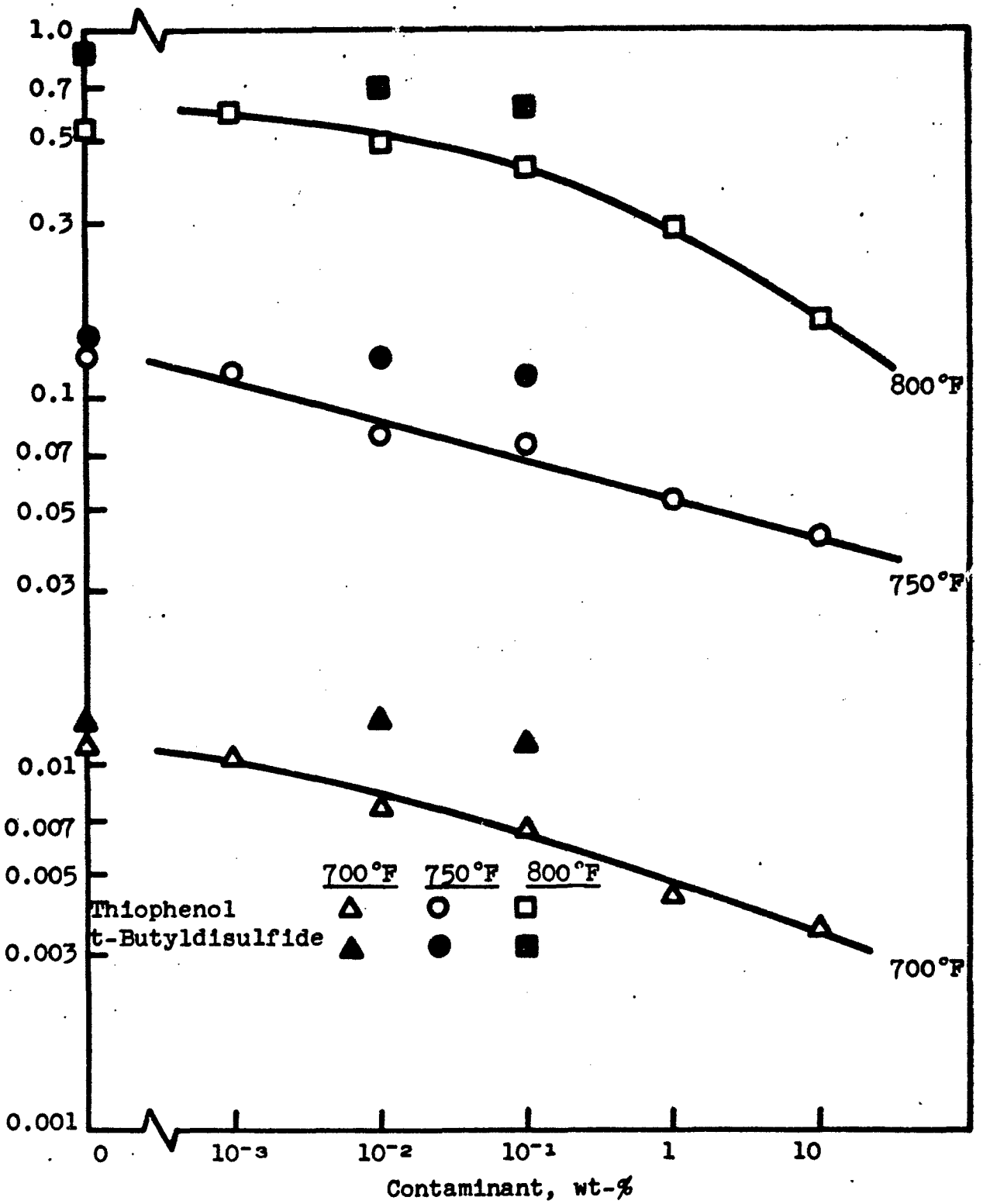

Figure 19. Effect of Contaminant Concentration on Rate of Decomposition of n-Hexadecane

1. Contaminant Concentration

Although contaminant levels such as 10 wt-% are impractical in a study of fuels, it was interesting from the standpoint of understanding the mechanism to observe that there was no leveling off of the contaminant effect even at such high concentrations as 10 wt-%. A study made earlier in this project demonstrated (by analysis) that the organosulfur contaminants were entirely used up when the hydrocarbon substrate was decomposed to the 50% level. No sulfur compounds were found in the reacted liquid at the end of the decomposition period, and the smell of sulfur compounds in the gas was very strong. The rate-inhibiting or -accelerating behavior of the sulfur contaminant was therefore not catalytic but rather direct involvement in the decomposition chain reaction of the hydrocarbon, resulting in the conversion to gaseous sulfur compounds as end products.

2. Contaminant Structure

The decomposition rates of pure thiophenol and t-butyldisulfide were determined at 800°F. The value for thiophenol was 0.7 hr^{-1}; that for t-butyldisulfide was greater than 15 hr^{-1}, making it extremely unstable relative to all of the other compounds of this study. The almost identical results obtained using these compounds as contaminants are therefore more surprising and indicate that the structure of the sulfur contaminant is not of prime importance.

3. Hydrocarbon Structure

The observation that the decomposition rate of 5-n-propylnonane was accelerated while those of decalin and n-hexadecane were inhibited prompted further investigation into the relationship of hydrocarbon structure to the observed phenomena. Several other hydrocarbons with widely differing structures were run. For simplicity, the contaminant type and concentration were fixed at 0.1 wt-% t-butyldisulfide and, for the sake of speed in screening the various types of hydrocarbons, the reaction temperature was mainly 800°F, a temperature that causes 50% decomposition in a very few hours in most cases. The data from this study are shown in Table 16.

The decomposition rates of ethyldecalin, 2,3-dimethyldecalin, isopropyldecalin, hydrindan, methylhydrindan, and n-dodecane were inhibited to varying degrees, while the decomposition rates of 3-methylundecane, 2,9-dimethyldecane, and 2,2,8,8-tetramethylnonane were accelerated. Only the branched-chain paraffins decomposed at a faster rate when contaminated with a sulfur compound. The decompositions of naphthenes and straight-chain paraffins were all inhibited.

A considerable difference in the degree of rate acceleration was noticed for the various branched-chain paraffins. In particular, the relatively stable 2,2,8,8-tetramethylnonane (symmetrical molecule and quaternary carbon atoms with no abstractable hydrogen) showed the greatest accelerating effect when contaminated by the 0.1% t-butyldisulfide. The only thing significantly different about 2,2,8,8-tetramethylnonane relative to the other branched-chain hydrocarbons studied was the fact that the molecule had more methyl groups, which presumably could form more methyl radicals to aid in the decomposition chain reaction.

To test this theory, the per cent change in the decomposition rates ($\%\Delta k$) was calculated for the four branched-chain paraffins. These are listed beside the number of methyl groups in the molecule in Table 17. The correlation between the $\%\Delta k$ and the number of methyl groups is striking and supports the theory extremely well.

It seemed reasonable to examine the hydrocarbons whose decomposition rates were inhibited to see if the number of methyl groups affected the degree of inhibition. For this reason, the four decalin types and the two hydrindans are listed also in Table 17. These data are not as uniform as for the branched paraffins. However, it can be concluded, at least, that rate inhibition by a sulfur contaminant also increases with increasing number of methyl substitutions.

4. Temperature Effects

In Figure 20 the per cent change in the decomposition rate ($\%\Delta k$) has been plotted for those hydrocarbons that were run at two different temperature levels. For four out of the six hydrocarbons, there was a very definite decrease in the effect of the sulfur contaminant as the reaction temperature was lowered, and this was true both for inhibition and acceleration of decomposition. The data for 5-n-propylnonane showed no temperature effect while that for isopropyldecalin demonstrated the exactly opposite effect. That is, the effect of the sulfur contaminant on the decomposition rate of isopropyldecalin was less at 800°F than at 700°F. The data for these two hydrocarbons probably should be checked, since a decrease in rate change with lower temperatures is very likely a general rule.

B. THEORETICAL CONSIDERATIONS

An attempt was made to explain the occurrence of both inhibition and acceleration of hydrocarbon decomposition by sulfur contaminants on the basis of the free radical reaction mechanism. Our further considerations are based on two conclusions reached in our experimental work:

(1) The decomposition reaction is first order in all cases

(2) The accelerating or inhibiting effect is proportional to the contaminant concentration.

Table 19

CHANGE IN DECOMPOSITION RATE BY 0.1% t-BUTYLDISULFIDE AS A FUNCTION OF NUMBER OF METHYL GROUPS

Hydrocarbon	% Δk^*	Number of Methyl Groups
2,2,8,8-Tetramethylnonane	+65.8	6
2,9-Dimethyldecane	+43.2	4
3-Methylundecane	+27.4	3
5-n-Propylnonane	+28.8	3
Decalin	-10.0	0
Ethyldecalin	-10.8	1
2,3-Dimethyldecalin	-38.5	2
Isopropyldecalin	-43.6	2
Hydrindan	-7.1	0
Methylhydrindan	-26.2	1

* $$\% \Delta k = \frac{k_c - k_o}{k_o} \times 100 \qquad (29)$$

where k_o = decomposition rate without sulfur contaminant, and

k_c = decomposition rate with sulfur contaminant

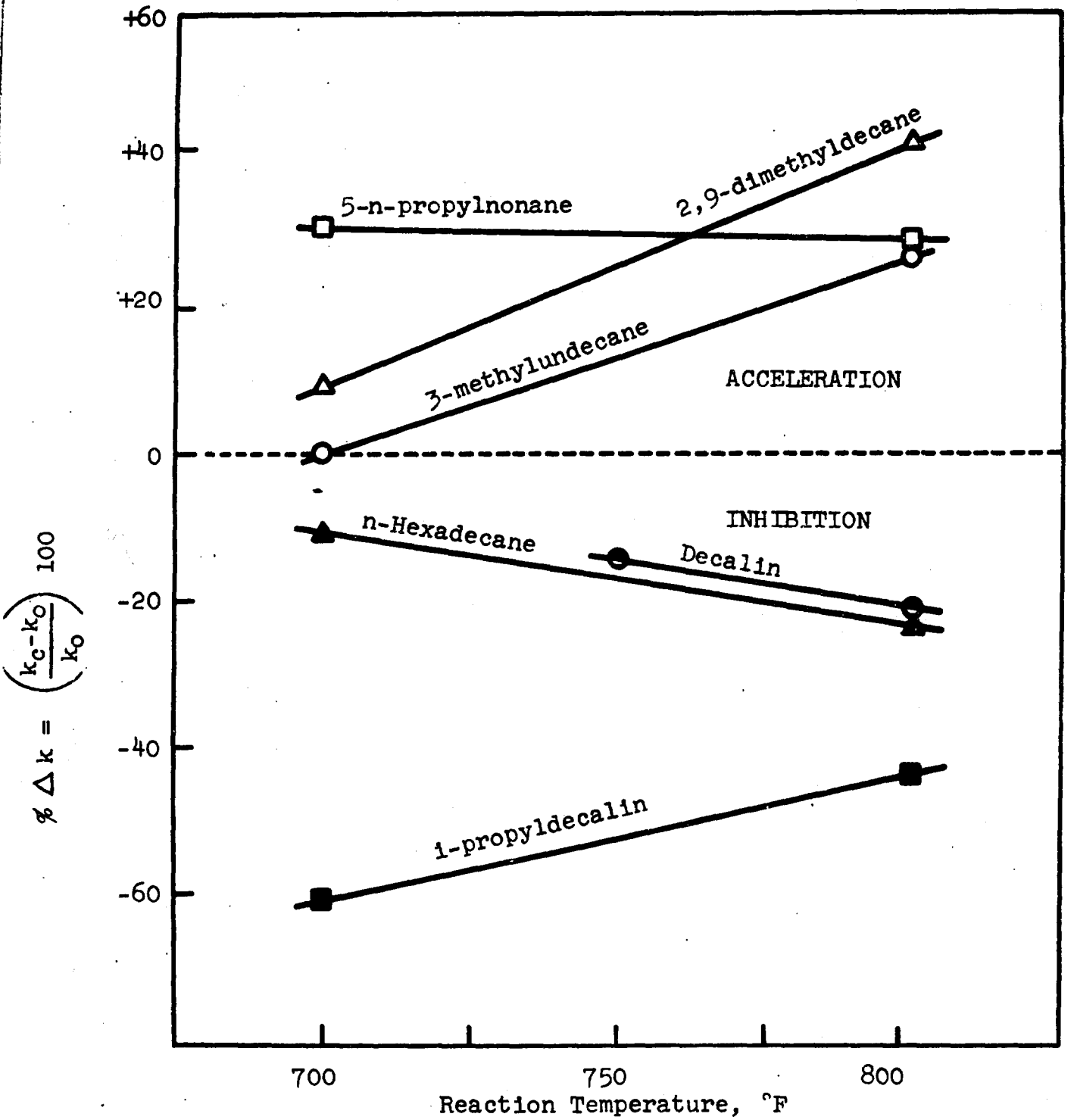

Figure 20. The Variation in the Effect of Sulfur Contamination with Temperature
(Contaminant: 0.1 wt-% t-butyldisulfide)

The free radical reaction mechanism of hydrocarbon decomposition can be given by the following reaction series (ref. 25):

Free radical formation:

$$R_1H \xrightarrow{k_1} R' + R'' \xrightarrow{2R_1H} 2R_1 + R'H + R''H \quad (30)$$

$$R_1H + S_1 \xrightarrow{k_2} S_1H + R_1 \quad (31)$$

Chain reaction:

$$R_1 \xrightarrow{k_3} Ol + R_2 \quad (32)$$

$$R_2 + R_1H \xrightarrow{k_4} R_2H + R_1 \quad (33)$$

Chain termination:

$$R_1 + \text{wall} \xrightarrow{k_5} \quad (34)$$

$$R_1 + R_2 \xrightarrow{k_6} \quad (35)$$

$$R_1 + R_1 \xrightarrow{k_7} \text{Inactive Products} \quad (36)$$

$$R_2 + R_2 \xrightarrow{k_8} \quad (37)$$

$$R_1 + S_1 \xrightarrow{k_9} \quad (38)$$

$$R_2 + S_1 \xrightarrow{k_{10}} \quad (39)$$

where, R_1H = original hydrocarbon

R',R'' = intermediate radicals

R_1 = long radical

S_1 = organosulfur radical

R_2 = short radical

Ol = olefinic product

R_2H = paraffinic product

*The free radical formation mechanism from hydrocarbons can be given by different mechanisms. The important fact is that free radicals are formed by first-order kinetics.

In the absence of sulfur contaminants, reactions (31), (38), and (39) cannot take place. The chain termination by reactions (34), (35), (36), or (37) determines the order of reaction. Since chain termination by interaction of long radicals according to reaction (37) gives a 1/2-order reaction rate equation, and since chain termination by interaction of short radicals according to reaction (37) gives a 3/2-order reaction, both reactions were disregarded in our further treatment. A detailed treatment of hydrocarbon decomposition by the Rice-Herzfelder mechanism can be found in textbooks (see ref. 37). The rate of the decomposition reaction can be expressed as

$$\text{Rate of reaction} = W = \frac{\text{(rate of free radical formation) x (rate of chain propagation)}}{\text{rate of chain termination}} =$$

$$\frac{[2k_1(R_1H) + k_2(R_1H)(S_1)]k_3(R_1)}{k_5(R_1) + k_6(R_1)(R_2) + k_9(R_1)(S_1) + k_{10}(R_2)(S_1)} \qquad (40)$$

This equation is too complicated to permit any conclusions to be drawn, and even for pure hydrocarbons, simpler forms of this equation must be considered.

For pure hydrocarbons, two chain terminations yield first-order reaction schemes; termination on the wall and interaction of R_1 and R_2 radicals.

For termination by reaction (34):

$$W = \frac{2k_1(R_1H)k_3(R_1)}{k_5(R_1)} = \frac{2k_1k_3}{k_5}(R_1H) \qquad (41)$$

and if termination by reaction (35) is considered:

$$W = \frac{2k_1(R_1H)k_3(R_1)}{k_6(R_1)(R_2)} = \frac{2k_1k_3(R_1H)}{k_6(R_2)} \qquad (42)$$

The rate of the chain reactions must be equal,

$$k_3(R_1) = k_4(R_2)(R_1H) \qquad (43)$$

and the rate of free radical formation (equation 30) and free radical disappearance (equation 35) must be also equal.

$$2k_1(R_1H) = k_6(R_1)(R_2) \qquad (44)$$

From equations (43) and (44):

$$[R_2] = \sqrt{\frac{2k_1k_3}{k_4k_6}} \qquad (45)$$

Introducing this value into equation (42):

$$W = \sqrt{\frac{2k_1k_3k_4}{k_6}}\ (R_1H) \qquad (46)$$

Both equations (41) and (46) are first-order rate expressions.

An inhibition by sulfur contaminants can be explained by rapid termination of chains by reactions (38) or (39). Assuming chain termination preferentially by reaction (38):

$$W = \frac{2k_1(R_1H)k_3(R_1)}{k_9(R_1)(S_1)} = \frac{2k_1k_3}{k_9}\ \frac{(R_1H)}{(S_1)} \qquad (47)$$

For chain termination by reaction (39):

$$W = \frac{2k_1(R_1H)k_3(R_1)}{k_{10}(R_2)(S_1)} = \frac{2k_1(R_1H)k_4(R_2)(R_1H)}{k_{10}(R_2)(S_1)} = \frac{2k_1k_4}{k_{10}}\ \frac{(R_1H)^2}{(S_1)} \qquad (48)$$

Equation (47) represents a first-order reaction with respect to R_1H hydrocarbon which is inhibited by increasing concentrations of the S_1 organosulfur radical produced from the sulfur contaminant. Equation (48) is a second-order reaction with respect to the hydrocarbon, and is therefore disregarded.

An acceleration by sulfur contaminants can be explained by rapid free radical formation by reaction (31) without affecting the chain termination step.

Assuming chain initiation by reaction (31) and chain termination by reaction (34) we obtain

$$W = \frac{k_2(R_1H)(S_1)k_3(R_1)}{k_5(R_1)} = \frac{k_2k_3}{k_5}\ (R_1H)(S_1) \qquad (49)$$

which is a first-order reaction with respect to the hydrocarbon, promoted by increasing concentrations of S_1 organosulfur radical. Assuming chain termination by reaction (35)

$$W = \frac{k_2(R_1H)(S_1)k_3(R_1)}{k_6(R_1)(R_2)} = \frac{k_2k_3}{k_6}\ \frac{(R_1H)(S_1)}{(R_2)} \qquad (50)$$

and using the same conditions as for equations (43) and (44)

$$k_3(R_1) = k_4(R_2)(R_1H) \qquad (43)$$

$$k_2(R_1H)(S_1) = k_6(R_1)(R_2) \qquad (51)$$

$$(R_2) = \sqrt{\frac{k_2k_3}{k_4k_6}}\ (S_1)^{1/2} \qquad (52)$$

Introducing this value into equation (50)

$$W = \sqrt{\frac{k_2 k_3 k_4}{k_6}} (R_1H)(S_1)^{1/2} \qquad (53)$$

This is a first-order reaction with respect to the hydrocarbon, promoted by increasing concentrations of S_1 organosulfur radical. The experimental data are not sufficiently precise to permit a choice between the reaction mechanisms assumed in deriving equations (49) and (53). Both mechanisms represent the trend of the experimental data.

We may also consider the case where both the chain formation is promoted (equation 31) and the chain termination is accelerated (equations 38,39) by organosulfur radicals. If reactions (31) and (38) are preferred, the result is

$$W = \frac{k_2 k_3}{k_9} (R_1H) \qquad (54)$$

and for reactions (31) and (39):

$$W = \frac{k_2 k_4}{k_{10}} (R_1H)^2 \qquad (55)$$

In both cases, the reaction rate is independent of the concentration of S_1 radicals, and therefore equation (54) and (55) do not represent the experimental results.

In summary, the rate of reaction can be expressed by the following equations:

For pure hydrocarbons

$$W = \frac{2k_1 k_3}{k_5} (R_1H) \qquad (41)$$

or

$$W = \sqrt{\frac{2k_1 k_3 k_4}{k_6}} (R_1H) \qquad (46)$$

For inhibition by S_1 radicals

$$W = \frac{2k_1 k_3}{k_9} \frac{(R_1H)}{(S_1)} \qquad (47)$$

And, for acceleration by S_1 radicals

$$W = \frac{k_2 k_3}{k_5} (R_1H)(S_1) \qquad (49)$$

These results explain the experimental facts and indicate the mechanism of the hydrocarbon decomposition in the absence and in the presence of sulfur contaminants.

To obtain in each case the first-order kinetics in the decomposition process for pure hydrocarbons, chains must be terminated either by deactivation of the long free radicals on the wall or, preferably, by interaction of long and short free radicals. Both of these chain terminations result in a first-order kinetic expression as given by equation (41) or (46).

For inhibition of the decomposition in the presence of sulfur contaminants, it was experimentally shown that the reaction rate is inversely proportional to the sulfur contaminant concentration. An interaction of long free radicals with organosulfur radicals according to reaction (38) yields a rate equation corresponding to this behavior (equation 47) according to which the rate of decomposition is proportional to the hydrocarbon concentration. This means first-order kinetics with respect to the hydrocarbon, and the rate is inversely proportional to the contaminant concentration.

For acceleration of the decomposition by contaminants, only equation (49) represents the experimental data. The acceleration can be explained here by hydrogen abstraction from the hydrocarbon by organosulfur radicals and faster chain generation due to the presence of the contaminant.

All other combinations of radical initiation and radical terminations lead to kinetic expressions that do not express the experimental results properly.

The different behavior of isoparaffinic hydrocarbons compared with n-paraffinic and naphthenic hydrocarbons can be explained by the ease of abstracting hydrogen atoms from the iso-paraffins, and by the higher stability of n-paraffins and naphthenics toward hydrogen abstraction. Because of this difference in the behavior of hydrocarbons, the organosulfur radicals formed in the decomposition of the contaminants are used up, either in the initiation step accelerating the reaction or in the chain termination step inhibiting the decomposition reaction.

C. SULFUR CONTAMINATION AND PARTICLE FORMATION

Earlier work showed that the formation of insoluble particles in the reaction tubes takes place after decomposition has proceeded (ref. 38) to a certain extent, usually about 30% or more. Because of the fundamental importance of particle formation in this project, it was of interest to determine whether the observed decomposition rate changes were accompanied by corresponding and normal changes in the extent of particle formation.

An experimental study was made of the decomposition of decalin whose decomposition rate was inhibited by sulfur compounds and also of 2,2,8,8-tetramethylnonane whose decomposition rate was accelerated. The usual particle counting techniques developed in this project were used as was the standard terminology (ref. 38). An added piece of information was obtained in the decalin study by measuring the light transmittance of the reacted liquid mixture contained in the glass reaction tube. A Coleman model 14 spectrophotometer was used, and the relative optical density of the samples was recorded to judge the effect of contamination.

The data of this study are shown in Table 20. For decalin, the inhibition of cracking caused by the presence of t-butyldisulfide was accompanied by a lighter color in the reacted sample, a lowered optical density, and a reduction in the number and size of particles. With 2,2,8,8-tetramethylnonane, the increased decomposition in the contaminated samples was paralleled by an increase in number and size of particles. In this case, however, the color remained the same.

From these results it is concluded that the effect of an organosulfur contaminant in changing the decomposition and particle formation rates of a hydrocarbon is similar to that obtained in changing the residence time or temperature in the reaction tube. This conclusion may not hold generally, however, at higher-than-normal contaminant concentrations (above 0.1%) where the organosulfur compound itself could perhaps form a significant amount of particles by cracking and/or polymerization.

D. DECOMPOSITION IN THE PRESENCE OF AIR AND CONTAMINANT

1. Synergetic Effect

When cetane containing 2.0 wt-% of phenyldisulfide as a contaminant was thermally decomposed in the presence of air a synergetic effect was observed between the air and the sulfur contaminant in the formation of particles. Thus, the number of insoluble particles formed in reacted samples was greater than could be logically predicted from the effects of sulfur and air acting alone. This observation was not made with 5-n-propylnonane and decalin, indicating that the substrate had much to do with the observed effect.

Because of the potential importance of this synergetic behavior it was decided to extend the experimental work in this area. Hydrindan, 2,2,8,8-tetramethylnonane, 2,9-dimethyldecane, and n-hexadecane were contaminated with 0.1 wt-% t-butyldisulfide and decomposed with and without the presence of air. Four samples were run in each experiment, which utilized the usual static apparatus and technique. Three of the samples were controls; a detailed description of the samples follows:

(a) Control, evacuated, no t-butyldisulfide

(b) Control, air bubbled through the substrate at room temperature for 5 minutes, no evacuation and no t-butyldisulfide

(c) Control, evacuated but with 0.1% t-butyldisulfide

(d) Air bubbled through for 5 minutes at room temperature, no evacuation, and contained 0.1% t-butyldisulfide.

Table 20

PARTICLE FORMATION IN SAMPLES CONTAMINATED WITH t-BUTYLDISULFIDE

Decalin at 800°F (Inhibition)				
Hours	22.5	22.5	22.5	
t-Butyldisulfide, wt-%	0	0.01	0.1	
% Cracked	49.7	46.2	45.9	
*Optical Density	0.22	0.22	0.09	
Particles	4AI-2μ	4AI-1μ	1AI-1μ	
Color	dark amber	dark brown	amber	
2,2,8,8-Tetramethylnonane at 800°F (Acceleration)				
Hours	1.5	1.5	3	3
t-Butyldisulfide, wt-%	0	0.1	0	0.1
% Cracked	31.1	55.4	53.7	72.1
Particles	none	1AS-1-2μ	1AS-2-4μ	50-300 pieces fused polymer
Color	amber	amber	dark brown	dark brown

*Optical density (= -log transmittance) measured on a Coleman Model 14 Spectrophotometer using a purple filter 14-214 and 650 mμ light.

No evidence of a synergetic effect on particle formation was observed in these experimental runs. Any increase in the number of particles in a particular reaction tube was accompanied by an increased level of conversion and was therefore to be expected.

Since no evidence for a synergetic effect had been found, a repeat of the original experiment using cetane and 2 wt-% phenyldisulfide was made. Once again, four samples were run. The reaction temperature was 800°F and the residence time at that temperature was two hours. The data are presented in Table 21.

The usual inhibition of decomposition rate by the sulfur contaminant was observed but there was no effect on the decomposition rate due to the presence of air. Therefore, the very considerable increase in the amount of particles found in the sample containing both air and the sulfur compound can only be explained by synergetic behavior.

In the past, it was generally observed that the extent of particle formation was closely related to the degree of conversion: the more conversion, the greater the particle formation. In this experiment, the two control samples which had no sulfur contamination were decomposed to the greatest extent but it was the sample containing both sulfur and air that showed the greatest particle formation. This was further evidence of synergetic behavior.

An experiment with 2 wt-% of t-butyldisulfide in cetane showed similar synergetic behavior when air was present in the reaction tube. When 0.1 wt-% of t-butyldisulfide in n-hexadecane was used, no increase in particle formation could be discerned. It therefore seems probable that the increase in particle formation is caused by polymerization of the organosulfur contaminant itself. The role of the hydrocarbon substrate is not clear. Synergetic behavior has been observed only where n-hexadecane was the substrate.

2. Prolonged Air Exposure

The question investigated was whether or not sulfur contamination plus prolonged exposure to air would bring about particle formation at low temperature with a short reaction time. The practical situation envisaged was that of a supersonic aircraft carrying fuel containing a sulfur contaminant making a flight of a few hours and then sitting idle for a few days. The question of interest was whether the residual fuel in the aircraft's tanks would be contaminated by the formation of particles.

The hydrocarbon substrate chosen was 2,2,8,8-tetramethylnonane, a relatively stable branched paraffin, but one whose rate of decomposition was much accelerated by the presence of 0.1 wt-% t-butyldisulfide, the contaminant for this experiment. All samples tubes were run for 4 hours at 700°F. Half of the tubes were evacuated, and the other half were sealed with air in them. In addition, air was bubbled through the hydrocarbon for five minutes at room temperature before sealing the tubes.

Table 21

PARTICLE FORMATION IN n-HEXADECANE DECOMPOSITION:
THE SYNERGETIC EFFECT OF AIR AND PHENYLDISULFIDE

Reaction Temperature: 800°F
Reaction Time: 2 hours
Contaminant: 2 wt-% phenyldisulfide

Sample	% Cracked	Particles (relative amount)
n-Hexadecane, evacuated	82.2	moderate, normal
n-Hexadecane, air in tube	81.1	moderate, normal
n-Hexadecane, air in tube, with 2% phenyldisulfide	65.8	most, abnormal
n-Hexadecane, evacuated, with 2% phenyldisulfide	62.4	least, normal

A pair of tubes (with and without air) was opened immediately after removal from the furnace and the extent of reaction determined while another such pair of tubes was left sealed for three more days. In addition, the liquid reaction products of each pair were run on the chromatograph every day for the ensuing three days. In this way, it was hoped to discover any tendency to form particles in samples exposed to air for prolonged periods of time after relatively mild cracking conditions.

All of the samples were decomposed about 15% and the results agreed with each other within experimental error. There was no change in the decomposition level or in the color of the reacted hydrocarbon upon standing whether exposed to air or not. No particles were observed in any sample. These results can be taken as further evidence that the real dangers of sulfur contamination of hydrocarbon fuels lie in high reaction temperatures (800°F) and high contaminant levels (over 1 wt-%).

VII. DECOMPOSITION OF BINARY MIXTURES

A. EXPERIMENTAL

Much data has been compiled on the decomposition rates of individual pure hydrocarbons. These data would be much more valuable if they could be used to predict the decomposition rate of mixtures of hydrocarbons. With this objective several binary hydrocarbon mixtures were studied experimentally.

Rates of decomposition or cracking were determined at constant temperature around 800°F using the usual sealed glass tubes to contain the hydrocarbons. The furnaces available held six tubes each. The mixtures were studied using only six tubes so that just one furnace was needed to contain the reaction tubes. Thus temperature variation between the tubes was eliminated.

Considering a binary mixture of A and B the six reaction tubes were made up as follows on a volume basis: pure A, 95% A + 5% B, 75% A + 25% B, 50% A + 50% B, 25% A + 75% B, and pure B. All six tubes were heated for the same time period.

A vapor phase chromatograph was used to determine the amount of unreacted A and B in the residual liquid after reactions. In Figure 21 the blank VPC peaks, A° and B° of the original unreacted mixture are shown, together with the residual peaks A and B. The liquid phase cracked products show up as a conglomeration of peaks.

The ratio of peak area A to peak area A° gives the fraction of A undecomposed and permits calculation of the first-order decomposition rate constant of A, k_A. Similarly k_B is calculated from the B/B° peak area ratio.

Pure A and pure B were cracked simultaneously with the blends and so the pure A and B rate constants, k_A and k_B, were available for comparison with the k_A and k_B values of the mixtures. In this way any interference in the cracking of A by the presence of B, or vice versa, could be detected.

The results showed such a definite interference that it seemed unlikely that an overall rate for the mixture could be predicted from the decomposition rates of the pure individual hydrocarbons. Nevertheless, the overall decomposition rate for each mixture was calculated from the experimental results as follows:

$$(k_{AB})_{exp.} = \frac{1}{t} \ln \left(\frac{A^\circ + B^\circ}{A + B} \right) \qquad (56)$$

In practice, the form of the equation used was:

$$(k_{AB})_{exp.} = \frac{2.303}{t} \log \left[\frac{1}{\alpha(1-x) + (1-\alpha)(1-y)} \right] \qquad (57)$$

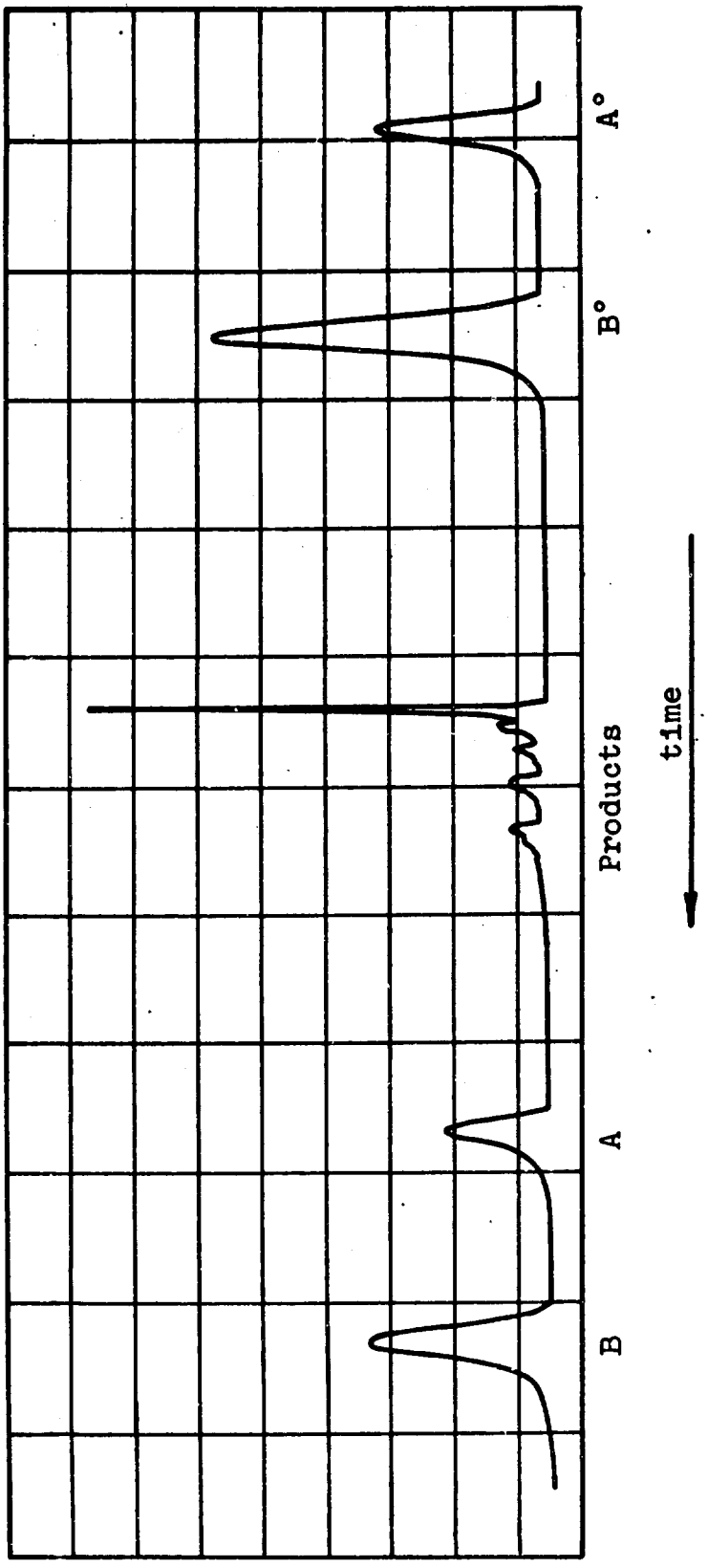

Figure 21. Typical Chromatograph for Binary Mixture Decomposition

where,

t = reaction time
α = fraction of A in mixture before reaction
1-α = fraction of B in mixture before reaction
1-x = fraction of A remaining after reaction
1-y = fraction of B remaining after reaction

These symbols are used in the data tables.

This procedure gives the rate constants of decomposition of the binary mixture assuming that only a single species (A + B) is present. This rate constant is referred to as (k_{AB}) exp. or the experimental value of the over-all rate constant.

If we assume that the two components of the mixture decompose independently, knowing the rate constants of decomposition of the pure compounds k_A and k_B, the residual concentration of each compound (A_{calc} and B_{calc}) can be calculated. If we now introduce these calculated residual concentrations into equation (57), we obtain a second set of k_{AB} values, which are called $(k_{AB})_{calc.}$ or the calculated theoretical over-all rate constants.

These two sets of rate constants are compared graphically in Figures 24, 27, 30, 33, 36 and 39.

B. RESULTS

The rate constant data presented here may not always agree exactly with those previously tabulated since generally the latter were average values. These new data are relative and can be readily compared with each other since the experimental conditions were entirely identical in the six samples of any mixture experiment.

For each of the binary mixtures investigated a summarizing table and three graphs are presented. The symbols used are as follows:

C = n-hexadecane
D = decalin
H = hydrindan
M = methyl hydrindan
N = 2,2,8,8-tetramethylnonane
X = t-butylcyclohexane

A superscript zero indicates that the value was determined by experimenting with a pure individual component. For example, k_c^0 means the decomposition rate constant for pure n-hexadecane.

1. n-Hexadecane - Decalin

This mixture was particularly interesting because of the very great difference in structure and decomposition rate for the two hydrocarbon. Referring to Figures 22 and 23, it is clear that the decalin and n-hexadecane interfered with each others' decomposition. The decomposi

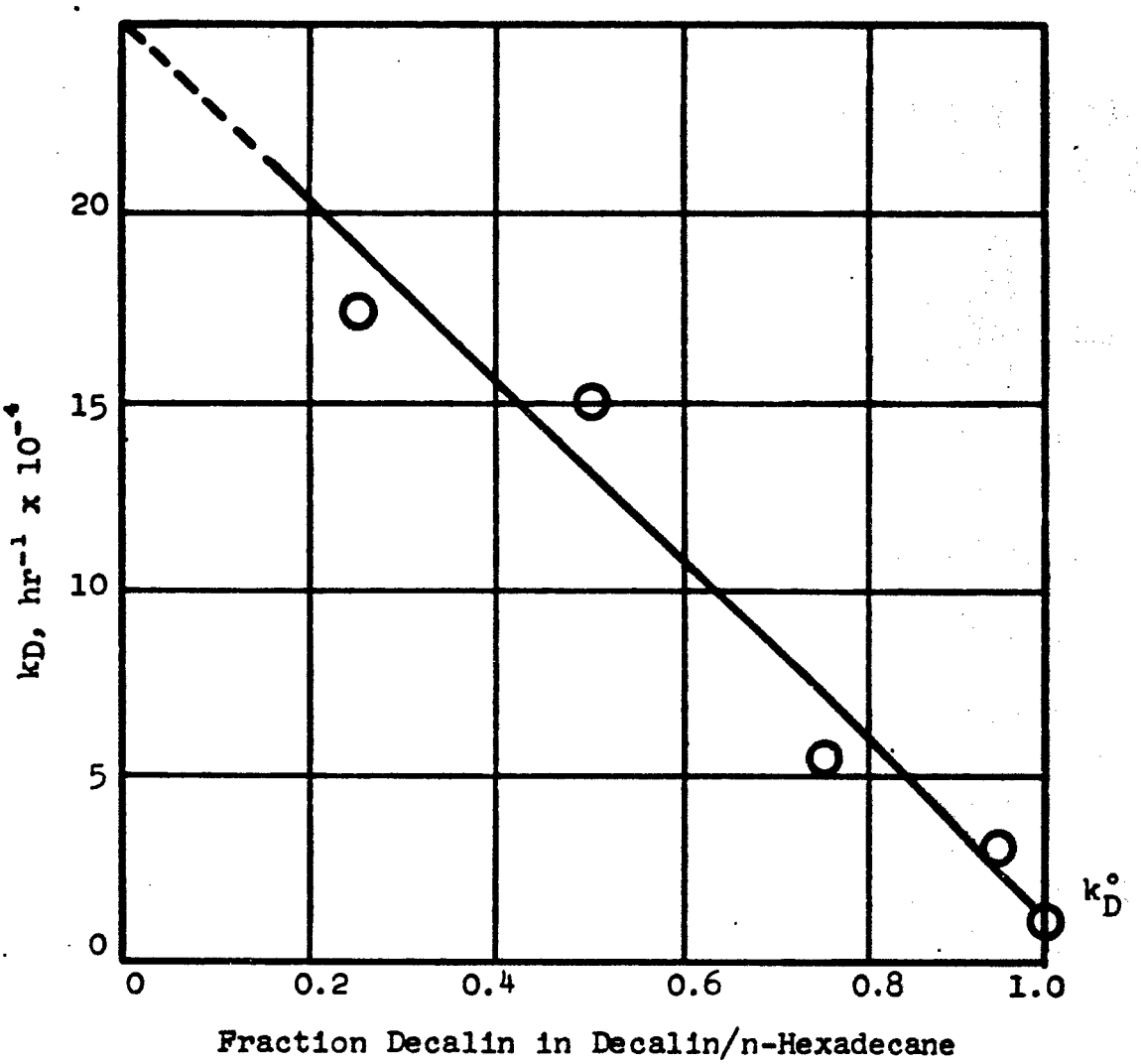

Figure 22. The Effect of Dilution with n-Hexadecane (C) on the Decomposition Rate Constant of Decalin (D) at 700°F

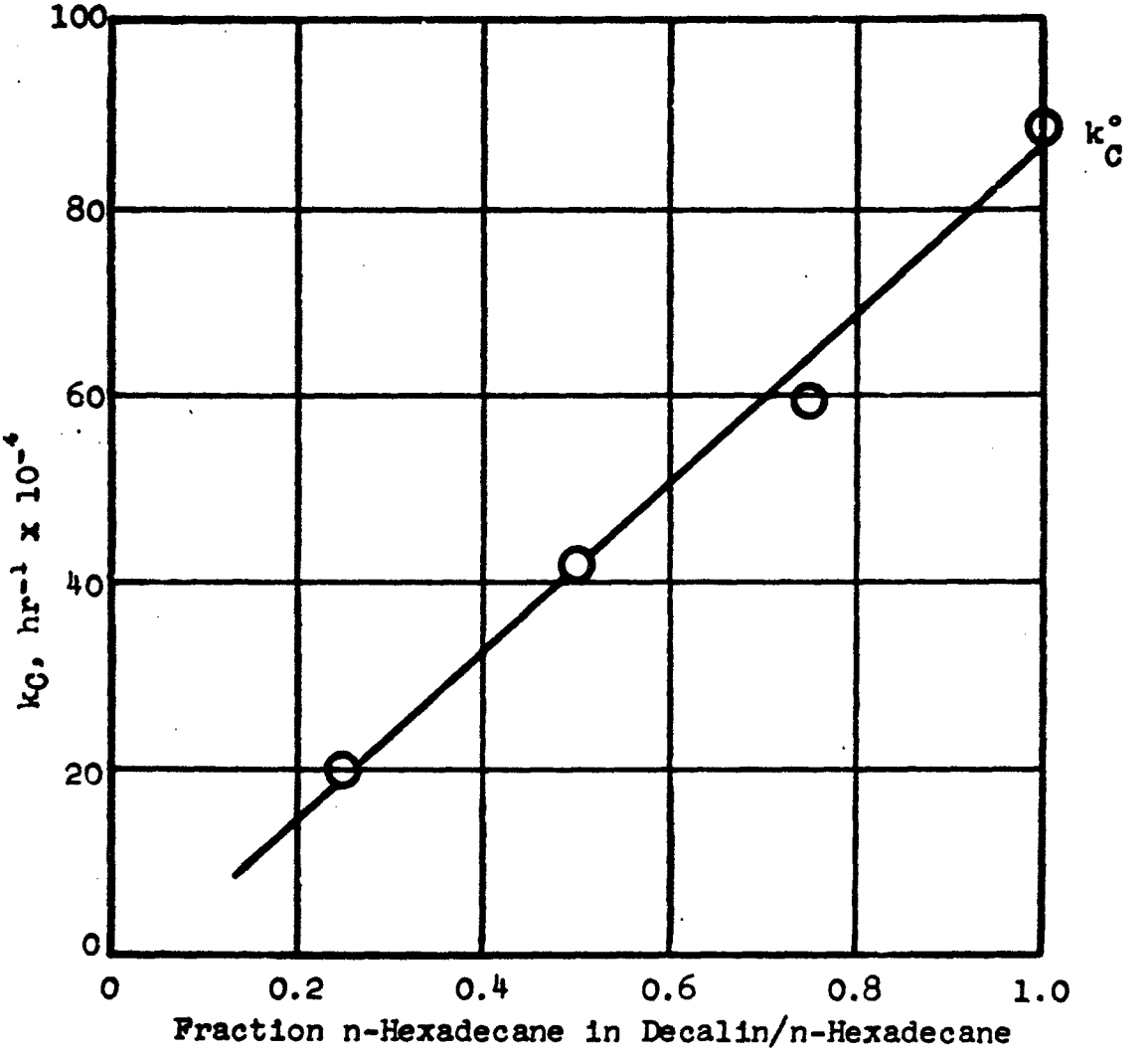

Figure 23. The Effect of Dilution with Decalin (D) on the Decomposition Rate Constant of n-Hexadecane (C) at 700°F

tion of the slow reacting decalin was significantly speeded up by the presence of the decomposing cetane. Conversely, the cracking of n-hexadecane was slowed by the presence of decalin in the reaction tube. A seemingly linear relationship between the individual rate constants and concentration in the mixture was demonstrated.

In Table 22 the overall k values for the mixture (k_{CD}) exp, which were calculated from the experimentally determined residual concentration of cetane and decalin (after pyrolysis), are listed together with the constants calculated knowing the decomposition behavior of the pure components only. In Figure 24 the two sets of k_{CD} values were plotted against the composition of the mixture. In this plot and the similar ones for the other mixtures, the correlating line is drawn through the experimentally determined values. The calculated values were then superimposed. Unless a very definite curvature in the correlation could be discerned (such as for the n-hexadecane decalin data) a straight line was drawn.

The agreement between the experimental and calculated values was exceptionally good. The decomposition rate of the n-hexadecane-decalin mixture changed smoothly with concentration from the lowest value for pure decalin to the highest for pure n-hexadecane. Knowing only the decomposition rates of pure n-hexadecane and pure decalin it was possible to calculate the rate for any blend of these two hydrocarbons with good accuracy.

2. Hydrindan-Decalin

Unlike n-hexadecane and decalin, hydrindan and decalin were much more alike in structure and decomposition rate. Both are fused-ring saturated naphthenes. It was therefore interesting to observe the same interaction between the decompositions (see Figures 25 and 26); hydrindan cracking was slowed down and decalin cracking was speeded up when they were pyrolyzed together in various binary mixtures. Furthermore, the predictability of the rate constant of the mixture k_{HD} from the individual rate constants of hydrindan and decalin, k_H° and k_D° was once again very good. The calculated values are shown in Figure 27 superimposed on the line through the values obtained by experiment.

3. Tetramethylnonane-t-butylcyclohexane

This mixture was cracked during 1962 as a first attempt at the study of mixtures, and the data were reported in the annual report of that year (ref. 38). These data were obtained by different workers than those presently investigating on the project. It is therefore gratifying that the values and the trends of these older results agree well with the data obtained in the recent experimental work. Once again the mutual interference in cracking of components was observed and the check between calculated and experimental values of the mixture decomposition rates was again sufficiently accurate for practical use. The recent experimental work is presented as Table 24 and Figures 28 to 30. The earlier work is given in Table 25 and Figures 31 to 33.

Table 22

THERMAL CRACKING OF BINARY MIXTURES
n-HEXADECANE-DECALIN

Run No. 157
Reaction temp. 700°F
Reaction time 166.5 hr

C = n-Hexadecane
D = Decalin

Component	Conc.		Fraction Remaining		k hr^{-1}	k_{CD} exp.	k_{CD} calc.
	α	1-α	1-x	1-y			
D	1.00	0	0.982	0	1.07×10^{-4}	1.07×10^{-4}	1.07×10^{-4}
D	0.25		0.913		5.44×10^{-4}		
C		0.5		0.718	19.9×10^{-4}	8.70×10^{-4}	13.9×10^{-4}
D	0.50		0.779		15.0×10^{-4}		
C		0.50		0.498	41.8×10^{-4}	27.0×10^{-4}	30.0×10^{-4}
D	0.25		0.749		17.3×10^{-4}		
C		0.75		0.372	59.3×10^{-4}	45.7×10^{-4}	52.5×10^{-4}
D	0.05		0.950		3.10×10^{-4}		
C		0.95		0	-	6.20×10^{-4}	3.44×10^{-4}
C	0	1.00	0	0.228	88.6×10^{-4}	88.6×10^{-4}	88.6×10^{-4}

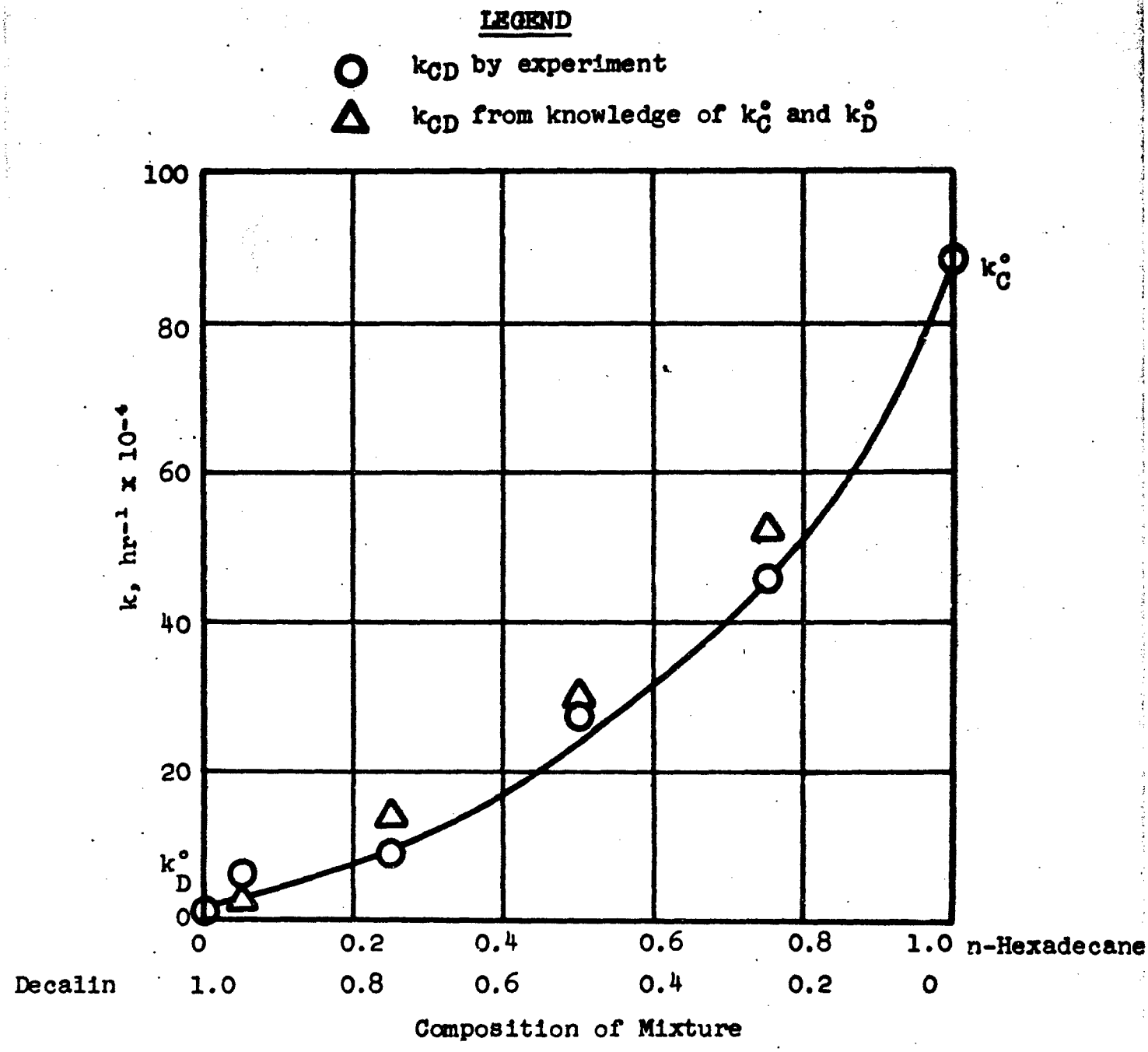

Figure 24. Decomposition Rate Constants of n-Hexadecane-Decalin Mixtures at 700°F

Table 23

THERMAL CRACKING OF BINARY MIXTURES
HYDRINDAN-DECALIN

Run No. 158
Reaction temp. 750°F
Reaction time 114 hr

H = Hydrindan
D = Decalin

Component	Conc.		Fraction Remaining		k hr^{-1}	k_{HD} exp.	k_{CD} calc.
	α	1-α	1-x	1-y			
H	1.00	0	0.505	0	5.99×10^{-3}	5.99×10^{-3}	5.99×10^{-3}
H	0.75		0.637		5.12×10^{-3}		
D		0.25		0.465	3.62×10^{-3}	4.33×10^{-3}	3.92×10^{-3}
H	0.50		0.558		4.12×10^{-3}		
D		0.50		0.662	3.36×10^{-3}	3.53×10^{-3}	3.05×10^{-3}
H	0.25		0.625		3.96×10^{-3}		
D		0.75		0.682	6.72×10^{-3}	4.55×10^{-3}	4.87×10^{-3}
H	0.05		0.720		2.88×10^{-3}		
D		0.95		0.671	3.50×10^{-3}	3.46×10^{-3}	2.41×10^{-3}
D	0	1.00	0	0.774	2.25×10^{-3}	2.25×10^{-3}	2.25×10^{-3}

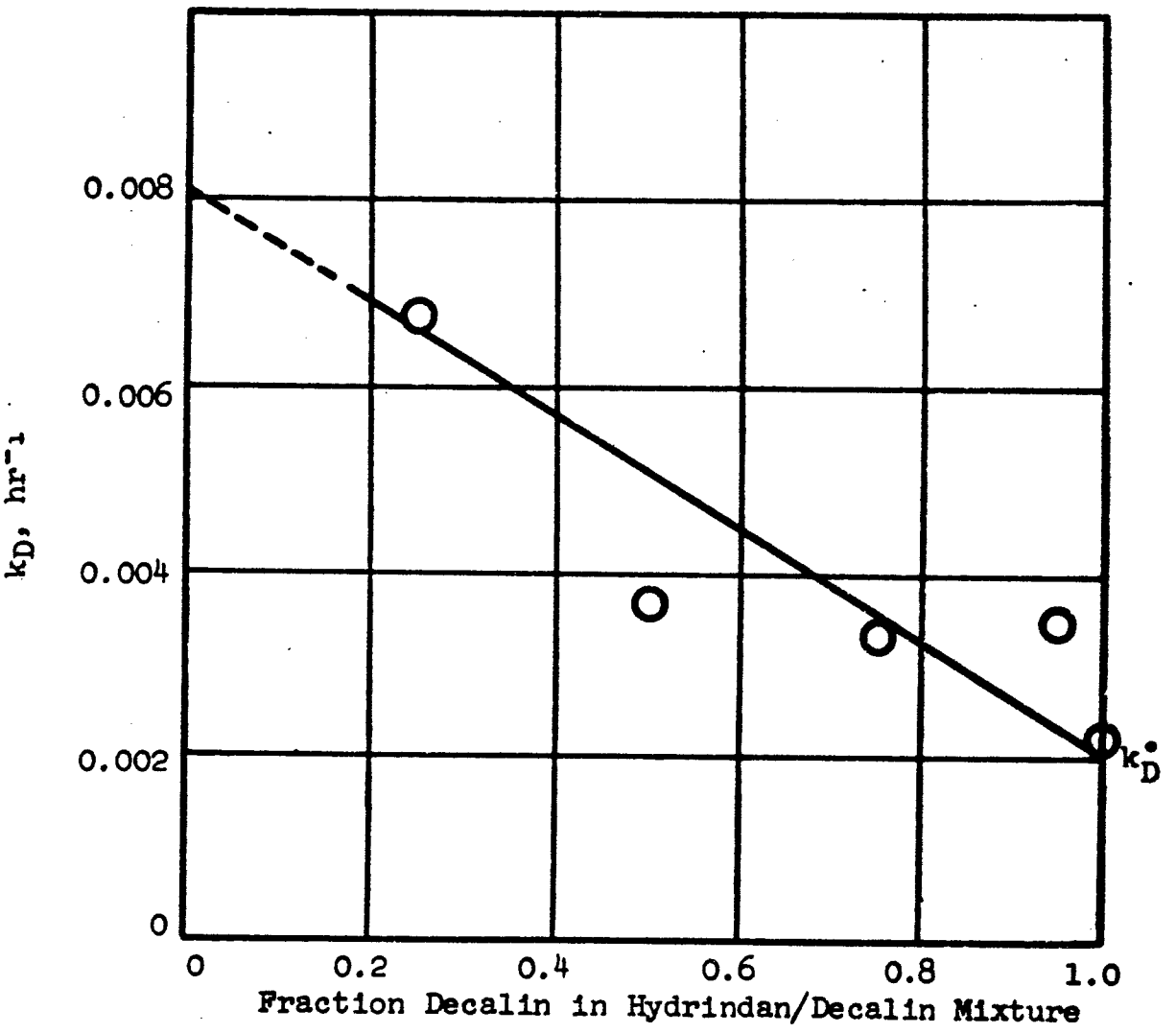

Figure 25. Effect of Dilution with Hydrindan (H) on the Decomposition Rate Constant of Decalin (D) at 750°F

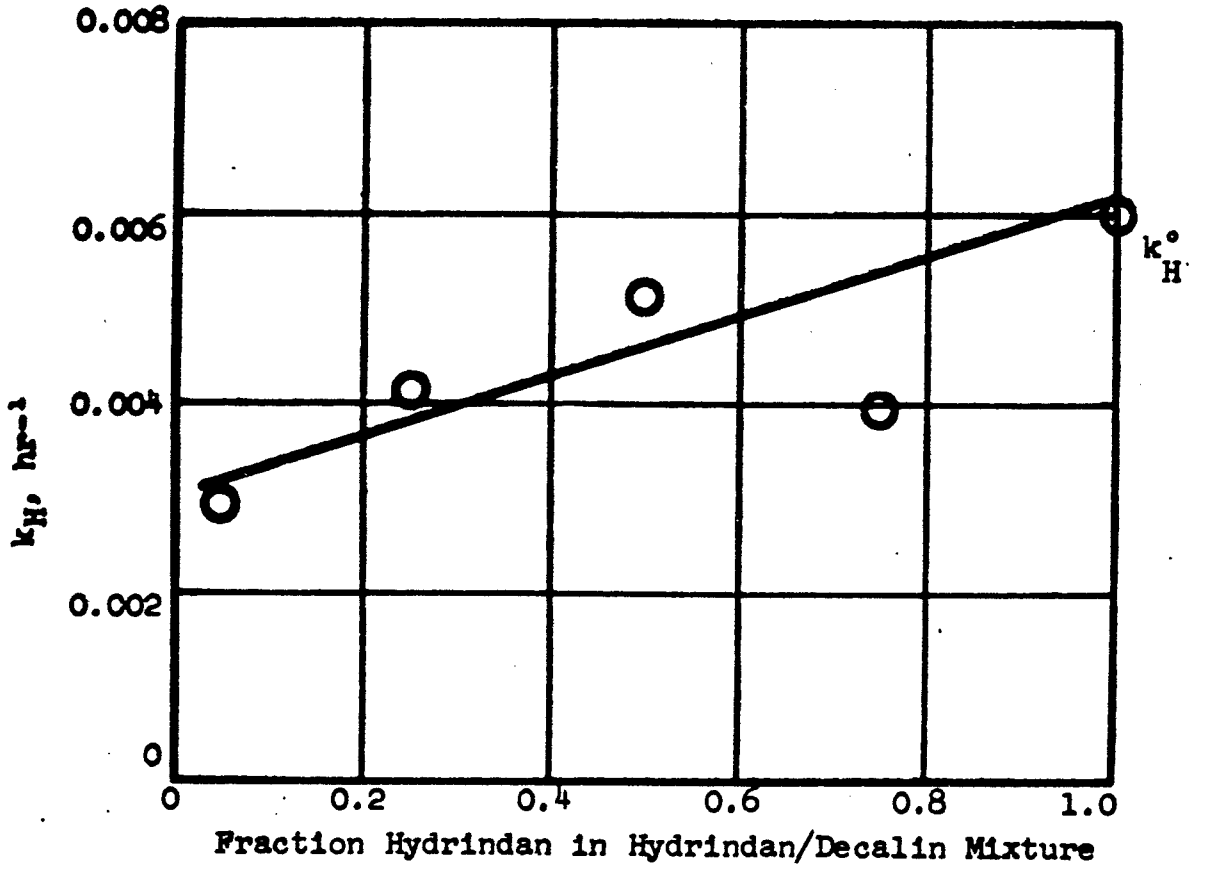

Figure 26. Effect of Dilution with Decalin (D) on the Decomposition Rate Constant of Hydrindan (H) at 750°F

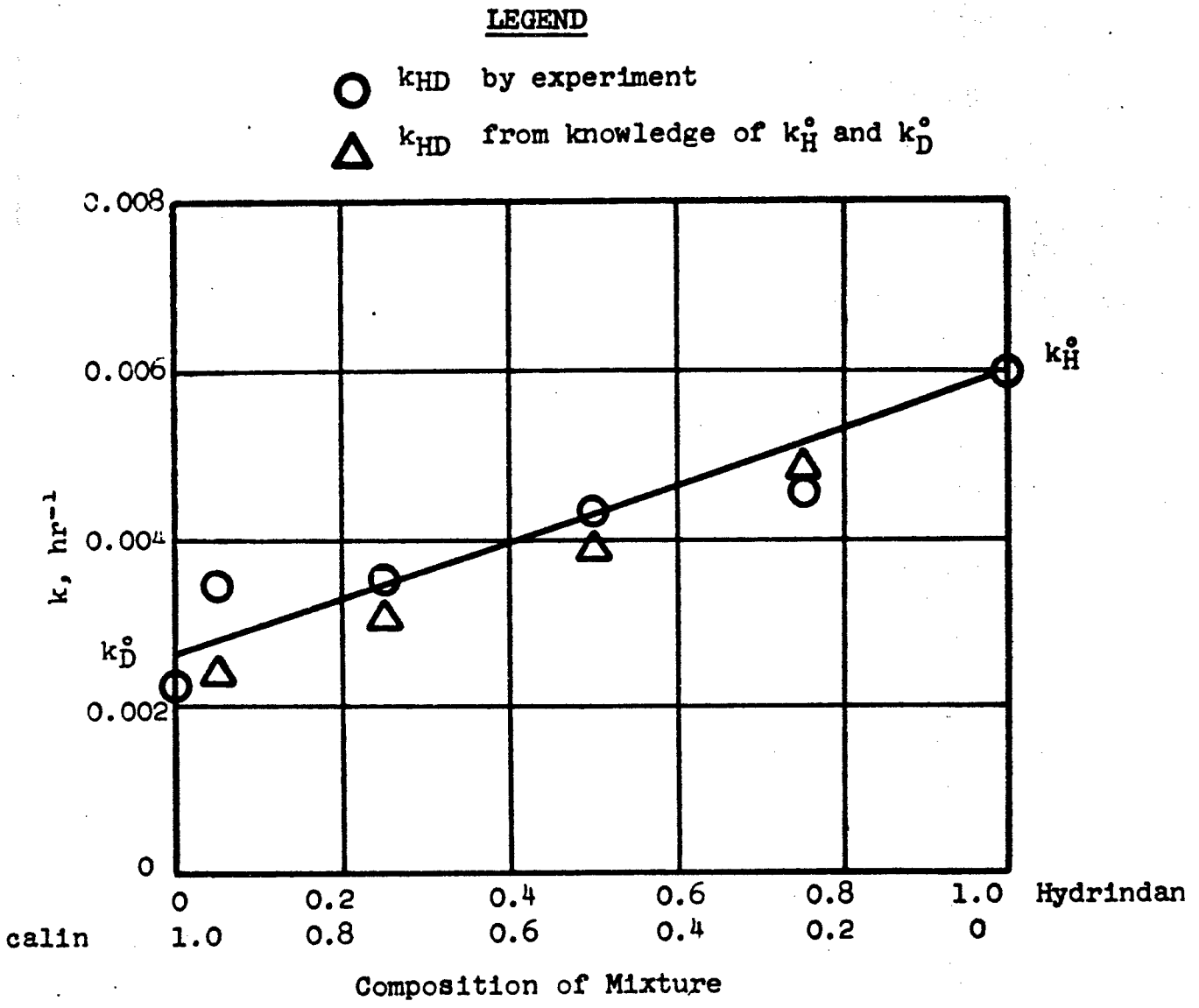

Figure 27. Decomposition Rate Constants of Hydrindan-Decalin Mixtures at 750°F

Table 24

THERMAL CRACKING OF BINARY MIXTURES
2,2,8,8-TETRAMETHYLNONANE-t-BUTYLCYCLOHEXANE (N-X)

Run No. 168
Reaction temp. 800°F
Reaction time 2 hr

N = 2,2,8,8-Tetramethylnonane
X = t-Butylcyclohexane

Component	Conc.		Fraction Remaining		k hr^{-1}	k_{NX} exp.	k_{NX} calc.
	α	1-α	1-x	1-y			
N	1.00	0	0.543	0	0.305	0.305	0.305
N	0.95		0.536		0.311		
X		0.05		0.588	0.265	0.309	0.297
N	0.75		0.552		0.296		
X		0.25		0.637	0.226	0.278	0.259
N	0.50		0.506		0.340		
X		0.50		0.553	0.296	0.317	0.215
N	0.25		0.648		0.216		
X		0.75		0.701	0.177	0.187	0.177
X	0	1.00	0	0.755	0.141	0.141	0.141

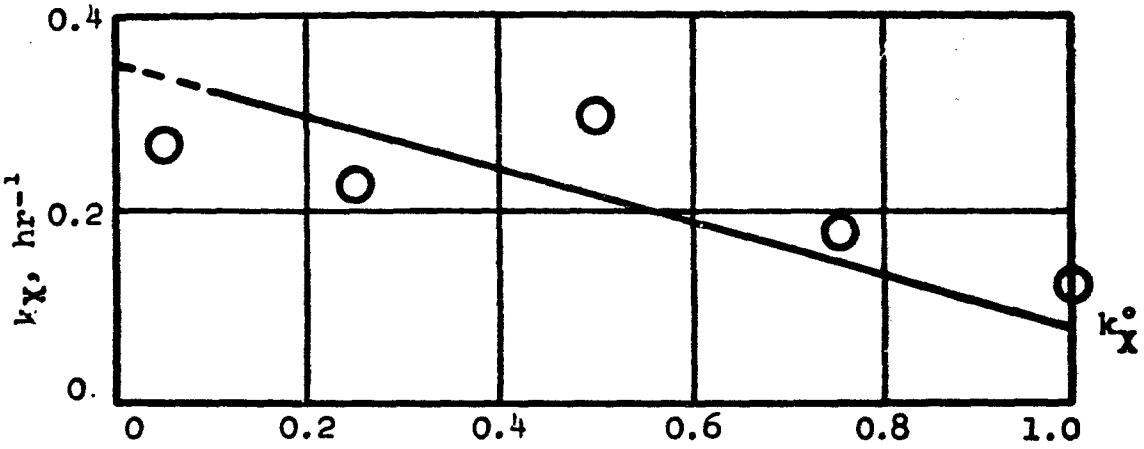

Figure 28. The Effect of Dilution with 2,2,8,8-Tetramethylnonane (N) on the Decomposition Rate Constant of t-Butylcyclohexane (X) at 800°F

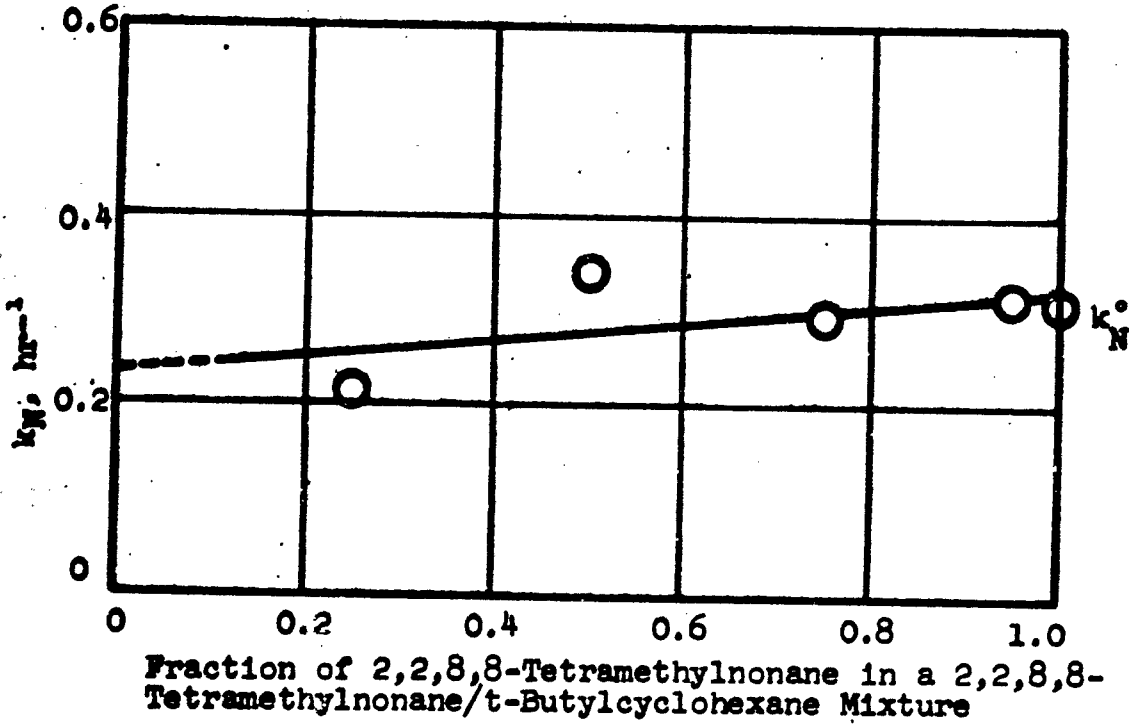

Figure 29. The Effect of Dilution with t-Butylcyclohexane (X) on the Decomposition Rate Constant of 2,2,8,8-Tetramethylnonane (N) at 800°F

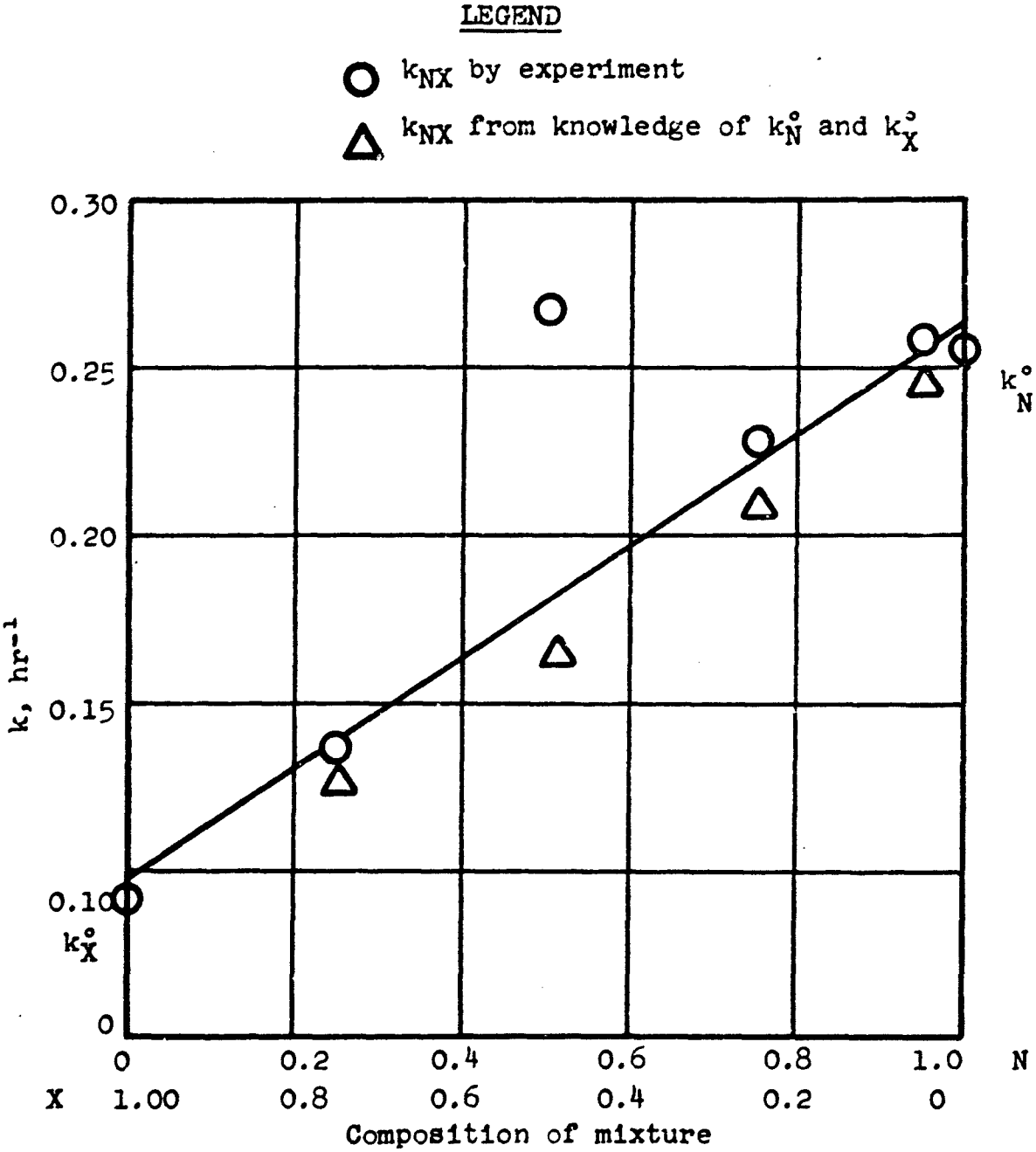

Figure 30. Decomposition Rate Constant of 2,2,8,8-Tetramethylnonane-t-Butylcyclohexane Mixtures at 800°F

Table 25

THERMAL CRACKING OF BINARY MIXTURES
2,2,8,8-TETRAMETHYLNONANE-t-BUTYLCYCLOHEXANE (N-X)

Run No: Annual report, 1962, Table 4 (Ref. 38)
Reaction temp: 800°F
Reaction time: Various (2 hr used)

N = 2,2,8,8-Tetramethylnonane
X = t-Butylcyclohexane

Component	Conc.		Fraction Remaining		k hr^{-1}	k_{NX} exp.	k_{NX} calc.
	α	1-α	1-x	1-y			
N	1.00	0	0.524	0	0.324	0.324	0.324
N	0.925		0.537		0.310		
X		0.075		0.695	0.182	0.300	0.304
N	0.807		0.598		0.257		
X		0.193		0.685	0.189	0.243	0.277
N	0.508		0.643		0.221		
X		0.492		0.733	0.156	0.187	0.214
N	0.506		0.658		0.209		
X		0.494		0.676	0.196	0.186	0.215
N	0.324		0.673		0.194		
X		0.676		0.759	0.140	0.157	0.180
N	0.116		0.652		0.214		
X		0.884		0.745	0.147	0.154	0.144
X	0	1.00	0	0.779	0.124	0.124	0.124

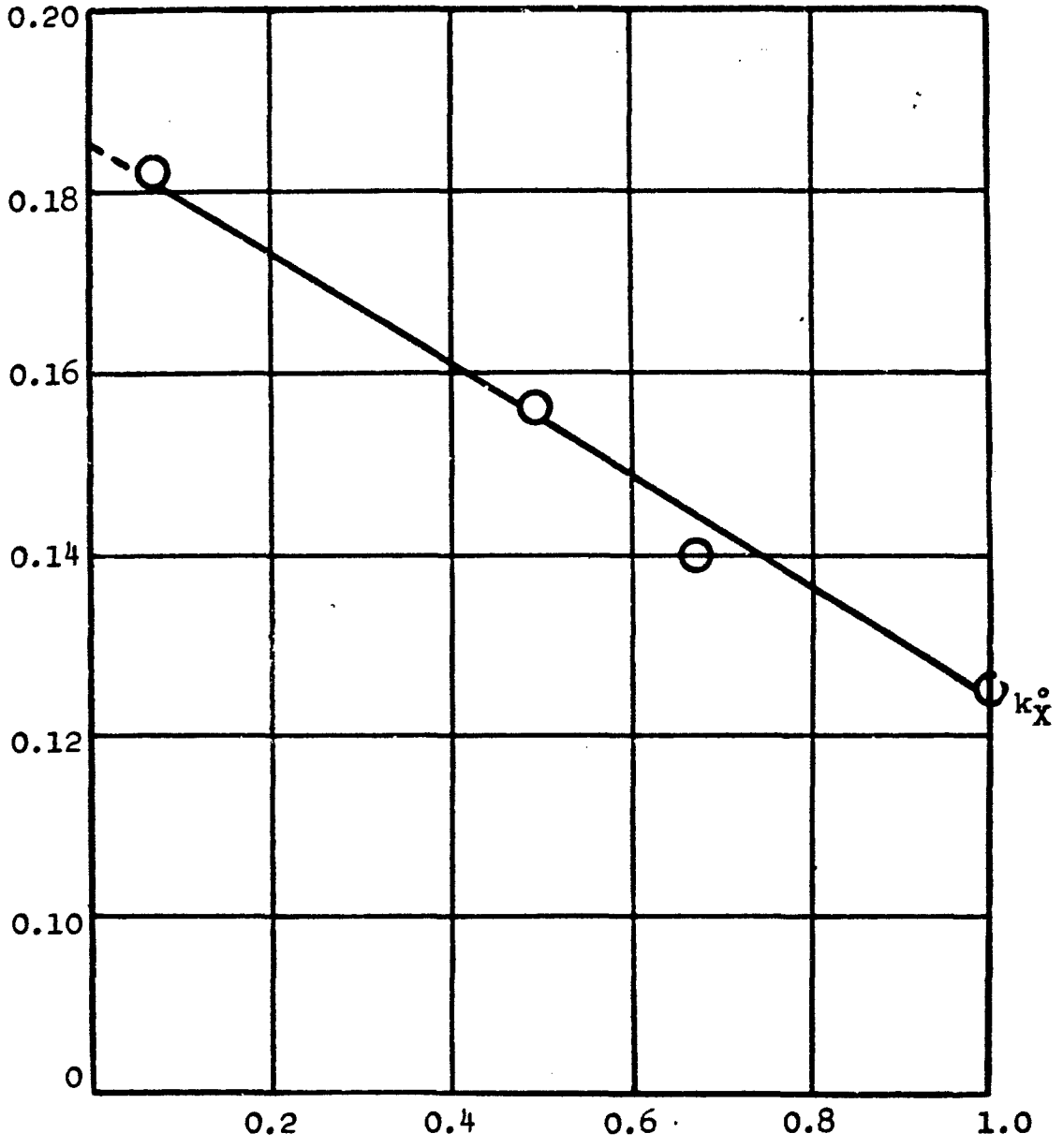

Fraction of t-Butylcyclohexane in Mixture of 2,2,8,8-Tetramethylnonane and t-Butylcyclohexane

Figure 31. Effect of Dilution with 2,2,8,8-Tetramethylnonane (N) on the Decomposition Rate Constant of t-Butylcyclohexane (X) at 800°F

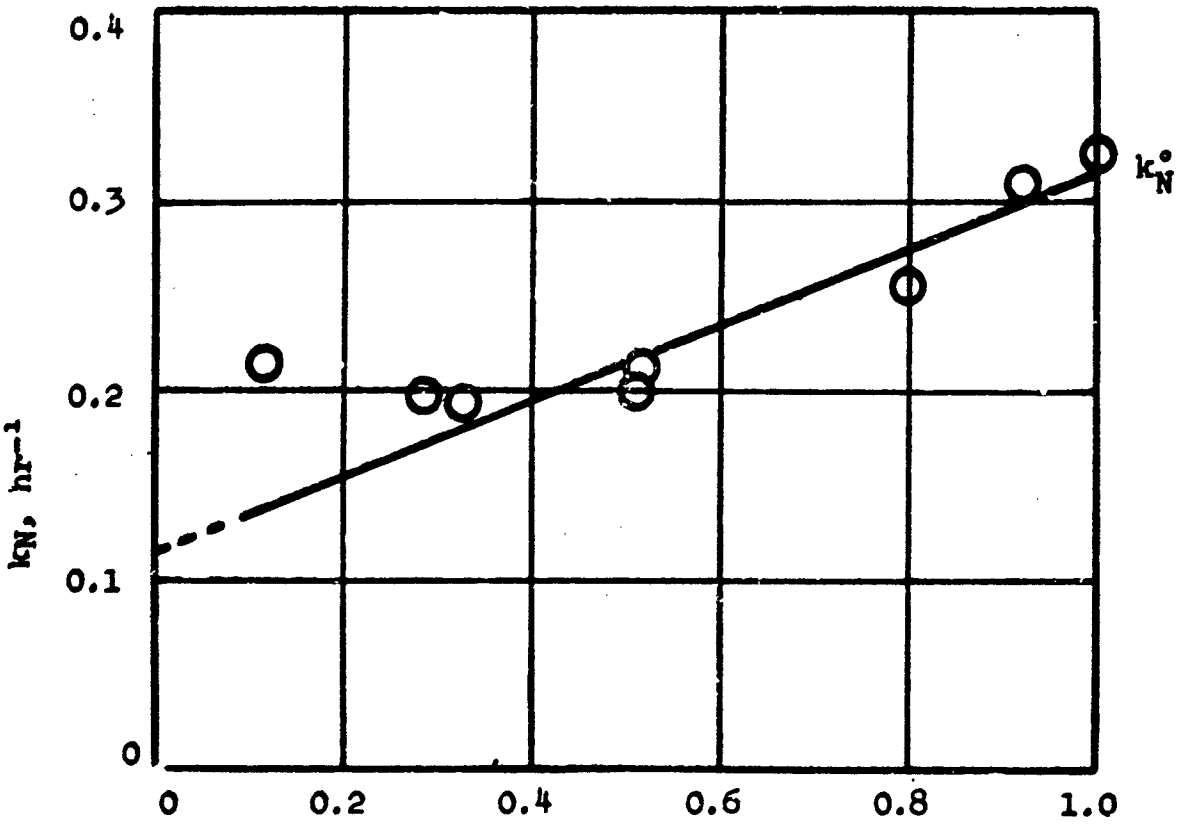

Figure 32. Effect of Dilution with t-Butylcyclohexane (X) on the Decomposition Rate Constant of 2,2,8,8-Tetramethylnonane (N) at 800°F

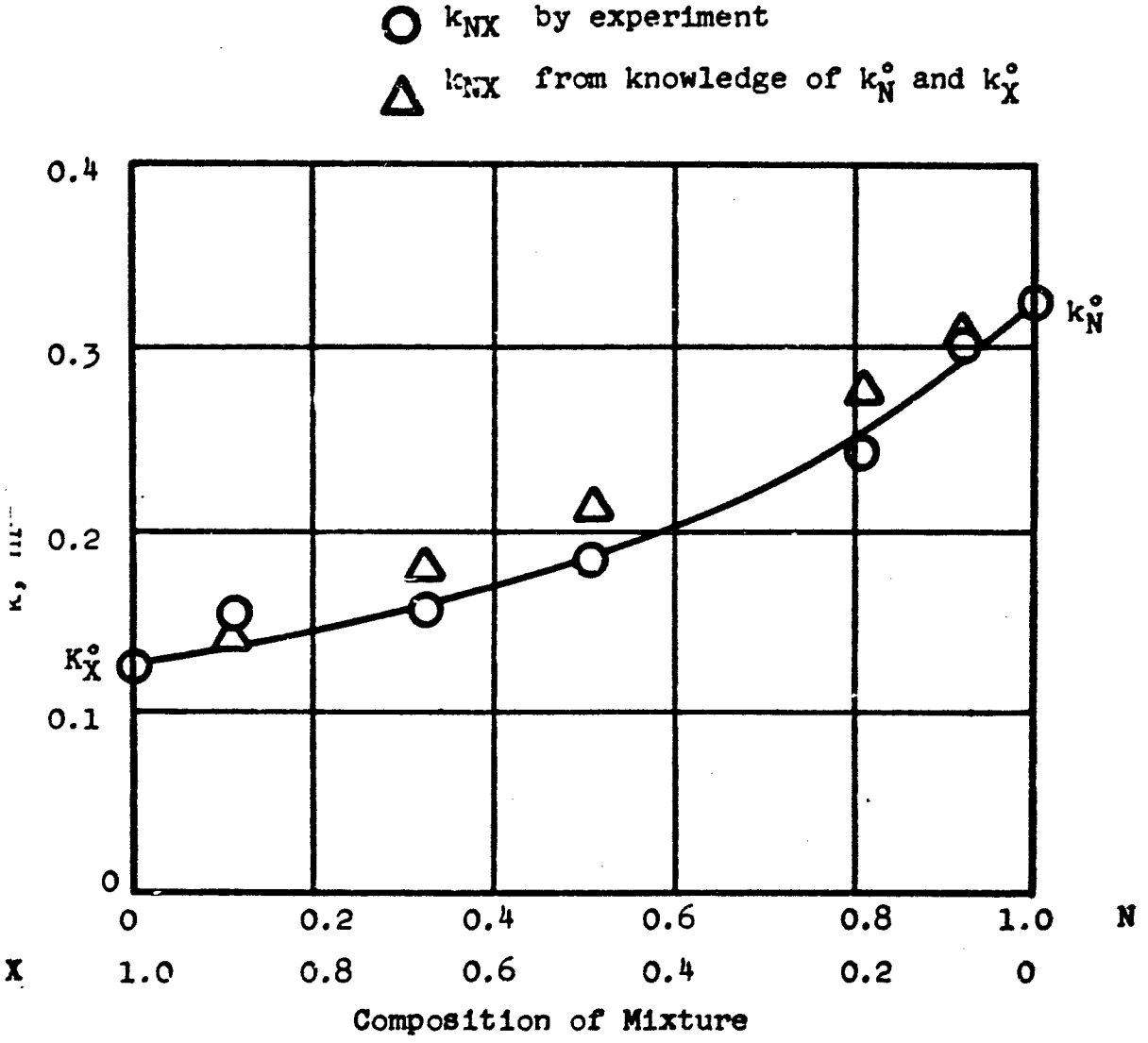

Figure 33. Decomposition Rate Constants of 2,2,8,8-Tetramethylnonane (N) —t-Butylcyclohexane (X) Mixtures at 800°F

4. t-Butylcyclohexane - Methylhydrindan

The data obtained in cracking this mixture were not as complete as those discussed for the other mixtures, but the same general results were obtained. The values of the rate constants for pure t-butylcyclohexane and methylhydrindan were close: 0.207 and 0.149 hr^{-1}, respectively. It was surprising therefore to see such a change in the individual rate constants caused by decomposing them in a mixture. The data for this mixture are presented in Table 26 and Figures 34 through 36.

5. n-Hexadecane - Tetramethylnonane

The data from cracking this mixture were the least reliable of all, but the results added some support to the findings from the other experiments. It is likely that the short residence time of this experiment (1 hour vs 166.5 hour for the cetane - decalin mixture) had an effect on the quality of the data. Table 27 and Figures 37 to 39 give the correlations.

Table 26

THERMAL CRACKING OF BINARY MIXTURES
t-BUTYLCYCLOHEXANE - METHYLHYDRINDAN

Run No. 163
Reaction temp. 800°F
Reaction time 3 hr

M = Methylhydrindan
X = t-Butylcyclohexane

Component	Conc.		Fraction Remaining		k hr^{-1}	k_{XM} exp.	k_{XM} calc.
	α	1-α	1-x	1-y			
M	1.00	0	0.640	0	0.149	0.149	0.149
M	0.95		no		-		
X		0.05	exp'l		-	-	0.152
			date				
M	0.75		0.820		0.066		
X		0.25		0	-	0.162	0.155
M	0.50		0.871		0.046		
X		0.50		0.267	0.440	0.187	0.177
M	0.25		0.549		0.200		
X		0.75		0.536	0.207	0.205	0.184
X	0	1.00	0	0.536	0.207	0.207	0.207

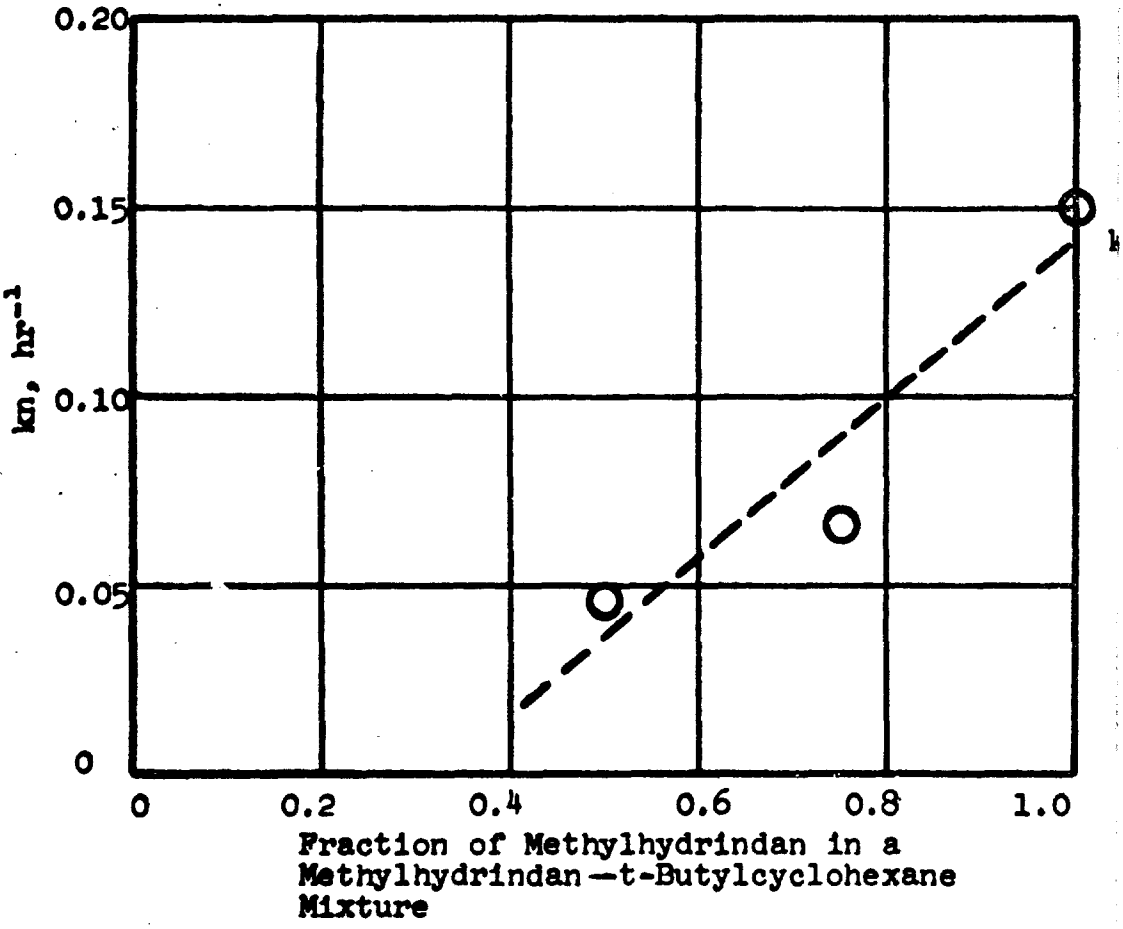

Figure 34. Effect of Dilution with t-Butylcyclohexane (X) on the Decomposition Rate Constant of Methylhydrindan (M) at 800°F

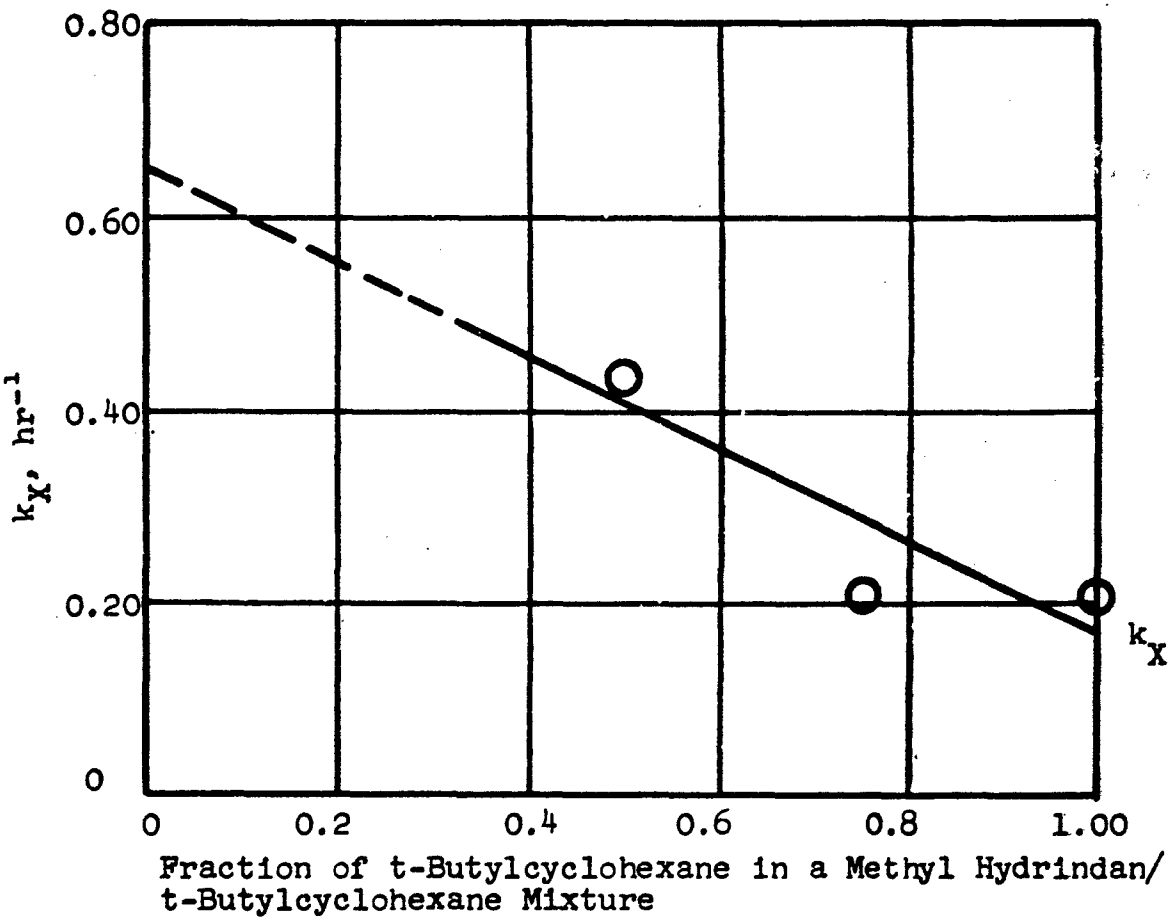

Figure 35. Effect of Dilution with Methylhydrindan (M) on the Decomposition Rate Constant of t-Butylcyclohexane (X) at 800°F

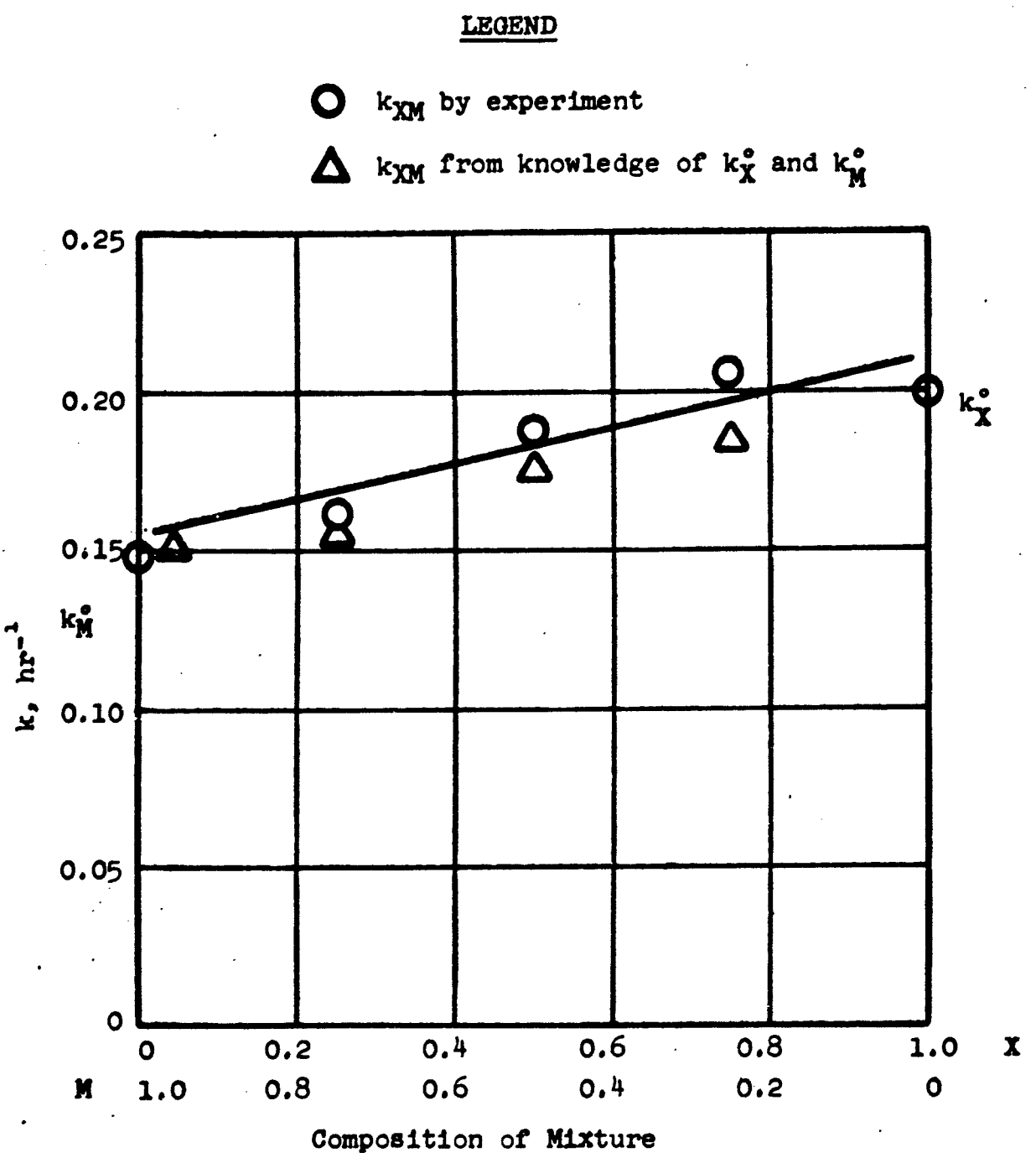

Figure 36. Decomposition Rate Constants of t-Butylcyclohexane-Methylhydrindan Mixtures at 800°F

Table 27

THERMAL CRACKING OF BINARY MIXTURES
n-HEXADECANE - 2,2,8,8-TETRAMETHYLNONANE

Run No. 154
Reaction temp. 800°F
Reaction time 1 hr

C = n-Hexadecane
N = 2,2,8,8-Tetramethylnonane

Component	Conc.		Fraction Remaining		k hr^{-1}	k_{CN} exp.	k_{CN} calc.
	α	1-α	1-x	1-y			
N	1.00	0	0.857	0	0.154	0.154	0.154
N	0.75		0.565		0.571		
C		0.25		0.955	0.046	0.410	0.271
N	0.50		0.387		0.950		
C		0.50		0.745	0.294	0.570	0.410
N	0.25		0.710		0.342		
C		0.75		0.509	0.676	0.581	0.564
N	0.05		0.776		0.254		
C		0.95		0.509	0.676	0.623	0.706
C	0	1.00	0	0.473	0.749	0.749	0.749

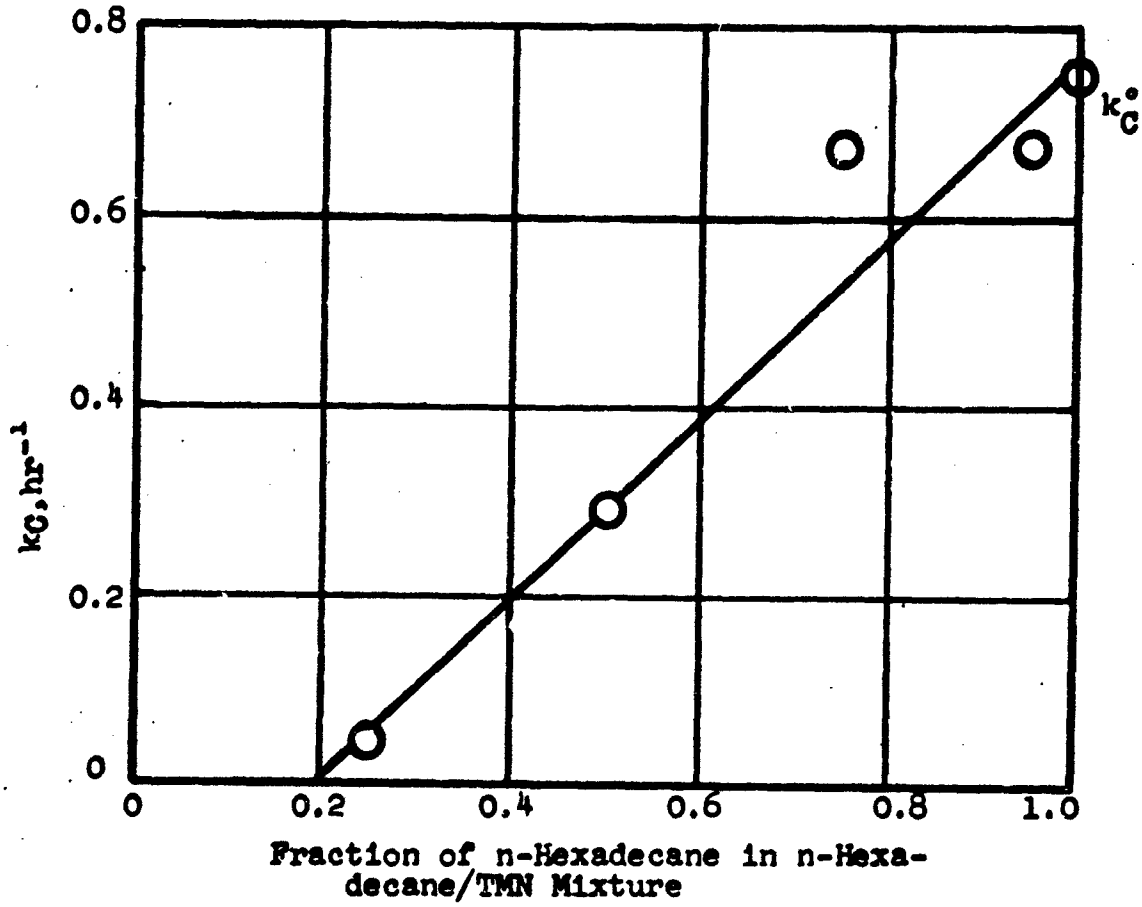

Figure 37. Effect of Dilution with 2,2,8,8-Tetramethylnonane (N) on the Decomposition Rate Constant of n-Hexadecane (C) at 800°F

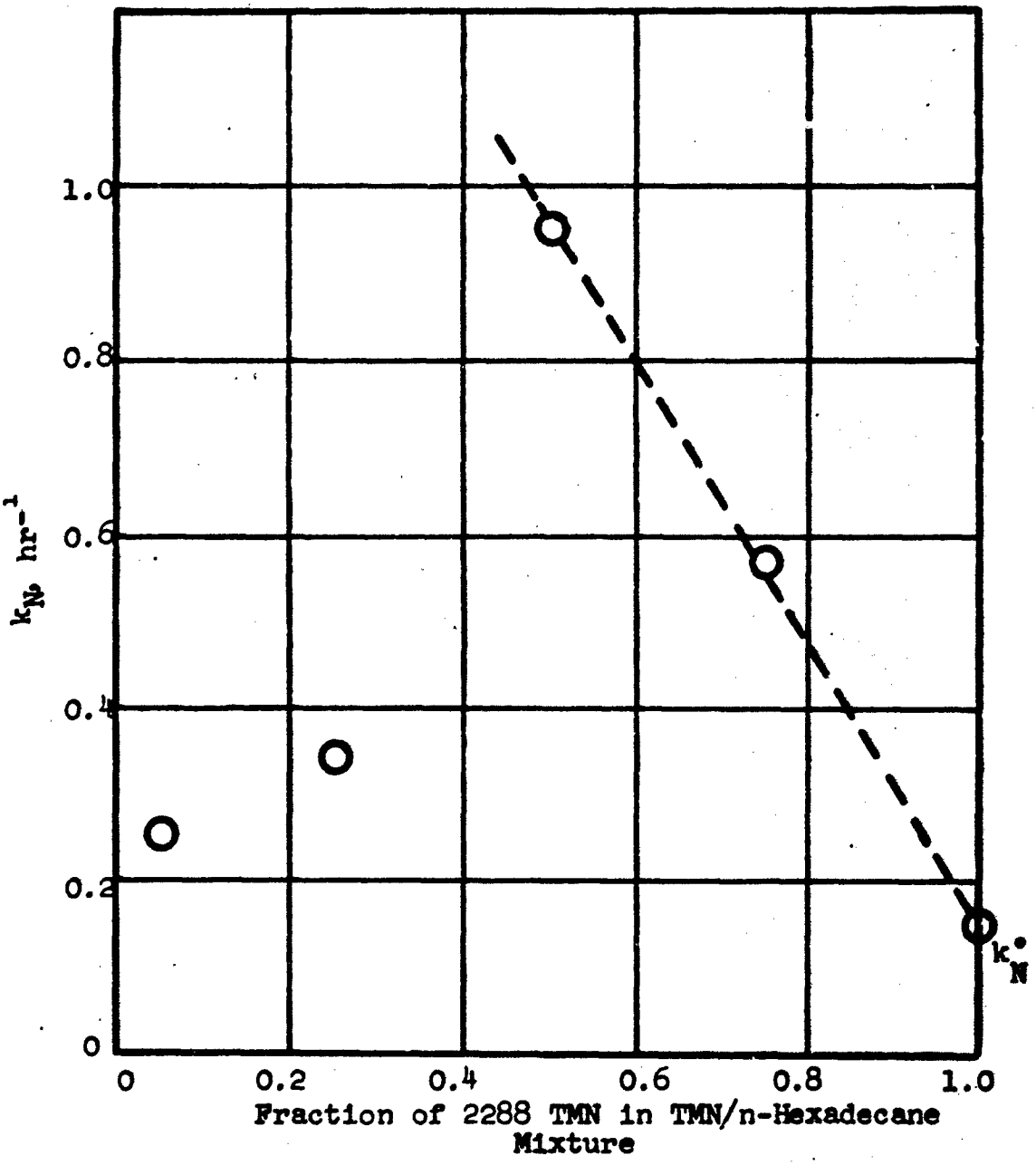

Figure 38. Effect of Dilution with n-Hexadecane (C) on the Decomposition Rate Constant of 2,2,8,8-Tetramethylnonane (N) at 800°F

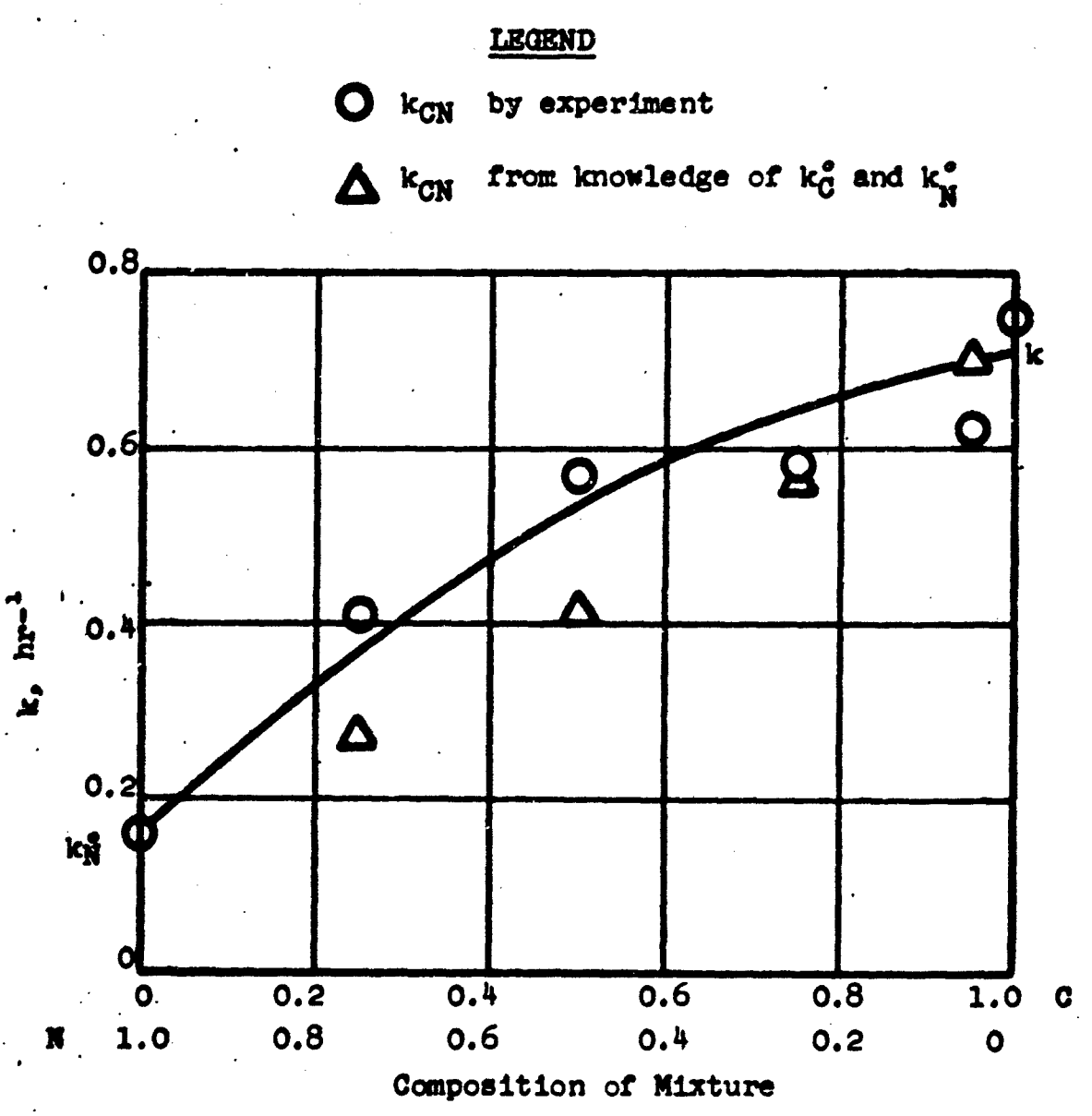

Figure 39. Decomposition Rate Constants of n-Hexadecane-2,2,8,8-Tetramethylnonane Mixtures (800°F)

VIII. MICRO-COKER DEVELOPMENT

Decomposition experiments have been conducted in the micro-coker covering a range of conditions with various fuels. These tests have showed that the micro-coker is a useful, reliable research tool.

A. EQUIPMENT

The equipment was described in detail in the previous annual report (ref. 39) on this contract and the general layout of the unit was shown in Figure 18, p. 42 of that report. No substantial changes have been made in the equipment or the test procedure. However, the reactor was modified. Preliminary experiments showed that modifying the helical reactor into a flat plate with grooves not only simplified the design but provided easy and reliable sealing, and had the additional advantage of providing the test plate with the deposit on it as a permanent record of the test. For these reasons, the flat reactor was preferred, and all the tests reported here were conducted with it.

The dimensions of the micro-coker were chosen so that it could be inserted into the high pressure vessel and still provide a 38.4-inch long test groove. The reactor is shown in Figure 40. The reactor consists of four main parts: (1) reactor body with the grooves, (2) test plate, which covers the test grooves, (3) cover plate, and (4) clamping bolts.

The reactor body covered with the test plate forms a duct of rectangular cross section for the fuel flow. The clamping bolts and the cover plate hold the test plate against the reactor body with sufficient force to seal against leakage.

The fuel is fed through a 0.041-inch I.D. stainless steel hypodermic tube. The feed line is joined to the body of the reactor by high pressure fittings. The preheated fuel flows through the test grooves, leaves the reactor and the high pressure vessel through stainless steel hypodermic tubing, and enters the pressurized sample chamber. Any instability of the fuel towards deposit formation due to thermal stressing is shown by deposition and discoloration of the test plate and grooves.

After completion of a run, the fuel path is flushed with nitrogen, and the reactor, after cooling to room temperature, is disassembled. The test plate is checked for signs of leakage and is evaluated. Each run is made with a new test plate, and the used plates are preserved as a record of the test.

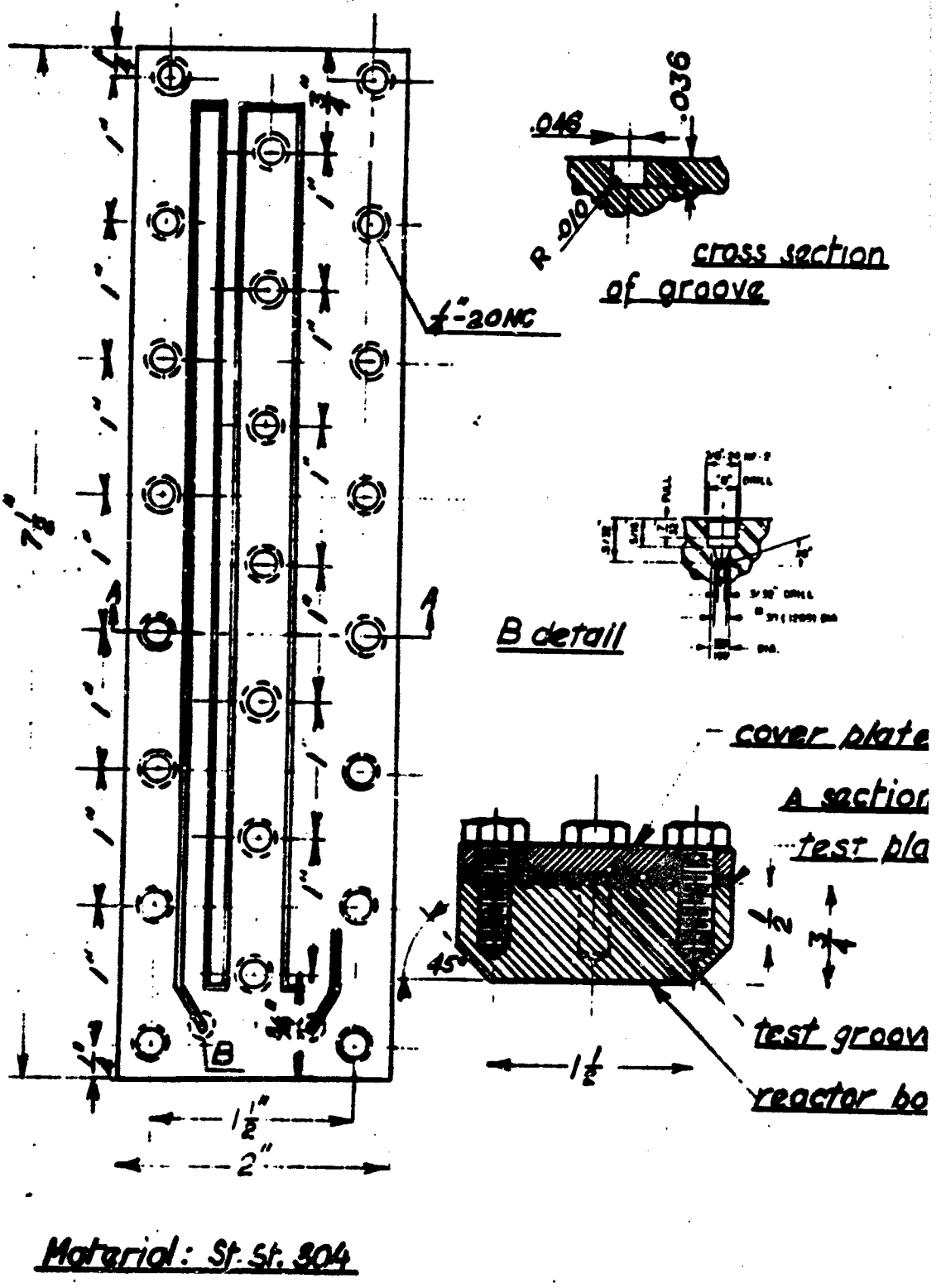

Figure 40. Micro-Coker Assembly.

The reactor body, the new test plate, and the cover are carefully cleaned and polished for the next run.

B. TEST RESULTS

Tests were conducted with the flat micro coker to determine the effect of temperature, pressure, test plate material, and different fuels on the nature and extent of test plate deposits.

1. Effect of Temperature, Pressure, and Plate Material

The test results of a ten-run series, conducted at a feed rate of 3 ml per hour, are given in Figure 41 from which the following conclusions can be drawn:

(a) There is hardly any deposit formed on the plates in the 600°F reactor temperature range at 500 psig pressure.

(b) In the 600-850°F range the correlation between temperature and deposit length shows a linear trend.

(c) Between 850 and 950°F there is a transient zone where deposits are no longer discernible at the inlet but begin to appear at the outlet.

(d) At 950°F, deposits can only be found at the outlet end of the test plate.

This behavior indicates that under these test conditions two temperature ranges for deposit formation can be distinguished, the transition between these two ranges being at 850-950°F. In the low temperature range, contaminants, dissolved oxygen, and oxidative degradation are probably responsible for the observed deposits. In the high temperature range, above 900°F, the processes leading to deposits must be similar to those studied in the static tester. The temperature limits for each of these zones must be a strong function of the experimental conditions, mainly the residence time at these elevated temperatures. Vapor phase chromatography of the stressed fuels showed no detectable changes in the fuel in the runs at lower temperatures. Yet, deposits were observed at the inlet in these tests.

The color of the deposit on type 302 stainless test plates characteristically changes from metal, to light gray, to dark gray, to dark black with increasing temperature. The reported deposit length includes the light gray through dark black sections.

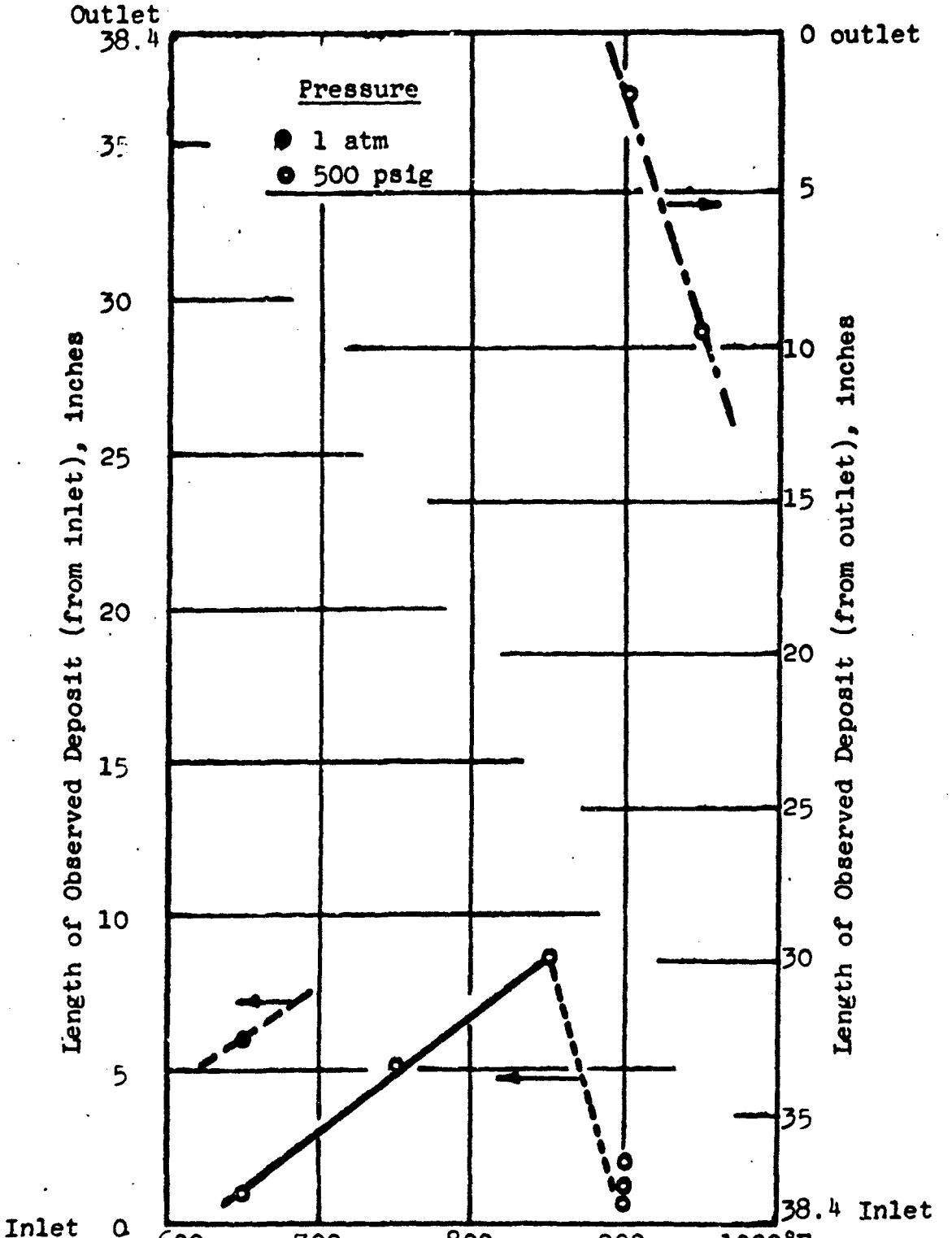

Conditions: Fuel, HTF 157-60; Flow Rate, 3 ml/hr.; Plate 302

Figure 41. Effect of Temperature on Deposit Length, Type 302 Stainless Steel Test Plates

Although there were not sufficient runs performed to elucidate the effect of pressure on deposit length using type 302 stainless plate, one run at atmospheric pressure and 650°F showed that the pressure change from atmospheric to 500 psig decreased the deposit length substantially.

Further investigations were conducted to obtain more data on the effect of pressure and test plate material. Since aluminum is widely used in both fuel test equipment and in airplanes, two sets of experiments were carried out with aluminum test plates. The results are presented in Figures 42 and 43.

The linearity of the deposit length vs temperature curve is similar to the curve obtained with stainless steel plates up to the transition point. Figure 42 shows that some deposit starts to build up at the outlet end while the length of deposit from the inlet continues to increase. As the temperature increases, the length of the deposit extends from both ends and around 970-975°F the two deposit paths meet resulting in a completely covered plate. The deposit length from the inlet does not decrease to a minimum as it does in the case of stainless steel. At atmospheric pressure, the length of deposit was increased as shown in Figure 43. The rate of increase with temperature is also somewhat higher at atmospheric pressure.

While the increase in deposit length with temperature is much greater (about 7 times) with aluminum than with stainless steel, the first appearance of deposits on aluminum occurs at a much higher temperature. The fact that higher temperatures are required for deposit formation on aluminum suggests that type 302 stainless steel catalyzes the reactions leading to deposit formation, lowering the activation energy for these reactions. This is further borne out by the rapid increase in deposit length on aluminum, since a higher activation energy with aluminum would make the reactions a much stronger function of temperature. The increase in deposit length (from the outlet) with temperature above the transition region is rapid with both stainless steel and aluminum being only slightly greater with aluminum (Figures 41 and 42). This would indicate that stainless steel is not catalytic for the decomposition reactions leading to deposits at the outlet. It has already been postulated that these reactions are of the same nature as those studied in the static test equipment where only minor variations were noted in decomposition with stainless steel present. The catalytic action of stainless steel, as compared to aluminum in deposit formation at lower temperatures, has been noted previously in CRC Fuel Coker tests.

2. Effect of Feed Material and Comparison of Results With CRC Coker Data

Preliminary experiments showed that type 304 stainless steel test plates produced a different type of deposit than that previously

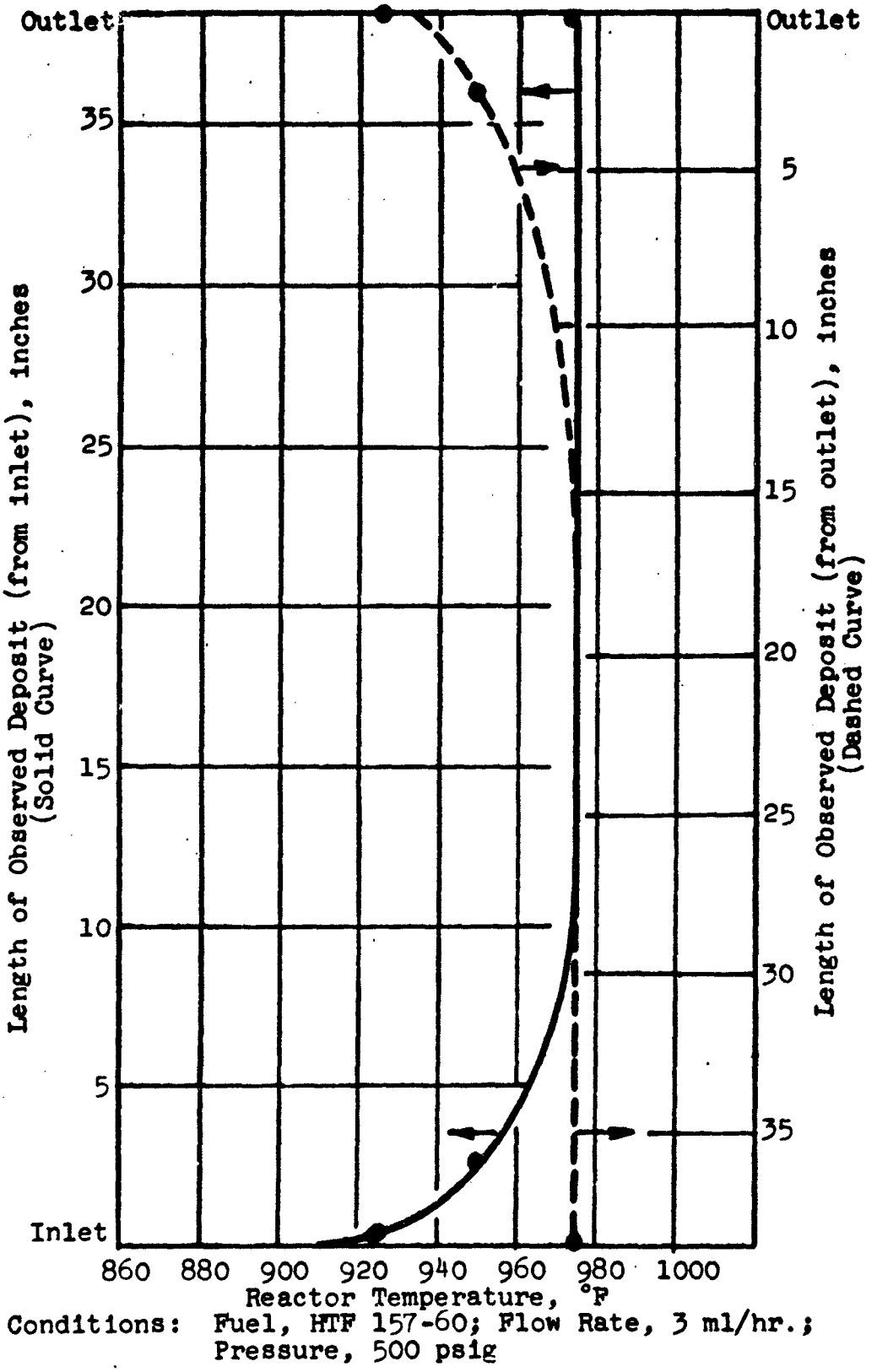

Figure 42. Effect of Temperature on Deposit Length, Aluminum Test Plates

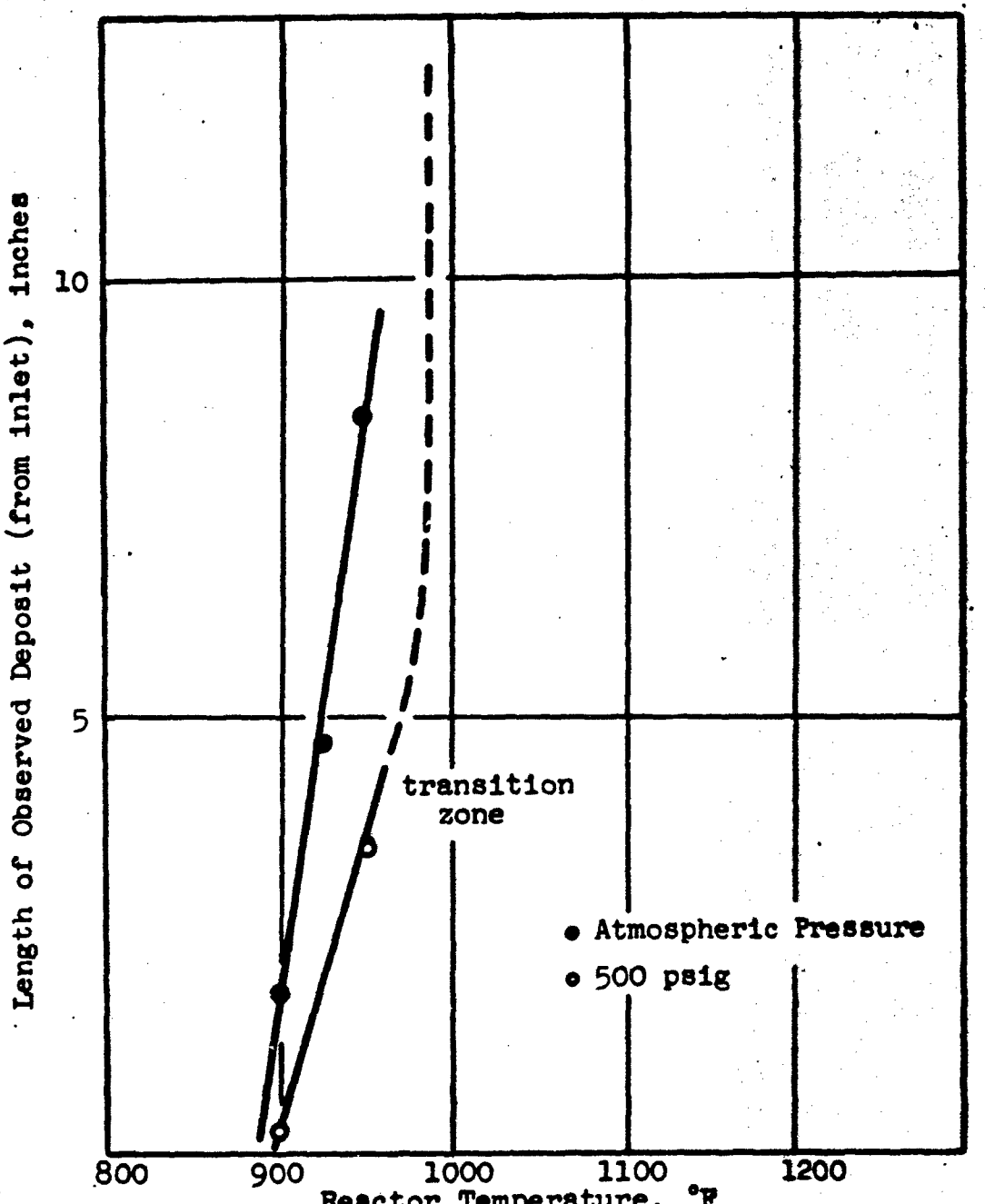

Conditions: Fuel, HTF-157-60; Flow Rate, 3 ml/hr.; Pressure, 500 psig

Figure 43. Effect of Pressure and Temperature on Deposit Length, Aluminum Test Plates

found on the aluminum and 302 stainless steel plates. While the latter two deposits fall into the gray-black category, the 304 stainless steel plates showed a variety of deposits comparable with the CRC preheater tube deposit rating. Tests were made on a number of fuels at 500 psig pressure, 750°F reactor temperature, and 3 ml/hr flow rate with 304 stainless steel plates. These con ditions were used since they resulted in ratings in the CRC scale range.

The deposit ratings of the test plates, according to the CRC depo scale, are plotted for each fuel against the CRC rating of the fu (ref. 40) in Figure 44. The test plate ratings are generally hig than the CRC ratings, but the maximum deviation is one rating uni

The micro-coker test plate permits the observation of the pattern the deposit in a flow reactor. It permits the study of the depos material by supplying samples for chemical analysis or x-ray fluorescence measurement. The micro-coker seems to be an instrum that could be employed for a more detailed investigation of the transient zone of deposit formation.

The comparative runs of CRC fuels showed that the micro coker res are consistent with the CRC coker data. The very small fuel con- sumption of the micro-coker (3 ml/hr) and the possibility of runn it at atmospheric pressure, make it a simple and reliable experim al device.

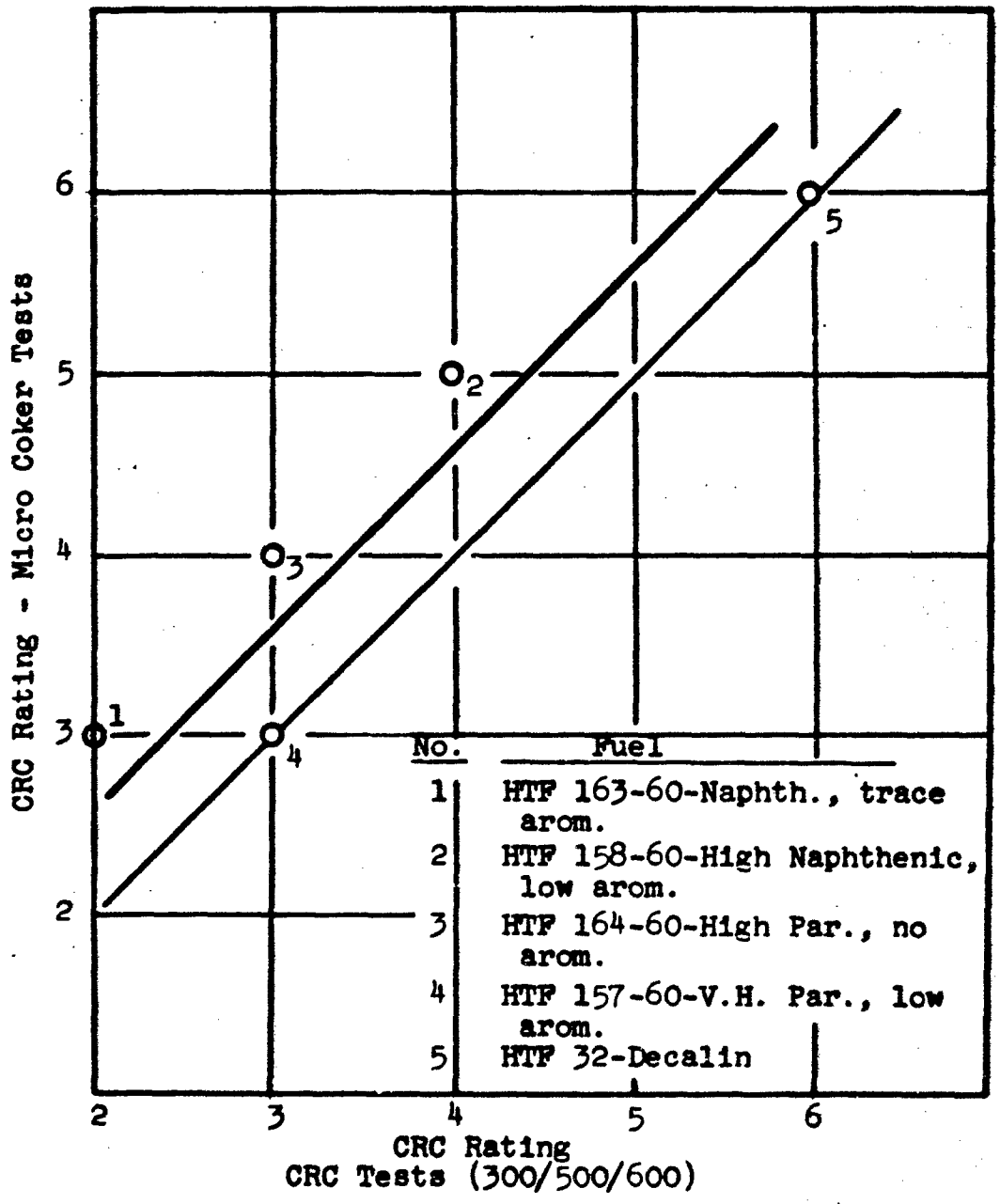

Figure 44. Comparison of Micro Coker and CRC Ratings on Various Fuels

IX. REFERENCES

1. Sherwood, T. K. and Reid, R. C., "The Properties of Gases and Liquids," McGraw-Hill Publ. Corp., N. Y. (1958).

2. Johns, I. B., McElhill, E. A., and Smith, J. O., Ind. Eng. Ch Proc. Res. and Dev., 1, 2 (1962).

3. Fabuss, B. M., Smith, J. O., Lait, R. I., Borsanyi, A. S., an Satterfield, C. N., Ind. Eng. Chem. Prod. Res. and Dev., 1, (1962).

4. Dintses, A. I., Compt. rend. acad. sci. USSR, 2, 153 (1933).

5. Dintses, A. I., Uspekhi Khim., 7, 404 (1939).

6. Dintses, A. I. and Frost, A. V., J. Gen. Chem., USSR, 3, 747

7. Frost, A. V., J. Phys. Chem., USSR, 8, 290 (1936).

8. Steacie, E. W. R., "Atomic and Free Radical Reactions," Reinl Publ. Corp., N. Y. (1954), p. 122.

9. Konovalov, D. S. and Migotina, E. N., Zhur. Priklad. Khim., 332 (1953).

10. Jost, W. and Muffling, L., Zeitschr. f. Elektrochem., 47, 76 (1941).

11. Schultze, G. R. and Wassermann, G , Zeitschr. f. Elektrochem. 47, 774 (1941).

12. Kasansky, B. and Plate, A. F., Ber., 67, 1023 (1934).

13. Kuchler, L., Trans. Far. Soc., 35, 874 (1939).

14. Pease, R. N. and Morton, J. M., J. Am. Chem. Soc., 55, 3190

15. Bachman, K. C., Matthews, E. K.and Zudkevitch, D.,"Evaluatio Hydrocarbon Materials as Vaporizing Fuels," ASD-TDR-62-254 (

16. Smith, J. O., Fabuss, B. M., Borsanyi, A. S., and Lait, R. I. "Evaluation of Materials as Endothermic Aviation Fuels," ASD-TR-60-841, Part II (1961).

17. Levenspiel, O., "Chemical Reaction Engineering," John Wiley Sons, Inc., New York (1962).

18. Tilicheev, M. D., Zhur. Prikl. Khim., 12, 735 (1939).

19. Malinovsky, M. S. and Stoyanovskaya, Ya. I., J. Applied Chem. USSR, 29, 1369 (1956).

20. Sundgren, A., Ann. Office Natl. Combustible Liquides, 5, 44 (1930).

21. Tilicheev, M. D., Zhur Prikl. Khim., 12, 105 (1939).

22. Voge, H. H., and Good, G. M., J. Am. Chem. Soc., 71, 593 (1949).

23. Fabuss, B. M., Kafesjian, R., and Smith, J. O., unpublished data.

24. Tilicheev, M. D. and Zimina, K. I., Khim i Tekhnol. Topliva, No. 8, 23 (1956).

25. Panchenkov, G. M. and Baranov, V. Ya., Izvest. Vyssh. Ucheb. Zaved. Neft' i Gaz, No. 1, 703 (1958).

26. Terres, E. and Gropenbacher, G., Erdol and Kohle, 10, 281 (1957).

27. Frey, F. E. and Hepp, H. J., Ind. Eng. Chem., 25, 441 (1933).

28. Tropsch, H. Thomas, C. L., and Egloff, G., Ind. Eng. Chem., 28, 324 (1936)

29. Hurd, C. D., and Spence, L. V., J. Am. Chem. Soc., 51, 3353 (1929).

30. Egloff, G., and Parish, C. I., Chem. Rev., 19, 145 (1936).

31. Dintses, A. I. and Klabina, Ts., I. Zhurn. Obshch. Khim., 7, 1507 (19).

32. Hepp, H. J. and Frey, F. E., Ind. Eng. Chem., 45, 410 (1953).

33. Steacie, E. W. R., and Puddington, I. E., Can. J. Research, B16, 176 (1938).

34. Gonikberg, M. G., Gravrilova, A. E., and Kozanskii, B. A., Dokl. Akad. Nauk. S.S.S.R., 89, 483 (1953).

35. Gonikberg, M. G. and Voevodskii, V. V., Izvest. Akad. Nauk S.S.S.R., Otdel. Khim. Nauk., 1954, 370.

36. Kossiakoff, A. and Rice, F. O., J. Am. Chem. Soc., 65, 590 (1943).

37. Frost, A. A. and Pearson, R. G., "Kinetics and Mechanism" John Wiley and Sons, Inc., New York, Second Edition (1961), p. 252.

38. Smith, J. O., et al., "Evaluation of Hydrocarbons for High Temperature Fuels," Technical Documentary Report No. WADC TR-59-327, Part II, Vol. I, Feb. 1962.

39. Fabuss, B. M., et al., "Research on the Mechanism of Thermal Decomposition of Hydrocarbon Fuels," Technical Documentary Report No. ASD-TDR-63-102, Jan. 1963.

40. Minutes of the Meeting of the CRC-Aviation Group on High Temperature Stability of Fuels for High Performance Aircraft, April 3, 1961, New York City.

APPENDIX

SAMPLE CALCULATIONS

A. RATE CONSTANTS OF PURE HYDROCARBONS: STATISTICAL EVALUATION OF DATA

To show the method used in evaluating the experimental data, the complete calculation will be given for t-butylcyclohexane shown in Figure 2. The experimentally determined conversions (x) and the calculated rate constants $\left(k = \frac{1}{t} \ln \frac{1}{1-x}\right)$ (58) are given for the 15 experiments at 800°F as follows:

Wt Fraction, x	t, hr	k, hr^{-1}	Wt Fraction, x	t, hr	k, hr^{-1}
0.286	2.0	0.168	0.629	8.5	0.117
0.422	3.5	0.157	0.688	10.5	0.111
0.476	4.5	0.144	0.732	11.5	0.115
0.505	5.5	0.127	0.750	12.5	0.111
0.572	6.5	0.131	0.795	13.0	0.122
0.558	6.5	0.126	0.840	16.1	0.114
0.622	7.5	0.130	0.901	22.0	0.105
0.608	7.5	0.125			

From these data

$$N = 15$$
$$\Sigma k = 1.903$$
$$\Sigma x = 9.384$$
$$\Sigma kx = 1.15383$$
$$\Sigma x^2 = 6.25331$$
$$\Sigma k^2 = 0.24576$$
$$\bar{x} = 0.626$$

To calculate the equation $k = a + bx$ by the method of least squares

$$b = \frac{N \Sigma kx - \Sigma k \Sigma x}{N \Sigma x^2 - (\Sigma x)^2} = \frac{(15 \times 1.15383) - (9.384 \times 1.903)}{(15 \times 6.25331) - (9.384)^2} = -0.09586 \quad (59)$$

$$a = \frac{\Sigma k - b \Sigma x}{N} = \frac{1.903 + 0.09586 \times 9.384}{15} = 0.18683 \quad (60)$$

and the equation is

$$\boxed{k = 0.187 - 0.096x}$$

for $x = 0$ $\quad k = k_o = 0.187$
$x = 0.5$ $\quad k = 0.139$
$x = 1.0$ $\quad k = 0.091$

If the above equation holds, as given, per cent confidence limits for the mean of the k values of all individuals having a particular x value are

$$Y_x - tS_{y,x}\sqrt{\frac{1}{N} + \frac{(x-\bar{x})^2}{(N-1)S_x^2}} < Y_x < Y_x + tS_{y,x}\sqrt{\frac{1}{N} + \frac{(n-\bar{x})^2}{(n-1)S_x^2}}$$

where t values are read from a table of percentiles of the t distribution for N-2 degrees of freedom and

$$S_x^2 = \frac{N\Sigma x^2 - (\Sigma x)^2}{N-1}$$

$$S_y^2 = \frac{N\Sigma k^2 - (\Sigma k)^2}{N-1}$$

$$S_{y,x}^2 = \frac{N-1}{N-2}(S_y^2 - b^2 S_x^2)$$

and in our case

$$S_x^2 = \frac{15 \times 6.25331 - 9.384^2}{14} = 0.41001$$

$$S_y^2 = \frac{15 \times 0.24576 - 1.903^2}{14} = 0.00464$$

$$S_{y,x}^2 = \frac{14}{13}(0.00464 - 0.09586^2 \times 0.41001) = 0.00094$$

$$S_{y,x} = (0.00094)^{1/2} = 0.0307$$

$$t = 1.771$$

$$\Delta = \pm t \cdot S_{y,x}\sqrt{\frac{1}{N} + \frac{(x-\bar{x})^2}{(N-1)S_x^2}} = \pm 1.771 \times 0.0307 \sqrt{\frac{1}{15} + \frac{(x-0.626)^2}{14 \times 0.41001}} =$$

$$= \pm 0.05437 \sqrt{0.06667 + 0.17421(x-0.626)^2} \qquad (66)$$

Using these equations, the k values are, for a series of x values,

x	Δ	k	k_{max}	k_{min}
0.1	$\pm$0.0184	0.177	0.196	0.159
0.3	$\pm$0.0159	0.159	0.174	0.142
0.5	$\pm$0.0144	0.139	0.154	0.125
0.7	$\pm$0.0141	0.120	0.134	0.106
0.9	$\pm$0.0153	0.101	0.116	0.085

This means that on the basis of 15 experimental results we are 95 per cent confident that the mean value of the rate constant of decomposition at 50% conversion is between 0.154 and 0.125. If we repeat this experiment with another series, we should obtain another set of limits instead of 0.154 and 0.125. In the long run, 95 per cent of such intervals would cover the value of 0.139. This is the interpretation of our statement of the degree of confidence.

The entire calculation was carried out by the method and tables given by W. T. Dixon and F. J. Massey "Introduction to Statistical Analysis" McGraw-Hill Book Co., N. Y. (1957).

B. RATE CONSTANTS OF BINARY HYDROCARBON MIXTURES

Problem

To calculate the decomposition rate of a 25% by volume decalin (D) and 75% n-Hexadecane (H) mixture given the reaction time as 166.5 hours at 700°F and the fractions of D and H unreacted as 0.749 and 0.372, respectively.

Solution

Assume that a first-order kinetic equation can be used to calculate the overall mixture rate using the sum of the residual decalin and n-hexadecane. Then,

$$(k_{DH})_{exp.} = \frac{2.3}{t}\log\left[\frac{1}{\alpha(1-x)+(1-\alpha)(1-y)}\right] = \qquad (57)$$

$$= \frac{2.3}{166.5}\log\left[\frac{1}{0.25(0.749) + 0.75(0.372)}\right]$$

$$= \underline{4.57 \times 10^{-3} hr^{-1}}$$

Problem

Calculate k_{DH} for a mixture containing 25 vol-% decalin(D) and 75 vol-% n-hexadecane (H) for a reaction time of 166.5 hours.

Solution

From Table 22, $k_D^\circ = 1.07 \times 10^{-4}$ and $k_H^\circ = 88.6 \times 10^{-4} hr^{-1}$. Assuming independent decomposition

for decalin, $\log\frac{1}{D} = \frac{1.07 \times 10^{-4} \times 166.5}{2.303} = 0.00773$

$$D = 0.982$$

for n-hexadecane, $\log\frac{1}{H} = \frac{88.6 \times 10^{-4} \times 166.5}{2.303} = 0.64055$

$$H = 0.229$$

and,

$$(k_{DH})_{calc} = \frac{2.303}{t} \log \left[\frac{1}{\alpha(1-x)+(1-\alpha)(1-y)} \right] =$$

$$= \frac{2.303}{166.5} \log \left[\frac{1}{0.25 \times 0.982 + 0.75 \times 0.229} \right] =$$

$$= 5.25 \times 10^{-3} hr^{-1}$$